Cell Permeabilization Using Supercritical Carbon Dioxide

by

Matthew Ng

A thesis
presented to the University of Waterloo
in fulfillment of the
thesis requirement for the degree of
Master of Applied Science
in
Chemical Engineering

Waterloo, Ontario, 2001

I hereby declare that I am the sole author of this thesis. This is a true copy of the thesis including any required final revisions, as accepted by my examiners.
I understand that my thesis may be made electronically available to the public.

Acknowledgements

I would like to thank Dr. Raymond Legge for the opportunity for working on this project. I also appreciate his patience, help, and guidence throughout my time at the university.

I would like to thank the readers, Dr. Christine Moresoli and Dr. Mark Pritzker for taking the time to read my thesis and provide suggestions for improvement.

I would like to thank the members of the downstairs lab group for the company over the past two years.

•Jeremy Steffler, for his help settling into Waterloo and introducing me to the wonderful world of wetlands
•Marc Aucoin, for the discussions on supercritical fluids and enzymes
•Joe Clifford, for his help with analytical procedures, especially on the GC
•Ahmad Yahya, for his help with the SDS-PAGE and as an experienced lab worker
•Dale Weber, for his help with the SEM
•Yooseong Hong, for his help with the AFM
•Wenbo Ma and Thomas Prade, for their help with the GFP and *E. coli*
•Andréanne Bouchard and Ben Youn, for keeping company during the weekends
•The technical staff (Ralph Dickhout, Bert Habicher, Rick Hecktus, and Jana Ortuba) for the help that they provided throughout my stay in Waterloo
•And all the students who have passed through the lab as a course of their co-op, undergraduate, or graduate work

I would like to dedicate this work
to my parents, Peter and Angela
who have always been supportive
of my choices.

Abstract

Supercritical fluids have unique properties which may make them ideal as reaction media for biotransformation or extractive solvents. Supercritical fluids are ideal for reducing diffusivity limitations over conventional fluids. Depending on the polarity of the fluid, a supercritical fluid can be similar to conventional organic solvents, but with few of the environmental drawbacks. The use of supercritical fluids in enzymatic research has the advantage of removing mass transport limitations so that they can act as a suitable solvent.

In this study, four permeabilization techniques were compared: control, toluene, supercritical carbon dioxide, and freeze/thaw cycles. The model cell systems studied were *Z. mobilis* and *E. coli*. The cells were analyzed for lipid profiles, recovery of proteins and enzymatic activity.

The use of supercritical carbon dioxide may not be the most effective of the treatments based on total protein or enzyme recovery since the greatest protein and enzyme recovery was with the freeze/thaw treatment. However, it can be selective in removing cofactors from *Z. mobilis* enabling sorbitol production and minimizing side reactions. In this application, supercritical carbon dioxide does show an advantage over the freeze/thaw treatment.

Aspects of the mechanism of permeabilization were investigated based on the lipid profiles of the cells, scanning electron microscopy (SEM) and atomic force microscopy (AFM). The SEM and AFM show changes of the cell surface morphology which indicate that the treatments affect the cellular surface.

The use of supercritical carbon dioxide as a reaction medium was investigated. Minute quantities of sorbitol were produced when *Z. mobilis* and sugars were placed in a supercritical carbon dioxide environment over a period of 24 hours.

Contents

List of Tables

List of Figures

Chapter 1

Introduction

Cell permeabilization is a technique used primarily for the recovery of microbial products. These products include proteins, enzymes and pharmaceuticals. Cell permeabilization can be used to produce a biotransformation system that can be an inexpensive alternative to purified enzyme systems. Conventional forms of cell permeabilization will be discussed with the addition of supercritical carbon dioxide as an alternative to organic solvents. With carbon dioxide, there are none of the toxicity problems found with the use of toluene. Using supercritical carbon dioxide to replace organic solvents would reduce the amount of toxic waste and be more environmentally-friendly.

The model organisms of *Z. mobilis* and *E. coli* are used to determine the effectiveness of the permeabilization using supercritical carbon dioxide. The studies with *Z. mobilis* focus on two aspects of cell permeabilization: protein/enzyme recovery and the production of cells suitable for the use as a biotransformation system. *Z. mobilis* was chosen as an experimental system because of interest in this organism for the production of sorbitol under supercritical conditions. Glucose-6-phosphate dehydrogenase was chosen as an enzyme marker for cytoplasmic proteins. Glucose fructose oxidoreductase (GFOR) was chosen as a marker for the periplasmic space and as an enzymatic system for the biotransformation of glucose to sorbitol. To better understand the molecular mechanisms behind cell permeabilization microscopic studies and lipid characterization were also conducted. Preliminary work on the viability of supercritical carbon dioxide as a reaction media was conducted as a basis for future work in the field of biocatalysis in non-convential media.

E. coli was studied to ensure that the results obtained for the *Z. mobilis* organism were

applicable to other organisms. For *E. coli*, protein recovery was the only aspect of cell permeabilization that was studied. The recovery of green fluorescent protein (GFP) from recombinant *E. coli* was used determine the effectiveness of the permeabilization process. Again, total lipid profiles were studied to determine changes in the lipids as a result of the permeabilization treatment.

Chapter 2

Literature Review

2.1 Cell Biochemistry

2.1.1 Cell Wall

The wall of the bacterial cell adds structural integrity so that the bacteria can withstand harsh environmental factors. The cell wall is the outermost layer of the bacteria and is exposed directly to the environment.

There are two types of bacteria classified by the type of wall: gram-positive and gram-negative. The different types can be differentiated by gram stain developed by Hans Christian Gram [91]. This procedure involves staining the bacteria with crystal violet and iodine. After exposure to the stain, the bacteria are decolourized with alcohol or acetone. The bacteria that retain the deep blue colour are gram-positive bacteria. The retention of the colour is attributed to the structure of the cell wall. Gram-positive bacteria have a wall consisting of a single, thick, polysaccharide layer. In contrast, gram-negative bacteria are rapidly decolourized due to the different cell wall structure. The cell wall consists of two thin layers: the inner membrane (plasma membrane) and the outer membrane. The periplasmic space lies between the two layers which can contain other elements such as proteins or enzymes. The outer membrane contains lipopolysaccharides and lipoproteins which link the outer membrane to the peptidoglycan layer. There are channels in the membrane allowing small water-soluble molecules to pass [91].

2.1.2 Cell Membrane

The next layer of the bacteria is the cell membrane, also referred as the plasma membrane, is composed of a lipid bilayer (double layer of lipid molecules) based on the fluid mosaic model by Singer and Nicolson [81]. The hydrophobic regions of the lipids face towards the interior of the layer, with the hydrophilic regions facing towards the surrounding aqueous environment. There are two main types of lipids that are found in the cell membrane. The most abundant lipids are the phosphoglycerides which provide most of the structure. A phosphoglyceride is composed of a glycerol backbone with a phosphate group and 2 fatty acyl chains. The next major constituent are glycolipids. They are structurally similar to phosphoglycerides, but the phosphate group is replaced with a carbohydrate group. Other types of lipids that can be found in the membrane are diglycosyl diglycerides, acylated sugars and minute amounts of glycerides. A diglycosyl diglyceride consists of a disaccharide bound to the hydroxyl group of a diglyceride. Acylated sugars do not contain a glycerol backbone with fatty acids esterified onto the sugar [76].

2.1.3 Cellular Components

Within the interior of the cell, there are many organelles and elements. For the purpose of this thesis, focus will be placed on DNA, RNA, proteins and enzymes.

The DNA is composed of three parts: an organic base, a phosphate group and a deoxyribose group. The different organic bases (adenine, guanine, thymine, cytosine) determine the type of DNA molecule. The different DNA sequences serves as a template for the construction of the different proteins used in the cell. In bacteria, the DNA molecule is a double helix that forms a closed circle in the cytoplasm [52].

The RNA structure is similar to DNA with the replacement of deoxyribose with a ribose group. Also, instead of a thymine base, uracil is used. RNA molecules are copied from the DNA strand which is then used as a template for protein synthesis. The transcription of the DNA involves the use of RNA polymerases that follow along the DNA strand and add the corresponding RNA base pairs according to the Watson-Crick base pairing system. The polymerase will join the adjacent RNA molecules through the removal of a pyrophosphate group. The product of the transcription process is the messenger RNA (mRNA) which is read by a ribosomal RNA (rRNA) for the translation process. The translation process produces a protein from the mRNA which matches the mRNA sequences to amino acids. The transfer

RNA (tRNA) consists of one end with the amino acid and the other end consisting of a three molecule RNA sequence (codon) that matches with the mRNA, allowing for construction of the protein [52].

Proteins are made up of combination of 20 natural amino acids. They can be used to form suppportive frameworks within the cell and on the cellular wall, where they can form channels [91]. Proteins are sensitive to environmental changes, such as pH, heat and chemicals. This sensitivity is due to the importance of the structure of the protein. The form of the protein is important for functionality, and any changes in structure (denaturation) will cause the loss of functionality.

Enzymes are specialized proteins that are used for catalyzing biochemical reactions. A catalyst will increase the rates of reactions by lowering activation energy. In the case of enzymes, they lower the energy required to transform a substrate to a product by stabilizing the transitional state. The transitional state is the intermediate form of the molecule as it transforms to the end product [28]. Enzymes are important since they can increase the speed of a reaction so that they can occur within the lifetime of bacteria under physiological conditions. There are many types of substrates and enzymes that are used by bacteria. Of note are the enzymes that use proteins as substrates and can degrade proteins. These enzymes are called proteases and can degrade proteins and enzymes [52].

2.2 Cell Permeabilization

Bacteria have been used for the production of many important products. They can be engineered to produce commerical products such as vitamins, hormones, antibiotics and enzymes. Bacteria may not only yield end-products, but can convert them into more valuable products. An example is the production of antibiotics. Bacteria may substitute the acyl group of penicillin with another organic group with a corresponding change in effectiveness or stability [2]. After the product is formed, it must then be recovered and purified for commercial applications. Dealing with the many types of product recovery is beyond the scope of this research and the focus is directed on the recovery or use of enzymes with cell permeabilization.

In the biotechnology field, bacteria can be used to produce large quantities of industrial products. With the fermentation products, there is a need for extraction and purification steps for further commercial and scientific use. The products can be classified into two main categories: extracellular or intracellular. The main difference between the two products is the

process of product recovery. Intracellular products need an extra unit operation to disrupt the cell for the release of the intracellular components [18].

Enzymes are used in a number of industrial processes, such as beer deproteinization, starch degradation and textile treatment [48]. For these treatments, large amounts of enzymes must be produced. The easiest method to obtain enzymes is to produce extracellular enzymes that require a simple recovery process. Even with recombinant technology, not all enzymes can be exported from the cell. There may be a need to recover intracellular enzymes. These enzymes can be isolated from plant or animal matter, but the use of bacteria can be more efficient and the supply more controllable since unlike plants, bacteria can be grown on a year-round basis [48]. There are some technical and economical advantages to using microorganisms over plant and animal cells. Bacteria can be easily modified and grown in large amounts fairly quickly, and the quality of the enzyme can be consistently maintained. Also, the product can be collected on a continuous basis as opposed to the batch processes involved with plant or animal cells [18].

Not all enzymes that are harvested from bacteria are native enzymes found in these specific organisms. There is a large amount of research focussed on genetic engineering to modify organisms to produce a specific enzyme. Organisms like *Escherichia coli* are regularly used and modified to obtain products (other than enzymes) that have pharmaceutical applications such as interferons, antibiotics and vaccines [72]. Figure 2.1 is a schematic of the stages needed for enzyme recovery, dependent on the type of enzyme and techniques used.

2.2.1 Extracellular Enzymes

For extracellular enzyme recovery, enzyme concentration is the critical process [23]. Biotechnology processes are characterized by a very dilute concentration of the product. This product needs to be purified and concentrated, which often represent the bulk of the cost associated with the process.

2.2.1.1 Purification

For this step, gravimetric techniques such as centrifugation or settling are used. Generally, after the cells settle, the supernatant can be removed. Besides gravimetric methods, filtration can be used to remove suspended solids that may not settle. These methods include gel filtration, ultrafiltration and membrane filtration [23]. After the solids have been removed from the broth, the product needs to be concentrated. The main techniques used for concentrating the

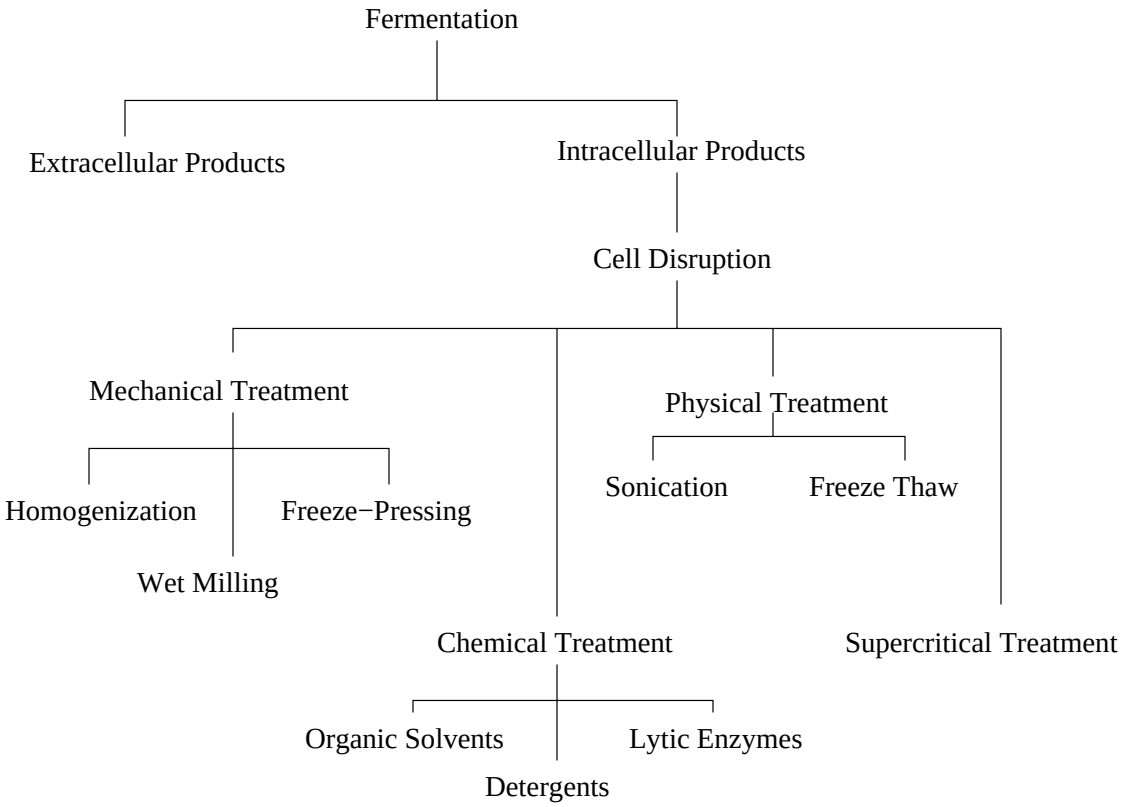

Figure 2.1: Flowchart of enzyme recovery (Adapted from *Fermentation and Enzyme Technology*[89]).

enzymes are precipitation, adsorption, ultra-filtration/reverse osmosis, chromatography, drying and freezing [18].

Precipitation of the enzymes can be done as a continuous process followed by purification using ion-exchange chromatography, affinity chromatography or gel filtration. Precipitation involves bringing the enzymes out of the solution as solid particulates. This is done by changing the nature of the solution so that the enzymes are less soluble. Precipitation may be performed using organic solvents or polyalcohols such as polyethylene glycol. Solid salts can be problematic since they cannot be easily added to obtain a high enough concentration for precipitation [48]. Changes in solubility due to pH adjustment may be used, but may cause deactivation of the

enzymes due to the narrow optimal pH range of most enzymes.

Affinity chromatography can be used to purify enzymes by constructing a matrix onto which the product species adsorb onto the matrix [18]. Antibody molecules are used to coat beads in the chromatography column. The antibodies will bind to a specific antigen so that only proteins containing that antigen will be retained by the column. After the bulk solution has passed through the column, the enzymes can be removed from the beads by passing an acidic solution that will disrupt the antigen-antibody complexes [52].

Another form of chromatography, ion exchange chromatography, can be used to remove the enzymes from the bulk solution. Cation and anion exchange chromatography are used for chromatography. Anion exchangers contain bound positive groups and cation exchangers contain bound negative groups. The bound groups will remove oppositely charged ions out of the bulk solution. In this case, the enzymes are carried by a pH buffered solution to ensure a positive or negative charge [33]. The resin will impede the enzymes differently based on the net charge of the enzyme. Enzymes with charges strongly opposite to that of the resin will be retained, allowing others to pass through with less impediment. The target enzyme can be chosen by modifying the ionic strength of the column. The resin can be collected and the enzymes removed using a strong ionic solution to strip the enzymes from the packing adsorbent [18].

Ultrafiltration can be used to concentrate the enzymes, through the use of selective pore sizes. The membrane can allow only molecules smaller then certain sizes to pass. This allows for fractionation on a molecular weight basis. Depending on the size of the pores, removal of salts and low molecular weight species can be accomplished, allowing the larger enzymes to stay in the solution [18].

Drying and evaporation is another technique that can be used to reduce the total volume of the solution. However, this is not used very often since it can damage the enzymes. An alternative technique is the use of freeze drying for long-term preservation of enzymes [18].

2.2.2 Intracellular Products

Permeabilization techniques have been used in industry for the recovery of intracellular products. These products would not normally be released into the media and require the disruption of the cell wall and membrane. Recombinant DNA proteins, and polyhydroxybutyrate are examples of products of commercial interest which may be recovered through disruption of the cell wall and further purification [34]. In industry, mechanical disruption techniques are generally

used, but other chemical, or physical techniques have also been used. The different techniques will be discussed in Section 2.3.

Intracellular enzymes need to be released from the cell through disruption prior to concentration and purification. Once the cell membrane and cell wall have been weakened or destroyed, the enzymes can extracted from the cell and then processed using fractional purification techniques.

Due to stability problems with enzymes, the environment used to recover the enzymes must be controlled to minimize deactivation. Enzymes are sensitive to pH changes, temperature effects, oxidation of sulphydryl groups and proteolytic action. These problems can be addressed using pH buffers and controlled temperatures during processing. Stability can be enhanced using dilute amounts of organic solvents such as ethanol or acetone. Protection can also be afforded by using metal ions such as calcium and manganese [61].

2.2.2.1 Protein Recovery

Permeabilization will release other cellular components into the media, so that more than the cell debris needs to be removed. Other cellular components such as nucleic acids and proteases need to be removed. The nucleic acids will increase the viscosity of the solution so that the use of nuclease may be required to remove them from the solution. After treatment, centrifugation can be used to remove the larger particles [18]. With recombinant organisms, there is a possibility of inclusion bodies being formed when a certain protein is expressed to a high degree. These inclusion bodies will contain only that protein and are resistant to shear effects, allowing for easier separation from the rest of the cellular debris [5].

The presence of other enzymes and proteins requires that numerous steps be performed to isolate the product of interest. The enzymes can be fractionated according to different protein properties. One of these properties is the enzyme stability. Denaturation of enzymes not of interest can be used to isolate the product. For example, the use of maleate and α-ketoglutarate can stabilize glutamic aspartic transaminase over a wide range of pH and temperatures as high as 75°C. At this temperature, most other enzymes will be denatured, leaving the glutamic asparatic transaminase as the only enzyme in the solution. Another criterion is the use of solubility to selectively salt-out enzymes so that unwanted enzymes can be removed and the product can be isolated [61].

The resulting purification treatments are similar to extracellular product purification, but with some differences. The enzymes that are being recovered generally have less stability than

extracellular enzymes due to the change in the environment. The enzymes are no longer inside a cell with hydrophobic environments that may be required for stability. In addition, to the previously mentioned methods of recovery there is the aqueous two phase separation. In a two phase environment, the enzymes will partition according to physical parameters such as their molecular weight and the surrounding environment (type and concentration of polymers in the solution) [18].

After the products are recovered, care must be taken for storage. Due to the stability problems mentioned in the previous paragraph, intracellular enzymes are more fragile and must be freeze-dried for long term storage. More robust enzymes (extracellular) can be spray or vacuum dried with little chance of denaturation [89].

2.2.3 Biotransformation Systems

A biotransformation system uses cellular machinery, such as enzymes and cofactors to produce a product. When dealing with pure products, purified enzymes are usually preferred as the basis for biotransformation systems since they eliminate side-reactions. However, the cost of using purified enzymes may be prohibitive [93].

An alternative is the use of permeabilized cell systems. In this application, complete disruption of the cell may not be the goal of the treatment. As previously stated, there can be occasions when partial disruption is preferred, eg., when recovering specific products or simplifying the product recovery process and minimizing cellular debris. Cells have a number of interconnected metabolic processes to yield a product and so the use of purified enzymes may be complicated. The enzymes will need to be stabilized requiring immobilization and may need to have cofactor regeneration which can become expensive. Also, with the lack of native cell structures, the products of one enzyme may not find their way to the next enzyme for further processing [25, 47]. In such a system, the cell is rendered non-viable, but the enzyme machinery is kept active. Since the cell is no longer viable, all the energy that is generated can be used for product production, allowing for more efficient use of substrate materials [26]. There are some benefits of such a system over a free enzyme system. With the cellular structure intact, the system is more stable since the structure can protect the enzymes. Another advantage is that the intact system may retain cofactors or that cofactors will be regenerated [25, 32, 26, 56, 12]. The use of permeable cell systems is usually cheaper since there is no cost for purification of the free enzymes. However, there are some disadvantages of using whole cells, including some problems with byproduct formation. Substrate and product transport across the membrane

may also be impeded resulting in diffusion limitations [50].

These type of systems have been studied as replacements for commercial enzymes. An example of such a system is reported by Liu *et al* [50] where recombinant yeast cells were used to overexpress glyoxalase I (GloI), isocitrate lyase (ICL), and β-galactosidase (β-gal). The different yeast cells were permeabilized using ethanol and isopropyl alcohol. For GloI and β-gal, stability in the alcohol solution was not a problem as their activities remained constant during a four hour incubation period. However, ICL showed a dramatic decrease in activity within ten minutes. Enzyme leakage was shown to be minimal for ICL and β-gal which would indicate that they can be used as good systems to replace isolated enzymes, while GloI showed a 50% decrease in activity from the cells over a four hour period [50, 44].

2.3 Cell Permeabilization Treatments

2.3.1 Small Scale

Many of the permeabilization techniques used are appropriate at laboratory scale, but only a few are used at the industrial scale. Three main categories can be identified: mechanical, chemical, and physical. One feature common to these treatments is the period during which the cells are harvested. Cumming *et al.* [16] have determined that the growth phase of the organism is important in obtaining an optimal release of enzymes. When comparing different treatments (ball milling, sonication and autolysis), the results have consistently shown that for *Bacillus amyloliquefaciens*, harvesting during the log phase of growth resulted in greater product recovery [16].

2.3.1.1 Mechanical Treatment

One of the potential problems with all the mechanical treatments is the deactivation of the enzymes. The shear forces needed to disrupt the cell membrane may also affect the enzymes. There are reports that the sensitivity to shear effects depends on the type of enzyme involved, i.e. globular enzymes seem to be insensitive to shear inactivation. The inactivation is due mainly to oxidation or denaturation at the air-liquid interfaces. One approach to minimize denaturation is to eliminate foaming and decrease the air-liquid interfacial area [5].

The most common method of cell disruption is the use of high pressure homogenization [45, 24, 13, 57]. A high pressure pump is used to compress the cell suspension in a tubular

reactor. A valve is allowed to open which causes the cell suspension to flow out of the tubing and impinge onto the impact ring. The forces of turbulence, cavitation, and liquid shear all play roles in disruption of the cells. With this process, there is no opportunity to target the recovery of periplasmic enzymes over cytoplasmic enzymes. Consequently, this method is non-selective and all enzymes will be released from the cell. While this method is generally suitable for most applications, it should not be used with highly filamentous microorganisms due to possible blocking of the homogenizing valve [89]. Also, this method is not very effective with organisms that have thick cell walls.

There are a few important parameters that can be used to optimize the process [45]. The first parameter is the pressure of the system. An increase in pressure has been shown to increase protein solubilization. However, a pressure increase will also increase the temperature of the system which may degrade the enzyme. The pressure increase requires that more energy be applied to the system. Once the optimum pressure level has been reached, the energy is no longer completely directed to cell disruption, but some is converted into heat and causes an increase in temperature [9]. The other parameter is the design of the homogenizer valve. There are two main types: a flat unit and a knife-edge unit and the difference in effectiveness depends on the pressure. At low pressures, recovery of enzymes is similar with both types of valves, but at higher pressures, a higher recovery is obtained when using the knife-edge valve. A change in the geometry of the orifice will also change the efficiency of cell disruption. In general, a decrease in bore size and impact distance will increase disruption efficiency [58]. The kinetics of cell disintegration can be described by the following first-order equation [45, 36]:

$$ln(\frac{R_m}{R_m - R}) = k * N * p^a \tag{2.1}$$

where R_m is the maximal obtainable protein mass per cell mass (mg/g), R is the mass of protein released per cell mass (mg/g), k is a dimensional constant, N is the number of passes, p is the pressure and a is an exponent dependent on the cell culture.

Another common technique is the use of wet milling. A wet mill is a horizontal chamber in which the cell suspension (with glass beads) is passed along an agitator shaft with impellers to disrupt the cells. Cell disruption is due to the high shear forces that act upon the cells as they pass through the milling chamber [45, 24, 13]. There are many operating parameters for wet milling, of which the most important are agitator speed, design of the stirrer and the geometry of the grinding chamber, feed rate of suspension, size of beads, packing density of beads and

temperature [45]. The agitation speed will affect the amount of energy used for cell disruption. When adjusting the speed of agitator rotation from 700-1100 rev/min, a corresponding increase in released enzymes has been found, but when the rotation was increased to 1400 rev/min, only a marginal increase was found with the excess energy being converted to heat [74]. While the outside construction of the chamber may be similar, differences with the internal agitator design affect the residence time of the cells. There is an inverse relationship between feed rate and percentage of cells disrupted. When changing the flow rate from 40-400 L/hr, a decrease of the cellular disintegration was found, with a slight decrease in the enzymatic activity of D-glucose-6-phosphate and α-D-glucoside glucohydrolase [74]. This relationship depends on the organism being treated, but it is generally advised to have a high flowrate with multiple passes through the mill. The optimum size of beads depends on the size of the organism being disrupted or the location of the products within the cell. Glass beads with diameters greater than 0.5 mm are ideal for yeast cells, while bacterial cells are more effectively disrupted using beads with diameters less than 0.5 mm. When trying to isolate periplasmic products, larger beads enrich their recovery. Cytoplasmic enzymes, such as glucose-6-phosphate dehydrognase, have a maximal activity when treated with 0.7 mm diameter glass beads, while periplasmic enzymes such as glucosidase, show an increase of activity when glass beads with diameters of up to 1.0 mm are used [74]. The temperature of the mill has an effect on the recovery of the enzymes. An increase of temperature from 5-20°C shows a decrease of 2% yield, but an increase to 40°C shows an 18% decrease of recovered enzymes. It is important that the temperature of the mill be maintained at a level less than 20°C [49]. The ideal volume of glass beads occupying the free space of the chamber is between 80%-90%. With less than 80%, the cell disruption is inefficient, while at loadings greater than 90%, heating becomes a problem and there is an increase in power consumption. Equation (2.2) relates the relationship between the recovered enzymes and time used to disrupt the cells [45]:

$$ln(\frac{R_m}{R_m - R}) = k * t \tag{2.2}$$

where R_m is the maximal obtainable protein yield per cell mass (mg/g), R is the protein released per cell mass (mg/g), k is a dimensional constant and t is the time.

Freeze-pressing of cell suspensions is another method for cell disruption. A Hughes press forces the cell suspension through a narrow slit or orifice with abrasives at 0°C or without abrasives at -25°C at high pressures. This treatment method leaves the cell wall relatively

intact and can be used for isolation of membrane-associated enzymes [13]. The disruption mechanism can be attributed to abrasion by ice crystals or changes in ice crystal states. The main factor influencing the protein recovery is the pressure. An increase in pressure will cause both an increase in protein recovery and temperature. The only concern with this method is the low temperature required for cells to remain frozen [9]. This method is effective for a variety of different cell types and has the advantages of biological activity retention and fewer cell fragments. However, this method cannot be used to isolate enzymes since the low temperature will denature enzymes [24].

2.3.1.2 Chemical Treatments

Organic solvents can be used to solubilize the cell envelope causing permeabilization [34]. Since this will not completely remove the cell membrane, only some of the enzymes will be released, allowing for selectivity of the product. This occurs since only certain cellular components (phospholipids) may be solubilized [22]. This allows for selection based on location, eg., cytoplasmic versus periplasmic products, or size, eg., enzymes versus nucleic acids. There is a danger of long-term exposure to organic solvents since deactivation of the enzymes may occur.

Another chemical method is the use of detergents for cell disruption. Commonly used detergents include sodium dodecyl sulphate (SDS), cetyltrimethyl ammonium bromide (CTAB), Tween and Triton X100. The use of detergents will cause disorganization of the cell membrane [22]. The detergents can partially solubilize the cell membrane and extract the membrane-bound enzymes. This technique has the advantage of producing an enzyme-rich solution with small amounts of non-catalytic protein and simplifying purification. However, biological activity may be lost due to the relatively high concentrations of detergent that are required [22]. Ionic detergents such as SDS and CTAB can cause deactivation of the enzyme due to their reactivity [18]. However, there are certain situations where SDS and CTAB may not inactivate the enzymes. SDS will normally weaken hydrophobic bonds and cause denaturation of the enzymes in the cell. However, manganous cations seem to stabilize enzymes and counteract the effects of SDS at low concentrations [67]. CTAB has also been shown to be useful for permeabilizing *Z. mobilis* and retaining enzymatic activity under certain conditions [68]. Triton X-100 will cause channel formation in the membrane, allowing cations to pass across the membrane. The Triton molecules may assemble as a tunnel-like channel across the membrane, or form micelles that can carry the ions across the membrane [73]. The use of Triton X-100 will yield a solution that does not allow all the cellular constituents to leave the cell. This makes further purification

easier and reduces the cost and time required for the isolation stages. With an increase of Triton X-100 concentration, there is a corresponding increase in protein released. The cell structure is kept intact, so there is a selective release of protein and a retention of DNA in the cell. Compared to mechanical methods half the amount of protein is recovered; however, there is little RNA or DNA released. As with other chemicals, excessively high concentrations of detergents may cause deactivation of the enzymes. Consequently, these chemicals need to be removed from the solution early in the purification stages [37].

Enzymes can be used as a method to permeabilize cells. Lytic enzymes can be used to digest the cell wall, weaken or causing its disruption [79]. The most commonly used enzyme is lysozyme that cleaves the β(1-4) linkage between the N-acetyl-muramic acid peptide and N-acetyl-glucosamine in the cell wall [22]. Lysozyme treatment is useful for a limited number of cells due its action on the specific β(1-4) linkage, but its low temperature conditions help preserve the biological activity of the product [24]. Lytic enzymes can target the release of a desired product based on product size since only a limited degradation of the wall may be required for product recovery [17]. Depending on the organism, additional treatment, such as freeze-thaw or EDTA, may be required to uncover the sites for lysozyme activity. The cost of lytic enzymes is very high, limiting their use as an industrial method. While enzyme treatment may not be appropriate as the sole method of disruption, pretreatment of the cells with lytic enzymes can weaken the cell walls. With a weaker cell wall, lower energy requirements using mechanical methods are needed [3]. One consideration with enzyme pretreatment is that the enzyme may interfere with the purification steps or affect the product so that the appropriate lytic enzyme must be carefully chosen [18]. If recovery of the lysozyme is desired, recovery may be simplified by immobilizing the enzyme and using ultrafiltration to collect the enzyme adsorbed onto its carrier [89].

2.3.1.3 Physical Treatments

Sonication is another technique that has been used to disrupt cells [24, 34]. The mechanism of sonication can be attributed to the formation of vapour cavities. These cavities are formed by the reduction in pressure that occurs due to the ultrasonic vibrations. When the cavities collapse, they will produce shock waves that cause shear stress and disrupt the cells. Microstreaming along the cavity surface may generate velocity gradients that can disrupt the cells. The laminar streaming caused by the cavitation of the cavities can cause the degradation of DNA and disintegration of yeast cells. During the collapse of the vapour cavities, sonic en-

ergy is released as mechanical force on the magnitude of 10^6 atm. The relationship between the power input (P) and volume fraction of cells disintegrated (F_v) is presented in Equation (2.3).

$$F_v(P) = 1 - exp\{-[(P - P_0)/\alpha_1]^{\beta}\} \tag{2.3}$$

where P_0 is the cavitation threshold power, α_1 is a constant with power dimensions, and β is dependent on the relationship between electrical power input and the dimension of the largest stable cell.

With subsequent derivations, the relationship between protein release (S_p) and time (T) can be expressed as terms given in Equation (2.4) [20].

$$1 - S_p = exp\{-[(P - P_0)/\alpha_4]^{\beta_3} T\} \tag{2.4}$$

where β_3 is 0.895, and α_4 is derived from intermediatary equations that involve values of α_1, α_2, α_3, β_1, and β_2.

The increase of power input will reach a sufficient force to disrupt the intermolecular cohesive forces and cause the cell structure to be disrupted [34]. This technique is not commonly used since it can cause degradation of enzymes. This occurs as oxidative free radicals are formed which then act upon enzymes, causing deactivation [22].

Cells may be subjected to extreme environments which cause disruption. One of the earliest methods of cell disruption was the use of freeze/thaw cycles. Cycles of freezing and thawing will cause the cells to rupture due to the formation of expanding ice crystals [24]. Researchers have determined that the rate of freezing has an effect on the effectiveness of the treatment. Use of a slow freezing cycle allows the formation of larger ice crystals which will cause more damage to the cells [79]. The different rates will also affect the type of enzymes released from the cell. Rapidly frozen samples (rate of 200°C/min) show considerable damage to the cytoplasmic membrane. This allows more cytoplasmic enzymes and components to be recovered from the cell. Slowly frozen cells (rate of 30°C/min) show little recovery of cytoplasmic markers, but an increase of released periplasmic markers [82]. This procedure has shown that even with repeated treatments, low yields are obtained. There is also a problem with possible deactivation of biological components due to the freezing of the cells. This procedure may not effectively disrupt the cell membrane since effectiveness depends on the membrane structure of the bacterium. However, this approach can be used as a technique to pre-treat the cells and weaken them for further treatment [18]. This method does have the advantage of being usable

with sealed pathogenic microorganisms so that the cells can be treated without exposure to the environment [89].

2.3.1.4 Supercritical fluids

A supercritical fluid is a fluid that is above its critical temperature and critical pressure. At this point, it cannot be liquefied because the molecular thermal energies exceed the attractive forces between the molecules. A fluid in a supercritical state has properties between that of a gas and that of a liquid. Its density may approach its density at liquid state, but will retain the viscosity and diffusion properties of a gas [39]. Supercritical fluids have been of interest in industry because of certain advantages. Supercritical extraction is a more energy efficient process than the usual conventional processes and can be used to simplify the separation process. When a solvent is in a supercritical state, its solvation properties can be readily adjusted by changing the temperature and pressure of the system. This allows for easier fractionation and purification of products [14, 39, 1]. The most commonly used supercritical fluid is carbon dioxide. Carbon dioxide is a nontoxic, nonflammable and cheap solvent whose low critical temperature (31.1°C) and pressure (73 atm) [65] make it an ideal medium for processing volatile products such as essential oils from plants [30].

Due to its low critical temperature, carbon dioxide is ideal for biological processing since cellular components will not undergo thermal degradation. When placed in a supercritical medium, enzymes are more thermostable than in aqueous environments. This feature has been used to increase lipase activity relative to aqueous environments [6, 7, 11]. Due to the lack of enzyme deactivation, it seems that supercritical exposure would not damage active enzymes if they were to be extracted from the cells. There have been studies where deactivation is hypothesized to occur during the depressurization stages of the supercritical exposure; however, it seems that this may be avoided with a gradual pressure reduction [95, 55].

Previous research indicates that the use of supercritical carbon dioxide affects the cell viability. Research on continuous supercritical carbon dioxide extraction of ethanol from a fermentation broth shows that phospholipids from the cells may also be extracted. Another effect that may occur is cell rupture, causing the death of the organism [86]. This effect allows for sterilization and recovery of intracellular products in one process [87].

Supercritical CO_2 has been used to extract lipids from algae (*Skeletonema costatum*, and *Ochromonas danica*). The lipids of interest were omega-3 fatty acids which have practical health benefits. Polak *et al* [66] were able to extract and recover about 50% of the total lipids

from the organism. Since supercritical CO_2 can extract lipids from cells, it is conceivable that supercritical CO_2 treatment will permeabilize the cells.

2.3.1.5 Comparisons between the permeabilization methods

Table 2.1 highlights some of the disadvantages and advantages of the previously discussed permeabilization methods. The table also indicates whether the technique can be used to create biotransformation systems in addition to releasing products.

Table 2.1: Summary of small scale cell disruption techniques

Type	Name	Advantages	Disadvantages	Bio System	Reference
Mechanical	Homogenization	Quick and simple High recovery	Heat problems Non-selective Cell debris	No	[45, 24, 13] [57, 9]
	Wet Milling	Quick and simple High recovery Selective	Heat problems Cell debris	No	[45, 24, 13] [74, 49]
	Freeze-Pressing	Quick and simple High recovery	Low temperature	No	[13, 9, 24]
Chemical	Organic Solvents	Selective Little cell debris	Use of solvent Low recovery	Yes	[34]
	Detergents	Selective	Denaturation Low recovery	Yes	[22, 18, 68]
	Lytic Enzymes	Little cell debris	Expensive Not always effective Low recovery	Yes	[79, 24, 22] [3, 18]
Physical	Sonication	High recovery	Cell debris Denaturation	No	[24, 34]
	Freeze Thaw	Quick and simple Selective	Low recovery Not always effective	No	[24, 79, 82]
Supercritical	Supercritical	Little cell debris Selective	Low recovery Capital costs	Yes	

2.3.2 Large Scale

2.3.2.1 Methods Used in Industry

Scale-up from laboratory scale to industrial scale may pose a few problems. The batch process may take longer to perform than on a lab scale due to the amount of material being processed. This also leads to a problem of maintaining a consistant environment since organisms and enzymes are sensitive to pH changes. It is difficult to maintain large tanks of media at a set pH. When acid or base is added to maintain the pH, high local concentrations of acids or bases may develop, causing deactivation of enzymes in those regions. Due to these problems of batch operations, the use of continuous fermentation is preferred. Since many of the cell disruption techniques are batch methods, only a few are usable on an industrial scale [48].

On an industrial scale, the main methods are mechanical including high pressure homogenization, wet milling and freeze pressing [57]. Most of the mechanical methods are energy intensive and generate heat. The generation of excessive heat may damage the protein products so cooling is needed to maintain a relatively low temperature [35]. The mechanical methods are high in capital and operating costs [24]. These factors encourage research for alternative industrial treatments. Harrison *et al.* [35] have shown that chemical or lysozyme pretreatment can weaken the cell wall sufficiently to decrease the amount of mechanical energy required. This allows for operation at lower pressures or fewer passes with the homogenizer. This reduces cell micronization which alleviates some of the possible problems during of the purification stage. With 45% of the equipment costs attributed to product recovery, decreasing its complexity will save money [34].

Autolysis is another treatment option related to lytic digestion that has been used in industry. Autolysis has been used for disruption of yeast cells [17]. This involves inducing the formation of lytic enzymes which will attack the beta-glucan component of the cell wall. The inducing agent can be aging, increased temperature, or the addition of organic solvents.

2.4 Model Systems

2.4.1 *Zymomonas mobilis*

Zymomonas mobilis is a gram-negative obligately fermentative bacterium. It is unique in that its sole source of energy production is the Entner-Doudoroff pathway to form adenosine triphosphate (ATP). This mechanism is inefficient, yielding one molecule of ATP for every molecule

of sugar consumed. To compensate for the low efficiency, the bacterium metabolizes glucose quickly and consumes up to one third of its mass of glucose per minute [63].

2.4.1.1 Industrial Use

Zymomonas mobilis is of industrial interest for two reasons. The first is its use in the production of ethanol for a biofuel. *Z. mobilis* has a number of advantages over yeast for ethanol production. *Z. mobilis* produces ethanol with a 98% efficiency at a rate twice as fast as yeast [62], resulting in higher yields and higher specific ethanol productivity [41, 40]. The increased efficiency leads to lower biomass production since most of the substrate is converted to ethanol. *Z. mobilis* has a tolerance for high ethanol levels, allowing a higher concentrations of ethanol to be produced before the bacteria are affected. The high tolerance to ethanol is due to the differences in the membrane composition that maintain cell viability [8]. In addition, there is no need for controlled oxygen addition during the fermentation and *Z. mobilis* can be genetically manipulated. Some disadvantages include its low salt tolerance and the fact that its carbon source metabolism is limited to glucose, fructose and sucrose [31].

The second area of research centers around the production of sorbitol. Sorbitol is industrially produced through glucose hydrogenation with a nickel catalyst at temperatures of 140-150°C and pressures of 40-50 atm [15, 21]. Sorbitol is an important commodity product that is valuable in the cosmetic, pharmaceutical, food and chemical industries [21]. Besides its use as an artifical sweetener, it can be used to preserve freshness [70]. Sorbitol also has use as a precursor to the synthesis of ascorbic acid (vitamin C). The D-sorbitol that is produced from *Z. mobilis* can be used by *Gluconobacter suboxydans* to produce L-sorbose.

In nature, *Z. mobilis* produces sorbitol as an osmoprotectant so that it may survive in environments with high sugar concentrations [53, 90]. This conversion is irreversible and *Z. mobilis* cannot be grown on a sorbitol-only media [94, 4]. When the cell is permeabilized, sorbitol production will occur with very little ethanol being produced [15, 53, 69, 80]. In a permeabilized cell system, the required cofactors for the Entner-Doudoroff pathway are removed from the cell so no ethanol production occurs and sorbitol will accumulate [38].

Both ethanol and sorbitol production occur due to the action of the enzyme glucose fructose oxidoreductase (GFOR) that converts glucose and fructose to sorbitol and gluconic acid [29]. The use of glucose and fructose as substrates is the preferred option since the sorbitol yield with sucrose-only media is much lower and production of levan as a side reaction is minimized. The yield of ethanol is unchanged when only sucrose is used [4].

2.4.1.2 Comparison of Cell Treatments

A microorganism can be characterized by its lipid composition. A lipid fingerprint can be used to differentiate one bacterium from another [76]. Analysis of the lipid composition of *Z. mobilis* shows that vaccenic acid (cis-11-octadecenoic acid) constitutes over 70% of the acyl chains contained in the cell. The remaining fatty acids are mostly myristic, palmitic and palmitoleic acids with trace amounts of other miscellaneous fatty acids [10]. *Z. mobilis* shows very little change in lipid composition when exposed to ethanol and different glucose concentrations. It is hypothesized that the high amount of vaccenic acid in the cell membrane helps *Z. mobilis* withstand the presence of high concentrations of ethanol [10].

The sorbitol production capabilities of *Z. mobilis* are well-known, but the enzyme responsible for the conversion was only isolated in 1986 [94]. The GFOR enzyme (E.C. 1.1.99.28) is a periplasmic enzyme that constitutes up to 1% of the soluble protein of *Z. mobilis*. GFOR is a tetramer with identical 40 kDa subunits with a bound NADP buried in the protein-subunit interior [38, 43, 53, 90, 54]. The activity of GFOR is optimal at a pH of 6.2 and has a high specificity for fructose and glucose, but low affinity for either substrates. Other sugars, such as D-mannose and D-xylose can be used as a glucose substitute and D-xylulose and dihydroxyacetone for fructose, but their relative activities are very low and require concentrations greater than one molar [94]. The NADP cofactor is regenerated through the oxidation of glucose and reduction of fructose. The enzyme is assembled with the NADP cofactor in the cytoplasm and then exported to the periplasm [90]. While the mechanism of the enzyme is unclear, it is known that it functions using a ping-pong mechanism with one substrate (glucose) catalyzed to yield a product (glucono-δ-lactone), before the other (fructose) can bind and form sorbitol [29, 43]. The glucono-δ-lactone is rapidly converted to gluconic acid, which enters the Entner-Doudoroff pathway and is converted to ethanol. Figure 2.2 shows the catalyzed reaction.

The cytoplasmic enzyme glucose-6-phosphate dehydrogenase (G-6-PDH) (EC 1.1.1.49) is a tetramer of four 52 kDa subunits. G-6-PDH will convert NAD^+ or $NADP^+$ to their respective reduced form. The optimal pH for this process is 8.0 [75]. Figure 2.3 shows the catalyzed reaction.

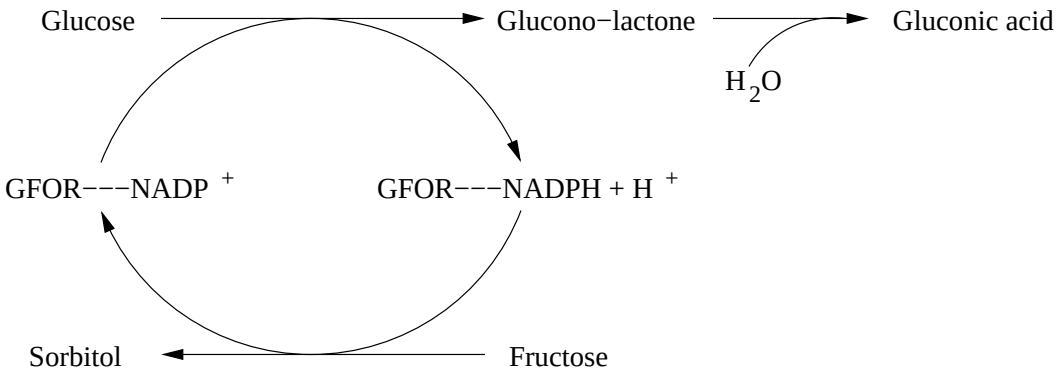

Figure 2.2: GFOR enzyme system [80]

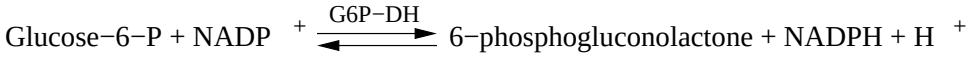

Figure 2.3: G-6-PDH enzyme system [19]

2.4.2 *Escherichia coli*

2.4.2.1 Industrial Use

Due to the ease of manipulating *E. coli*'s genes, there has been a lot of research directed towards producing pharmaceutical products based on recombinant DNA with *E. coli* as the host [88, 78, 46]. The first pharmaceutically approved recombinant product from *E. coli* was human insulin in 1984. *E. coli* has since been used extensively for pharmaceutical purposes [83]. Recombinant *E. coli* have been used to produce various products, including D-amino acids used for production of semi-synthetic antibiotics such as amoxicillin, cefadroxil, cefatrizinen, cefaparole and cefaperazon [93]. Other commercial uses involve recombinant enzymes for washing detergents [51].

2.4.2.2 Green Fluorescent Protein

Green fluorescent protein (GFP) was first isolated from *Aequorea* jellyfish and has been cloned into other organisms. GFP can be used in biological applications as a tag or indicator of

recombinant gene expression. Adding the gene sequence of GFP near the recombinant gene of interest will give an indication of incorporation into the genome when fluoresence is detected. Another option is to add the GFP sequence to the gene of interest, rendering the protein of interest fluorescent and able to act with little impediment due to the presence of the GFP. GFP can also be made an active indicator if its sequence is modified. By making the chromophore sensitive to pH or environmental changes, the fluorescence will be altered thereby indicating a change in the environment [85]. This feature can be useful for determining pH gradients within cells revealing signal pathways based on H^+ concentrations [59]. GFP can be used as a surface cell marker to determine surface properties. This can be useful when determining protein markers for antigen identification [77].

Chapter 3

Materials and Methods

3.1 Source of materials

3.1.1 Chemical sources

All the chemicals were of reagent grade unless otherwise stated.

Aldrich Chemical Company (Oakville, Ontario): Ammonium sulfate, Calcium proprionate, Myristic acid, Pentadecanoic acid
Anachemia (Toronto, Ontario): Agar powder
Bio-Rad (Mississauga, Ontario): Bromophenol blue, Coomassie blue R-250, Sodium dodecyl sulfate (SDS), Tris(hydroxymethyl) methylamine (Tris)
BDH (Toronto, Ontario): Glycerol, Hydrochloric acid, Sodium chloride, Sulfuric acid, Toluene
Difco Laboratories (Detroit, Michigan): Yeast extract
EM Science (Gibbstown, New Jersey): Hexane, Methanol, Methyl t-butyl ether (MTBE)
Fisher Scientific Company (Nepean, Ontario): Acetic acid, Bovine Serum Albumin (Fract V) (BSA), Isopropyl β-D-thiogalactoside (IPTG), Luria-Bertani (LB) Broth, Potassium phosphate monobasic
Fluka (Toronto, Ontario): Sorbitol
Mallinckrodt (Pointe-Claire, Quebec): Magnesium sulfate 7 hydrate
Manville (Denver, Colorado): Celite R-633
Pierce (Rockford, Illinois): BCA protein assay reagents
Praxair (Paris, Ontario): Carbon dioxide (research and supercritical extraction grade)

Sigma (Oakville, Ontario): 30% Brij-35, Fructose, Gluconic acid, Glucose, Glucose-6-phosphate, Glutaraldehyde, Glycine, Kanamycin, Magnesium chloride, β-Mercaptoethanol, (2-[N-Morpholino]ethane sulfonic acid (MES), β-Nicotinamide adenine dinucleotide phosphate (NADP), Sodium hydroxide, Triton X-100
W.A. Hammond Drierite Company (Xenia Ohio): Anhydrous $CaSO_4$

3.1.2 Cell sources

Two microorganisms were studied for the research. *Zymomonas mobilis* (ATCC 29191) and *Escherichia coli* (ATCC 87452) were obtained from American Type Culture Collection (ATCC) (Manassa, VA). The *E. coli* contained the p519gfp plasmid, with a *lac* promoter for green fluorescent protein. The production of active GFP is promoted by the inducer IPTG.

3.2 Preparative Methods

3.2.1 Preparation of *Zymomonas mobilis* Cells

The *Zymomonas mobilis* cells were stored at 4°C. The cells were subcultured on 3 month intervals. The growth medium detailed in Table 3.1 was prepared as described by Chun and Rogers [15] except 50 g/L glucose instead of 100 g/L was used. For subculturing, 10 mL of growth medium was placed in screw-top test tubes. For innoculum growth, 100 mL of medium was measured into 250 mL flasks. The growth medium was autoclaved for a cycle of 15 min of sterilization at a temperature of 120°C and 1.5 atmosphere and 15 min of depressurization to room temperature. The medium was then cooled to room temperature before use or stored at 4°C.

Transfer of cultured cells into subculture tubes or into innoculum flasks was performed using aseptic techniques in a laminar flowhood. For subculturing purposes, 0.5 mL of culture solution was transfered into the new test tubes containing 10 mL of growth medium. For innoculation of the flasks, all of the culture was poured into the flasks.

The innoculum flasks or subcultured tubes were then incubated at 30°C without agitation. The cells were harvested during the logarithmic growth phase (t=20 hours). The subculture tubes were then stored at 4°C for future use. The 10 mL of the innoculum flask was used to innoculate another 100 mL of medium to yield a total of ten fresh flasks. After 20 hours of incubation, the ten flasks were combined and separated into four samples and subjected to the

separate treatments.

Table 3.1: Solutions used for *Zymomonas mobilis* growth

Solution	Chemical	Concentration
Growth Medium	Glucose	50 g/L
	Yeast extract	5 g/L
	Potassium phosphate monobasic	1 g/L
	Magnesium sulfate 7 hydrate	1 g/L
	Ammonium sulfate	1 g/L
MES Buffer	MES adjust to pH 6.2 (NaOH)	0.05 M

3.2.2 Preparation of *Escherichia coli* Cells

The growth medium and other solutions were prepared in concentrations as detailed in Table 3.2. For the medium, LB base was added to 100 mL of water. For the agar plates, the LB broth solution was heated to dissolve the agar. The liquid and agar media were autoclaved at 120°C and 1.5 atm for 30 min.

The kanamycin was prepared in deionized water and then filter sterilized using sterile 0.20 μm Acrodisc syringe filters (Gelman Sciences, Inc., Toronto, Ontario). After the media had cooled sufficiently, the kanamycin was added. The agar medium was poured into petri dishes and allowed to solidify before storage at 4°C. If the liquid medium was not immediately used, it was also stored at 4°C.

Stock *E. coli* stored at -20°C was used to streak the agar plates and incubated at 37°C for 16 hours. A colony from the agar plate was used to innoculate 100 mL of liquid medium and then incubated at 37°C and 100 rpm in a Lab-line Orbit Environ-Shaker for 20 hours. The liquid medium was used to innoculate another flask to yield a 1% innoculum concentration. After 3 hours of incubation under the same conditions, IPTG solution (sterilized using the aforementioned syringe filters) was added.

Table 3.2: Solutions used for *Escherichia coli* growth

Solution	Chemical	Concentration
Growth Medium	LB broth base	25 g/L
	Kanamycin	50 μg/mL
	IPTG (induce after 3 hours of growth)	1 mM
Agar Plate	LB broth base	25 g/L
	Kanamycin	50 μg/mL
	Agar	1.5%
Kanamycin stock	Kanamycin	50 mg/mL
IPTG stock	IPTG	0.1 M

3.2.3 Determination of Biomass Concentrations

A sample of the culture was removed and the absorbance was measured using a Genesys Spectrophotometer 5 at 500 nm and 550 nm. The absorbance was compared to a standard curve of absorbance and *Zymomonas mobilis* dry cell weight. The curve was created by harvesting cells at different times of growth, i.e. 2, 4, or 6 hours of incubation and determining their absorbance. The media solution was filtered using dry pre-weighted filter membrane which was dried overnight at 110°C. The membrane was equilibrated in a dessicator prior to being weighed.

3.2.4 Cell Harvesting

After the biomass concentration was determined, the remaining sample was centrifuged to remove the whole cells. A Beckman type 16 rotor was used in a Beckman L7 Ultracentrifuge at 4000 rpm (1550 x g) for a duration of 15 min. The media was decanted from a 250 mL centrifuge bottle and 30 mL cold MES buffer was added to resuspend the cells. The solution was centrifuged again under the same conditions and then the buffer was decanted. The remaining pellet of whole cells was used as described in the cell treatment section.

3.3 Cell Treatment

3.3.1 Control Cells (No treatment)

Cold 0.05M MES buffer solution (4 mL) (Table 3.1) was added to the recovered cell pellet (approx. 100 mg dry weight). The solution was vortexed to suspend the cells. The solution was placed in 30 mL Corex centrifuge tubes and centrifuged. A IEC HN-S Centrifuge with a catalogue number 801 was used for 11 min at 3500 rpm (1480 x g). The supernatant was collected in 7 mL glass scintillation vials and stored at -20°C. The resuspension and centrifugation steps were repeated twice to obtain three wash samples for protein and enzyme analyses.

3.3.2 Cell Permeabilization using Toluene

The cells were resuspended in 27 mL of 0.05 M MES buffer(Table 3.1) and 3 mL of toluene was added. The solution was cooled in an ice bath and magnetically stirred for 13 minutes. After the treatment, the solution was separated into glass centrifuge tubes and placed in a IEC HN-S Centrifuge (rotor: catalogue no. 801) for 11 min at 3500 rpm (1480 x g). The resulting cell pellet was then washed three times with the MES buffer using the same wash treatment as the untreated cells.

3.3.3 Cell Permeabilization using Supercritical Carbon Dioxide

The supercritical reactor was custom-made by Parr Instrument Company (Moline, Illinois), based on model 4766 (300 mL, 2.5 in inside diameter, 4.0 in inside depth). Two quartz windows were added to the reactor for verification of the supercritical state. An aluminum stand was constructed to support the cells in the reactor. A magnetic stir bar was used to agitate the reactor contents. The cells were spread on a Nytex cloth (200 μm mesh size) (B. & S.H. Thompson, Scarborough, ON). and supported in the reactor on the stand. A schematic is shown in Figure 3.1.

Three cycles of pressurization and depressurization with research grade carbon dioxide (Praxair, Paris, ON) were performed to purge the reactor; the pressure was brought to 180 psi and then reduced to 10 psi. Meanwhile, heating tape was used to bring the internal temperature of the reactor to 36°C. After the last evacuation, extraction grade liquid carbon dioxide was used to gradually (over a period of 10 min) bring the system to 1100 psi. The reactor was observed through the quartz windows to watch the change of state. The subcritical state was reached when the suspension became cloudy and opaque. When the reactor contents cleared and showed a mirage effect described by Tang *et al.* [84], the supercritical state of carbon dioxide was verified. The exposure time was 2 hours with a final operating pressure of 1260 psi. After the 2 hours, the system was gradually depressurized over a period of 10 min.

The recovered cells were then removed from the Nytex cloth and washed three times using the same procedure as described for the control cells.

3.3.4 Cell Permeabilization using Freeze/Thaw Cycles

The recovered cells were treated with three cycles of freezing at -20°C and thawing at room temperature (24°C). The duration of a cycle was a total of 24 hours. After the last thaw stage, the cells were washed three times with MES buffer using the same procedure as for the control cells.

3.3.5 Crosslinking of Cells using Glutaraldehyde

After permeabilization treatment, the cells were suspended in 48 mL of 0.05 M MES buffer (Table 3.1) and 2 mL of glutaraldehyde (25% aqueous stock solution). The mixture was stirred for 30 min on ice. The mixture was then centrifuged for 11 min in the IEC HN-S Centrifuge (1400 x g). The resulting pellet was then suspended with 0.05 M MES buffer (Table 3.1) and centrifuged in the IEC HN-S Centrifuge for 11 min at 3500 rpm (1400 x g).

3.3.6 Immobilization of Cells onto Celite

Celite R-633 (2.5 g) was spread out on a petri dish to which 2.5 mL of deionized water was added to ensure prewetting and easier adsorption of cells onto the Celite. The dry cells were rehydrated in 2.5 mL of deionized water and spread throughout the petri dish. The dish was then placed in a Lab-line Orbit Environ-Shaker at 37°C and 17% humidity at 100 rpm. The targeted total water content was 20-25% by total weight. A small sample was removed and

placed in a watch glass for moisture determination. The sample was then placed overnight in an oven at 110°C to remove all water and to verify the water content of the cells.

3.3.7 Supercritical Carbon Dioxide as a Reaction Medium

A sample of cells was placed on the Nytex cloth with 0.6 g of glucose and an equal amount of fructose. The cloth was then placed in the supercritical reactor and exposed to supercritical condition for a period of 24 hours and then depressurized. Thereafter, the cloth was placed in 50 mL MES buffer to extract the sugar. The buffer solution was then analyzed with HPLC for sugar quantification.

3.4 Analytical Methods

3.4.1 Scanning Electron Microscopy (SEM) Preparation

The cells were suspended in deionized water, spread out on a petri dish and then placed in a Lab-line Orbit Environ-Shaker for drying. The dish was stored overnight in a dessicator (with anhydrous $CaSO_4$) for further analysis using scanning electron microscopy (SEM). The samples were placed on studs and sputter-coated with gold using a Polaron Sputter Unit (P53). After the coating, the studs were viewed in a Hitachi S-570 SEM to obtain micrographs of the cell surfaces.

3.4.2 BCA Assay

BCA reagent solution of reagents A and B was made in a 50:1 ratio. Samples (100 μL) of the cell washes from the treatments were added to 2 mL of the BCA solution. The resulting mixture was incubated for 30 min at 37°C. After incubation, the absorbance of the solution was determined at a wavelength of 562 nm in a spectrophotometer. A calibration curve was constructed using BSA as the standard protein, over a concentration range from 0 to 2.0 g/L.

3.4.3 Glucose-6-Phosphate Dehydrogenase Assay

A spectrophotometric assay for G-6-P as described by Deutsch [19] was used to determine dehydrogenase activity. A 0.02 mL sample of the wash was added to 1.0 mL of the assay solution (Table 3.3). The absorbance of the solution (at 339 nm) was observed for a period of 11 minutes to monitor NADPH formation. The specific activity was determined using Equation(3.1) [19].

$$Specific\ activity = \frac{8095 * \Delta A}{\Delta t * c}, \tag{3.1}$$

where ΔA is the change in absorbance, Δt is the change in time and c is the protein concentration in g/L.

Table 3.3: G-6-P Dehydrogenase Assay Solutions

Solution	Chemical	Amount
NADP solution	NADP (sodium salt)	29 mg
	Water	10 mL
Tris-HCl buffer	Tris base	6.05 g
	Water	100 mL
Magnesium chloride solution	Magnesium chloride-6-hydrate	320 mg
	Water	25 mL
Glucose-6-phosphate solution	Glucose-6-phosphate (sodium salt)	93.1 mg
	Water	10 mL
Assay solution	Deionized water	5.8 mL
	NADP solution	1.0 mL
	Tris-HCl buffer (pH 7.5)	1.0 mL
	Magnesium chloride solution	1.0 mL
	Glucose-6-phosphate solution	1.0

3.4.4 Glucose-Fructose Oxidoreductase Assay

The assay was conducted in a small 50 mL glass jacketed reactor. A recirculating water bath at 40°C was used to control the temperature. A pH probe and 0.1 N sodium hydroxide were used to maintain a constant pH of 6.2. The treated cells were added to the reaction medium (Table 3.4) and 500 μL samples were taken periodically: 0 min, 1 min, 10 min, 20 min, 30 min, 1 hr, 2 hr, 4 hr, 6 hr, 20 hr, and 23 hr. The samples were immediately centrifuged for 8 min in the Eppendorf Centrifuge 5415. A 400 μL sample of the supernatant was removed from the centrifuge tube and immediately stored at -20°C until the HPLC analysis. A schematic of the experimental setup is shown in Figure 3.2

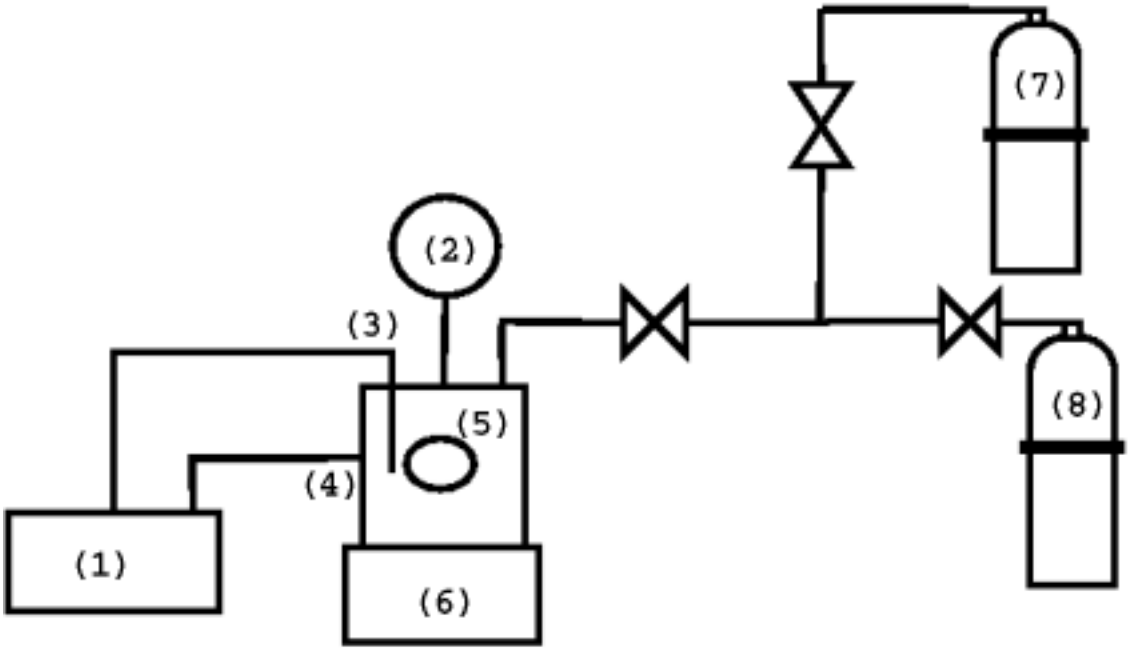

(1) Temperature Controller
(2) Pressure Gauge
(3) Temperature Probe
(4) Heating Element
(5) Supercritical Reactor
(6) Magnetic Stir Plate
(7) Research Grade Carbon Dioxide
(8) Supercritical Grade Carbon Dioxide

Figure 3.1: A Schematic of the Supercritical Reactor Equipment

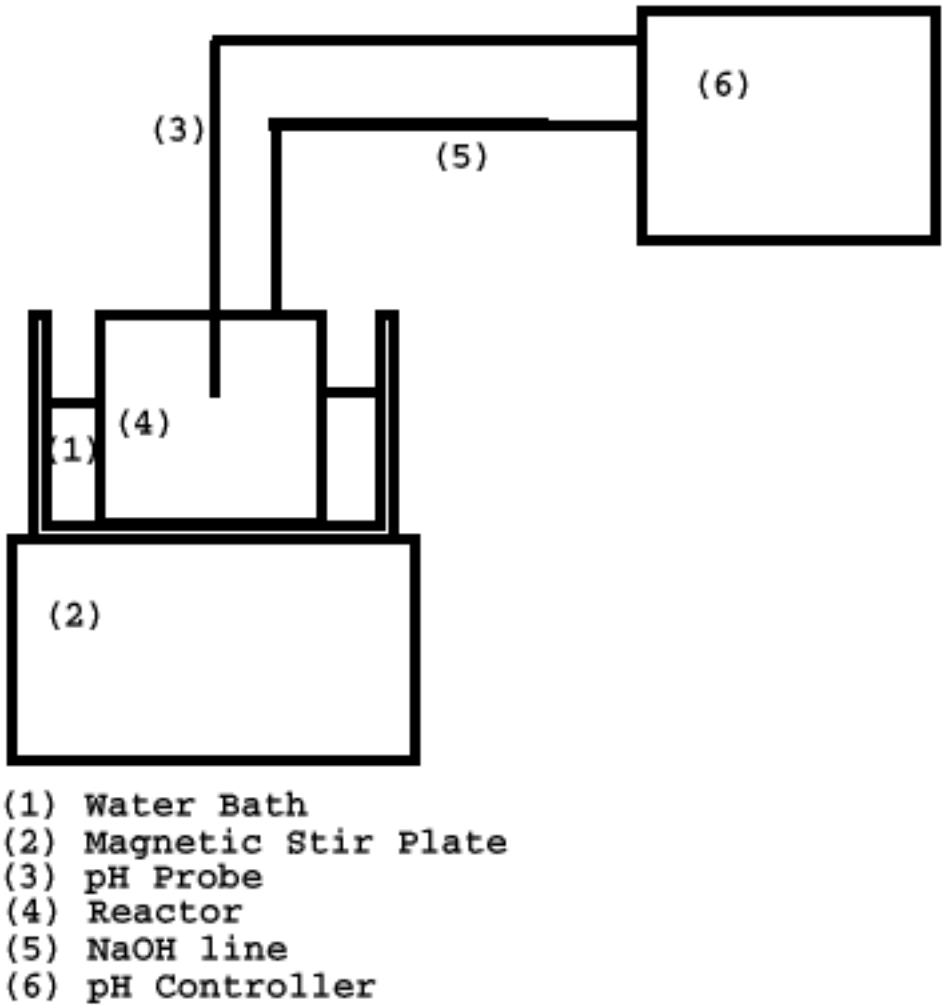

Figure 3.2: The Schematic of the GFOR Reactor System

Table 3.4: GFOR media

Chemical	Amount
0.05 M MES Buffer solution (pH 6.2)	50 mL
Glucose	0.6 g
Fructose	0.6 g

After the samples were thawed, 2 mL of buffer was added for dilution. The solution was filtered using 0.20 μm Acrodisc syringe filters (Gelman Sciences, Inc., Toronto, Ontario). The samples were analyzed using a Waters HPLC equipped with a Waters SugarPak I column and prepared eluent (Table 3.5). The analysis was done using a flowrate of 0.6 mL/min at 90°C, with a helium sparge at 20 mL/min. A Waters R401 refractive index detector was used to monitor the eluent. A 20 μL sample was injected into the column and ran for 27 min. The mixture was separated and quantified into 4 main peaks: glucose, fructose, sorbitol and gluconic acid. A similar procedure has been used by Kim [42].

Table 3.5: HPLC solutions

Solution	Chemical	Amount
HPLC buffer solution	HPLC grade water	1.0 L
	Calcium propionate	0.8379 g
HPLC standard solution	HPLC buffer solution	10 mL
	Glucose	0.5 g
	Fructose	0.5 g
	Sorbitol	0.5 g
	Gluconic acid	0.5 g

3.4.5 Fatty Acid Analysis

The extraction procedure was based on a modified Miller and Berger method used by Sasser [71]. A sample of bacteria (approx. 20 mg dry weight) was treated with 1 mL of reagent 1 (Table 3.6) and heated for 30 min at 100°C on a Pierce Reacti-Therm Heating Module. After cooling to room temperature, 2 mL of reagent 2 (Table 3.6) was added. The vial was replaced on the heating module at 80°C for another 10 min. The solution was allowed to cool to room temperature and extracted three times with 1 mL of reagent 3 (Table 3.6). After each extraction, the organic

phase was removed and collected in a separate container. The organic solution was washed with 3 mL of reagent 4 (Table 3.6). The organic layer was removed and evaporated under nitrogen. The sample was resuspended in 1 mL of hexane before analysis by gas chromatography.

Table 3.6: Fatty acid extraction solutions

Solution	Chemical	Amount
Reagent 1	NaOH	3.0 g
	Methanol	10.0 mL
	Water	10.0 mL
Reagent 2	Hydrochloric acid (conc)	10 mL
	Methanol	5.0 mL
	Water	5.0 mL
Reagent 3	Hexane	10.0 mL
	MTBE	10.0 mL
Reagent 4	NaOH	480 mg
	Water	20.0 mL

The organic layer was analyzed using a Agilent 6890 Series GC System and a HP-1 column (30 m x 0.32 mm ID, 0.25 μm film). The program for the oven began at 60°C with a 90°C/min gradient for 2 minutes to 150°C. The temperature was held constant for 4 min before a 4°C/min gradient was applied. The program ran the GC at a final temperature of 250°C for the remainder of the 31 min program. Helium was used as the carrier gas at a flowrate of 25 cm/sec at 150°C. A FID detector at 280°C was used. Samples of 1 μL were injected using an auto-injector with a splitless flow at 250°C.

3.4.6 SDS-PAGE

Protein samples obtained from extracting the treated and untreated cells were analyzed using gel electrophoresis. The protein samples were first heated in boiling water for 5 min with a sample buffer solution (Table 3.7) in a 1:2 part ratio. A 10% Tris-HCl gel (Bio-rad, Mississauga, Ontario) was used with a Mini-PROTEAN II cell. The running conditions were 200 V at 55 mA with a total run time of 35 min in the Tris running buffer (Table 3.7). The developed gel was stained with a 0.1% Coomassie Blue R-250 stain (Table 3.8) for 20 hrs and destained (Table 3.8) for another 1.5 hrs. The final product was then sealed in plastic for storage.

Table 3.7: SDS-PAGE solutions

Solution	Chemical	Amount
SDS-PAGE sample buffer	Water	2.9 mL
	0.5 M Tris-HCl (pH 6.8)	1.0 mL
	Glycerol	2.0 mL
	10%(w/v) SDS	1.6 mL
	β-Mercaptoethanol	0.4 mL
	1.0% Bromophenol blue	0.1 mL
10x running buffer	Water	500 mL
	Tris base	15.0 g
	Glycine	72.0 g
	SDS	5.0 g

Table 3.8: Protein staining solutions

Solution	Chemical	Amount	Final Concentration
Coomassie Blue Staining Solution	Methanol	200 mL	40%
	Acetic acid	50 mL	10%
	Coomassie blue R-250	1.0 g	0.1%
	Deionized water	250 mL	—-
Coomassie Blue Destaining Solution	Methanol	200 mL	40%
	Acetic acid	50 mL	10%
	Deionized water	250 mL	—-

3.4.7 Zymogram - Protease activity

Protein samples obtained by extracting the treated and untreated cells were analyzed using zymogram gels to determine protease activity. The sample solution was prepared with 1 part protein sample and 2 parts zymogram sample buffer solution(Table 3.9). A 10% zymogram gel (with gelatin) (Bio-rad, Mississauga, Ontario) was used with a Mini-PROTEAN II cell. The running conditions were 100 V, at 25 mA with a total run time of 85 min in the Tris running buffer (Table 3.9). The developed gel was treated with the renaturation buffer (Table 3.10) for 30 min with some agitation. The solution was replaced with development buffer (Table 3.10) and incubated at 37°C with low agitation for 20 hours. The gel was stained with a 0.5%

Coomassie Blue R-250 stain (Table 3.10) for 20 hrs and destained (Table 3.10) for another 1.5 hrs. The final product was then sealed in plastic for storage.

Table 3.9: Zymogram solutions

Solution	Chemical	Amount
Zymogram sample buffer	Water	2.15 mL
	0.5 M Tris-HCl (pH 6.8)	1.25 mL
	Glycerol	2.5 mL
	10%(w/v) SDS	4.0 mL
	1.0% Bromophenol blue	0.1 mL
10x running buffer	Water	500 mL
	Tris base	15.0 g
	Glycine	72.0 g
	SDS	5.0 g

Table 3.10: Zymogram staining solutions

Solution	Chemical	Amount	Final Concentration
Renaturation Buffer	Triton X-100	12.5 g	2.5%
	Deionized water	500 mL	—-
Development	Tris base	3.03 g	50 mm
	NaCl	5.85 g	200 mm
	$CaCl_2$ (anhydrous)	0.28 g	5 mm
	30% Brij-35	0.335 mL	0.02%
Coomassie Blue Staining Solution	Methanol	200 mL	40%
	Acetic acid	50 mL	10%
	Coomassie blue R-250	5.0 g	0.5%
	Deionized water	250 mL	—-
Coomassie Blue Destaining Solution	Methanol	200 mL	40%
	Acetic acid	50 mL	10%
	Deionized water	250 mL	—-

3.4.8 Green Fluorescent Protein assay

After the cell treatment, the *E. coli* cells were washed with 0.01 M Tris-HCl buffer (adjusted to pH 8.0 with HCl). The solution washed from the cells was then analyzed with a Varian photospectrometer at an excitation wavelength of 485 nm and an emission wavelength of 530 nm [85]. The emission intensity was used as an indication of concentration of GFP in the sample.

Chapter 4

Results and Discussion: *Zymomonas mobilis*

The first studied organism was *Z. mobilis* because of its sorbitol producing properties.

4.1 Growth Curves

Growth (Figure 4.1) and calibration curves (Figures A.1 and A.2) were obtained for *Z. mobilis* under the specified growth conditions (Section 3.2.1). The exponential growth phase of *Z. mobilis* has been reported to occur 16-20 hours after innoculation of the medium [27]. However, in these experiments, it was found that the exponential growth phase occurred much earlier, 8 hours after subculture. This may have been due to the change of the strain since it had been subcultured many times. For the purpose of consistency, the cells were harvested after 16 hours and gave a yield of 0.95 g/L. This does not compare well to the 20-30 g/L reported by Rehr *et al.* [69], or to 9 g/L reported by Gollhofer *et al.*[29]. This can be partially explained by the conditions used to grow the cells. The cells were grown statically in an incubator at 30°C. The lack of agitation could reduce the amount of available oxygen. When samples of *Z. mobilis* were grown with agitation, the yield doubled to twice that obtained under the conditions used in this study. While the yield was not as high as that reported by Gollhofer, maintaining optimal pH or glucose concentrations would also increase the biomass yield. Further experiments concerning the optimal biomass yield may be performed, but they are outside the scope of this research. Gollhofer used media with glucose concentration of 100 g/L instead of 50 g/L that

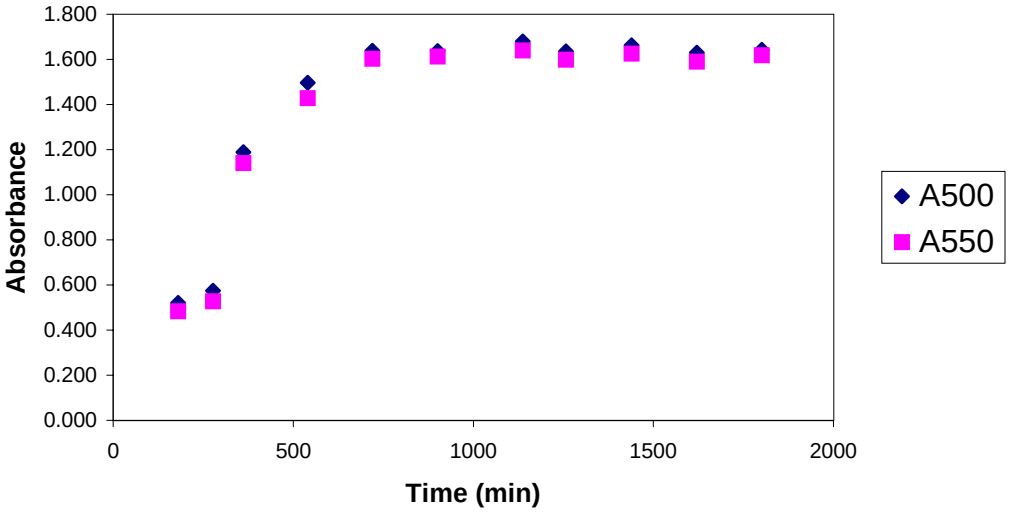

Figure 4.1: Growth curve of *Z. mobilis* measured at both 500 and 550 nm (one trial).

was used in this study. Since this study did not maintain an optimal level of glucose, the yield may have been affected. Also, since the cells showed a different time of exponential growth, this may have affected the total yield.

4.2 Protein Recovery

Table 4.1: Summary of the four permeabilization treatments on protein release (mg protein/g cell). (Data is the average of 6-10 replicates)

Treatment	Wash 1	Wash 2	Wash 3	Total
Control	2.94 ± 2.71	1.00 ± 0.52	2.83 ± 2.21	6.76 ± 4.65
Supercritical CO_2	5.30 ± 3.63	3.93 ± 3.25	1.44 ± 0.97	10.40 ± 6.65
Toluene	4.02 ± 3.27	8.21 ± 8.57	14.18 ± 11.03	39.23 ± 27.60 *
Freeze/Thaw	28.52 ± 10.38	15.87 ± 16.43	10.73 ± 9.53	55.12 ± 33.09

* includes protein found in the permeabilization solution (wash 0)

One measure of the effectiveness of the cell permeabilization treatment is the amount of protein that can be recovered by repeated washing of the cells. To determine this, cells were washed three times with buffer and the buffer wash analyzed for total protein content. In the case of toluene-treated cells, the toluene wash was also analyzed for protein content. For toluene-treated cells, this sample is referred to as wash 0; the other treatments do not have a corresponding wash. Table 4.1 summarizes the comparisons between treatments based on the average amount of protein released per dry weight of cell. The dry weight of the cells was calculated using the absorbance measurement and calibration curve for *Z. mobilis*. Of the treatments, the freeze/thaw treatment shows the largest amount of total protein release. Toluene treatment shows the next largest amount of total protein release. Treatment with supercritical carbon dioxide treatment showed the third largest amount of protein release, while the control treatment shows the least amount of release. When analyzed statistically, the following ANOVA table can be constructed (Table 4.2):

Table 4.2: ANOVA table of protein release data

Source	df	SS	MS
Treatments	3	10 780.51	3593.50
Within Treatments	24	9789.64	761.86
Total	27	20 570.16	

where df is the degrees of freedom, SS is the sum of squares, and MS is the mean square.

Using these values a standard error of 14.75 is obtained. When analyzing the averages at a 90% confidence interval a value for the least significant difference (LSD) of 41.31 is obtained. A significant difference occurs if the values differ by more than the LSD. In this case, the amount of protein released by the supercritical carbon dioxide, toluene and control methods are not significantly different from each other. The amount of protein released by the freeze/thaw method is signifcantly different from the supercritical carbon dioxide and control methods, but is not significantly different from the toluene method. The large standard deviations will be discussed for each of the treatments in the following sections.

A noticeable trend of percentage of total proteins released per wash is seen with the four treatments. With the supercritical carbon dioxide and freeze/thaw treatments, wash 1 shows the greatest amount of protein recovery. After wash 1, the amount of recovered protein decreases with subsequent washes. In the case of toluene, the trend is reversed where subsequent

washes show greater recovery of protein. The control cells show no noticeable trends as the amount of recovered protein changes very little between washes. These trends indicate different mechanisms of permeabilization. This will be discussed more in detail in Section 4.2.3.

4.2.1 Control Treatment

Figure 4.2 compares the results from the 6 individual control replicates. The control treatment shows a protein recovery range of 2 to 15 mg protein/g cell. The amount of total protein recovered does not deviate very much from the average. The overall trend in terms of the amount of protein released as a function of the wash is inconclusive since the second wash usually recovers much lower amounts than either the first or last wash. Protein recovery appeared to be more variable in the case of non-permeabilized cells. This may be explained by the fact that since the cells have not been permeabilized, the physiological state of the cells may affect the pattern of cell release [16].

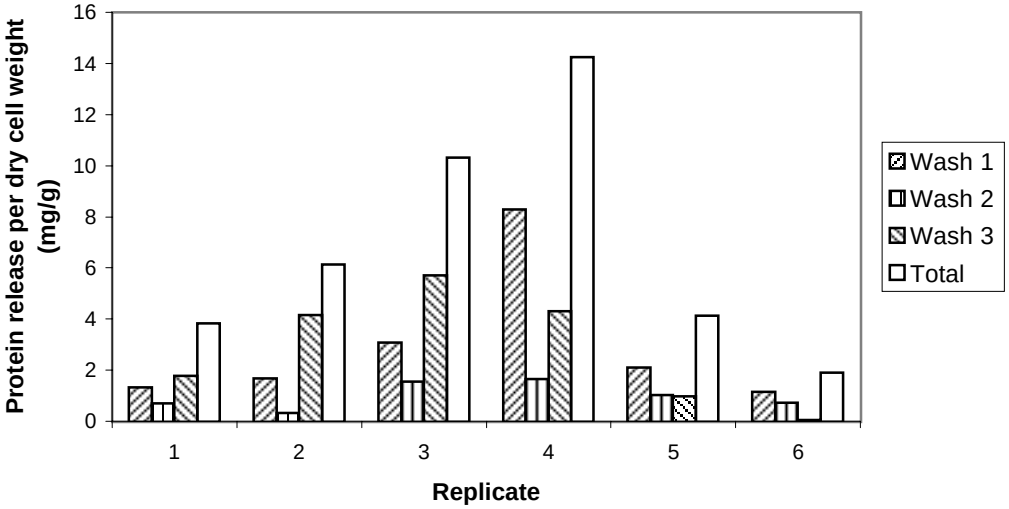

Figure 4.2: Comparison of the effects of control treatment on protein release. (The raw data may be found on figure C.1)

4.2.2 Supercritical Carbon Dioxide Treatment

Figure 4.3 is a comparison between the different replicates of protein recovery using supercritical carbon dioxide treatment. The amount of protein release with the supercritical treatment fluctuates from 2 to 22 mg protein/gram cell. One explanation for this behaviour is the difficulty of cell recovery. For each treatment, wet cells were spread between folded sheets of Nytex cloth. After treatment, the cells were scraped off the cloth. This procedure caused a loss in recovered cell weight. The cells and cloth would be weighed before and after the scraping procedure and yielded a significant difference in mass. The difference in mass was up to three times the amount of recovered cells. The lost mass may be cells that were not fully recovered after scraping the cloth which would result in a loss in total protein, and a decrease in actual amount of cells available. The problem was addressed after replicate 7 by increasing the amount of treated cells to minimize the effects of cell loss. The general trend was a decrease in protein recovered during each successive wash of a sample. This pattern of protein release is more consistant than for the control cells where protein release appeared variable depending on the wash.

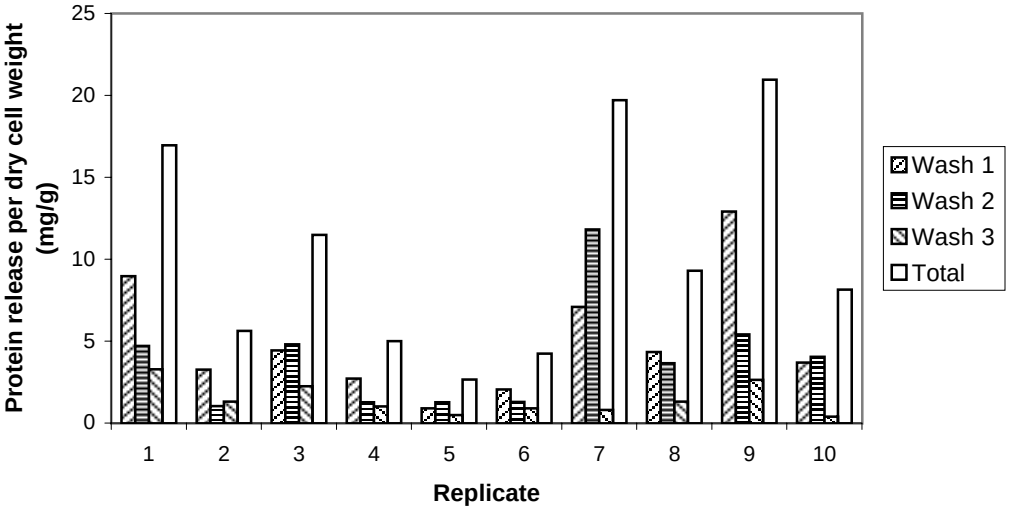

Figure 4.3: Comparison of the effects of supercritical carbon dioxide treatment on protein release. (The raw data may be found on figure C.1)

4.2.3 Toluene Treatment

Toluene treatment resulted in a recovery of 20 to 88 mg protein/g cell (Figure 4.4). Compared to the total amount of recovered protein, the loss of protein during the toluene treatment (wash 0) seems to be minimal. Replicate 4 shows a significant difference from the other replicates as it yields more than twice the amount of protein as the others. This skews the average of the runs and makes it very comparable to the freeze/thaw treatment. When replicate 4 is not considered the average amount of recovered protein and the standard deviation drop significantly. The average protein recovery drops to 29.53 $\pm$ 15.71 mg/g cell, instead of 39.23 $\pm$ 27.60 mg/g cell.

Overall, a distinguishing trend of the toluene treatment is the increasing amount of protein released in subsequent washes, even though individual trials may not show this. Unlike the other treatments (supercritical carbon dioxide and freeze/thaw), the greatest percentage of the total recovered protein is not obtained in the first wash. This indicates that the mechanism of permeabilization may play a role in this difference. In the freeze/thaw treatments, the cell wall is physically ruptured with the formation of ice crystals. With the toluene treatment, cellular components are being solubilized by toluene. This may lead to a gradual weakening of the cellular structures, indicated by the increasing amount of protein released with each wash. The first wash may be removing membrane proteins further weakening the cell membrane and allowing larger cytoplasmic proteins to be subsequently removed from the cell. This means that increasing the length of toluene treatment or more washes may yield greater protein recovery.

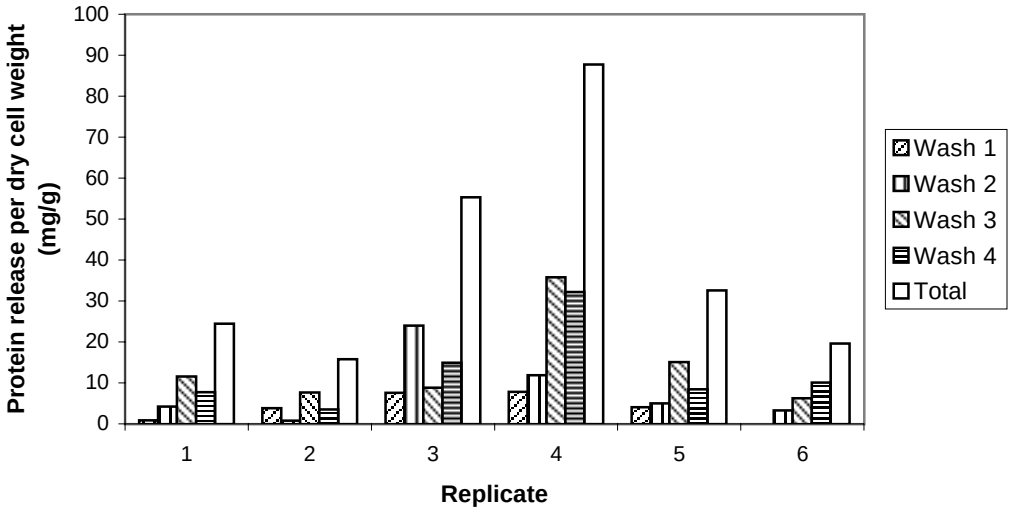

Figure 4.4: Comparison of effects of toluene treatment on protein release. (The raw data may be found on figure C.1)

4.2.4 Freeze/Thaw Treatment

Figure 4.5 presents the results of the individual freeze/thaw replicates. The freeze/thaw treatment was the most effective of the 4 methods with the highest average total protein release per cell weight. The amount of protein released ranged from 30 to 124 mg protein/g cell. In most cases, the majority of the protein was recovered in the first wash. Replicate 4 showed a marked difference from the other experimental runs. The amount of protein recovered in each of the first two washes is shown to be comparable to the total protein recovered in the other treatments. Again, this experimental run shows a markedly increase in the protein recovery. Upon removal of replicate 4 data, an average of 42.17 $\pm$ 10.54 mg/g cell is obtained, instead of 55.12 $\pm$ 33.09 mg/g cell. With these numbers, the overlap between the toluene treatment and freeze/thaw treatment is reduced, making the difference in treatments more statistically significant.

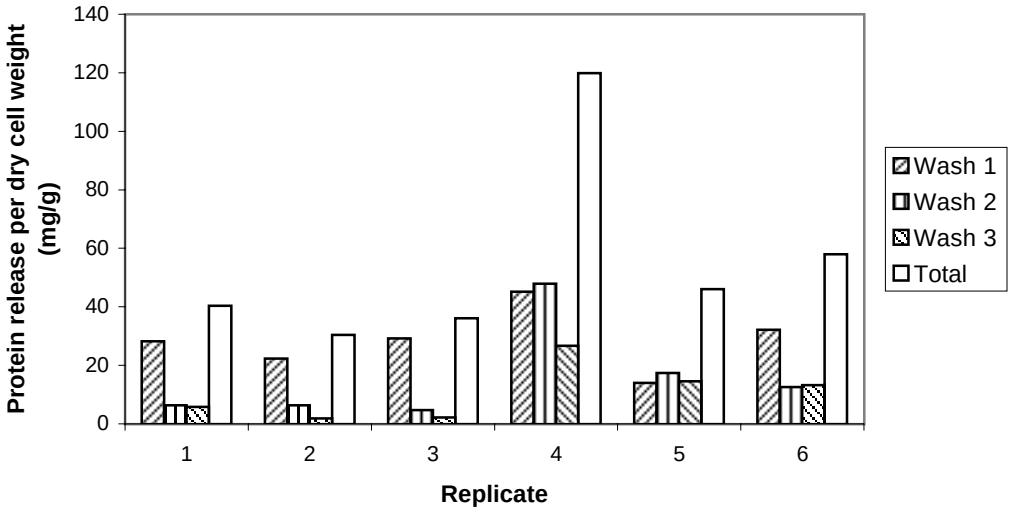

Figure 4.5: Comparison of the effects of freeze/thaw treatment on protein release. (The raw data may be found on figure C.1)

When the data for the toluene treatment and freeze/thaw treatment is modified to reduce the standard deviation, the following ANOVA table can be constructed (Table 4.3):

Table 4.3: Modified ANOVA table of protein release data

Source	df	SS	MS
Treatments	3	4873.78	1624.59
Within Treatments	22	1938.68	88.12
Total	25	6812.46	

These values reduce the standard error to 5.42 and the LSD is reduced to 15.28. This means that the supercritical carbon dioxide and the control treatments are still not significantly different from each other, but the toluene treatment is statistically different from either treatment. The difference of means between the toluene and freeze/thaw methods is 12.6, which is very close to the LSD, but there is still no statistically significant difference between the two.

4.3 Electrophoresis Gels

Electrophoresis gels are useful tools for obtaining quantitative and qualitative information on proteins. Proteins can be characterized qualitatively with the use of molecular weight markers. The markers can be used to determine the approximate molecular weight of the unknown proteins. In this study, cell washes were analyzed using gel electrophoresis to characterize the pattern and abundance of proteins in the cell washes.

4.3.1 SDS-PAGE Gels

The gels were loaded with the same volume of wash sample (5 μL diluted to 15 μL with sample buffer). The washes with the largest amount of protein determined by the BCA method were used as samples. Figure 4.6 is an SDS-PAGE gel comparing the protein content for wash 1 and 2 for the various cell permeabilization treatments. A comparison of lanes 2-7 for the three treatments reveals that for the most part, the same complement of proteins based on molecular weight were observed in the washes, independently of the permeabilization procedure. Lanes were loaded with washes from comparable levels of dry weight of cells so the trend in terms of quantity of protein follows that suggested by the BCA assay (Table 4.1). The most intense bands are found for the freeze/thaw treatment. Toluene and supercritical carbon dioxide treatments appear to be somewhat comparable except for wash 2 of the toluene-treated sample. The toluene, supercritical and freeze/thaw treatments show proteins ranging from 7-200 kDa. Based on previous gels published by Scopes *et al.* [75] and Pawluk *et al.* [64], some of the bands may be identified. The identifiable bands are G-6-P DH (52 kDa), pyruvate kinase (48 kDa), glucokinase (32 kDa) and fructokinase (29 kDa). The lanes containing control extracts show almost no presence of proteins, indicating that cell permeabilization is required for protein removal. The toluene lanes appear to show a smaller number of larger proteins, indicating that the toluene treatment may not be as effective for recovery of large proteins. Both the supercritical and freeze/thaw lanes show similar patterns except that the lanes with freeze/thaw treated extracts indicate larger amounts of recovered protein.

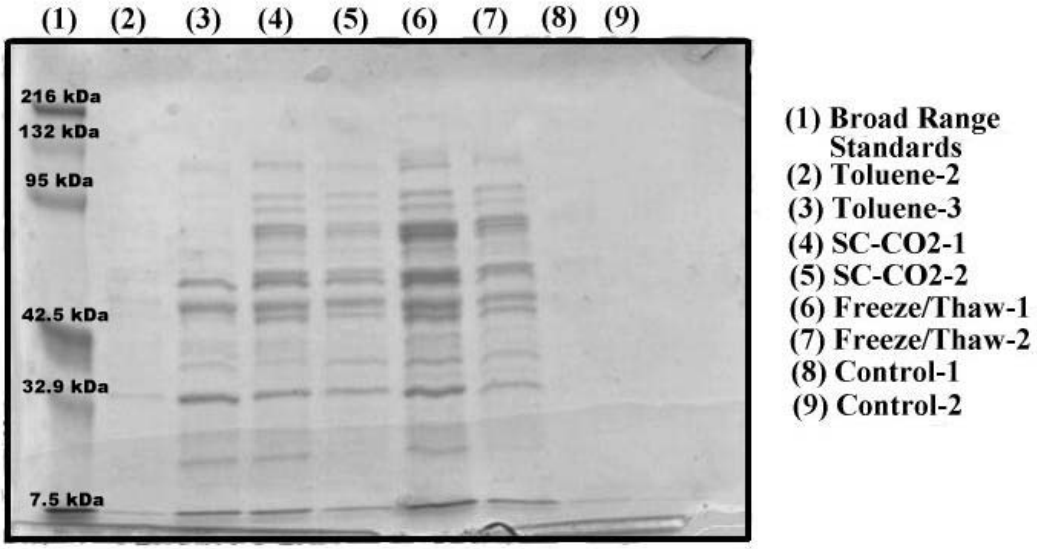

Figure 4.6: Comparison of proteins isolated from different treatments and washes (i.e. supercritical carbon dioxide - wash 1).

4.3.2 Zymogram Gels

One problem of significance in the biotechnology industry is that once cells have been ruptured to release their contents, proteases are also released. The proteases can then degrade the desired protein products. To determine if the permeabilization procedures used in this study released proteases, Zymogram gels were used to assess protease activity. Protein is incorporated into the gel which will stain blue with Coomassie stain. If proteases are present, clear lines indicating protease activity will appear. In this study, the gels are stained uniformly blue with no clear

bands, indicating no protease activity from any treatment samples. This lack of activity can be attributed to either a lack of recovered protease or inactivation of protease during the treatment. This is important since isolation of the protein product would be less effective if it is hydrolyzed by proteases [60]. This result indicates that these permeabilization treatments do not release active proteases into the cell washes.

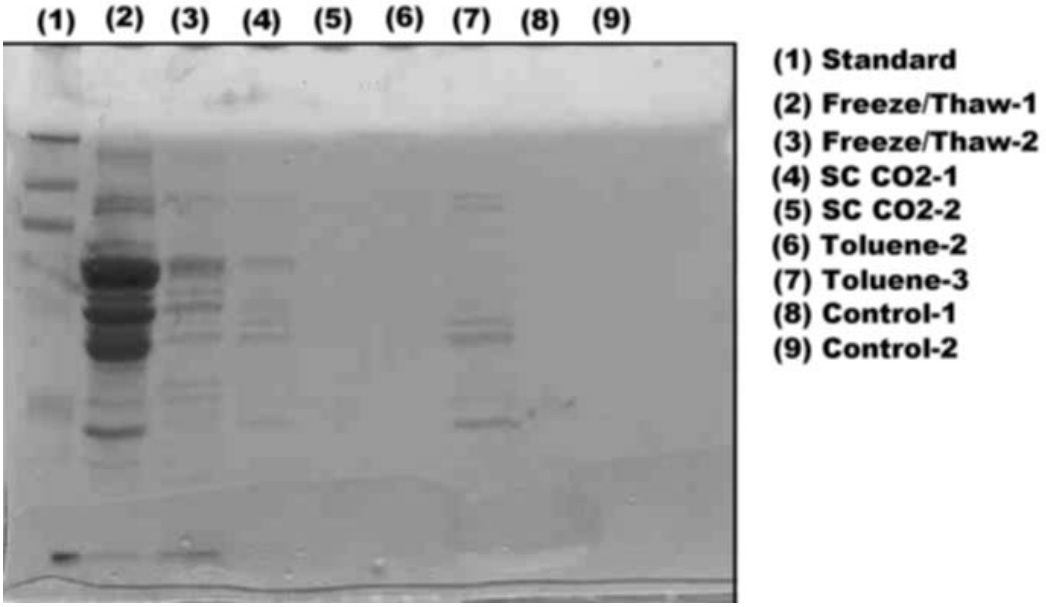

Figure 4.7: Comparison of protease activity from different treatments and washes using a Zymogram gel.

4.4 Glucose-6-Phosphate Dehydrogenase Activity

Table 4.4: Summary of G-6-P dehydrogenase reaction rates (mU/g protein)

Treatment	Wash 1	Wash 2	Wash 3	Total
Control	4.81 ± 4.48	10.73 ± 11.14	6.08 ± 5.37	21.62 ± 20.99
Supercritical CO_2	5.91 ± 4.37	7.38 ± 10.26	8.75 ± 8.15	22.04 ± 22.78
Toluene	11.43 ± 10.80	1.97 ± 1.43	1.85 ± 1.58	15.25 ± 13.81
Freeze/Thaw	48.22 ± 28.32	23.64 ± 15.04	9.96 ± 7.69	81.82 ± 51.05

Glucose-6-phosphate dehydrogenase activity was measured to determine if cytosolic proteins were in the mixture of proteins released by the cells under different permeabilization strategies and what effect these treatments had on enzyme activity. If the desired product is to be an active enzyme, lack of activity would render the permeabilization technique useless. Glucose-6-phosphate dehydrogenase is a cytoplasmic enzyme that can be extracted from cells [75]. The activity in units was defined as the concentration of NADPH (g/L) formed per minute. Specific activities were recorded to compare activity on the basis of units of G-6-P DH activity per gram of protein. Table 4.4 compares the averages of the different G-6-P dehydrogenase activities based on the wash number and treatment type.

Overall, the freeze/thaw treatment yielded the highest activity, while the other treatments were comparable to each other. This indicates that the freeze/thaw treatment favours the release of cytoplasmic proteins including G-6-P DH since the results were normalized to the total amount of recovered protein. Both the toluene treatment and freeze/thaw treatments show most of the activity recovery in the first wash. This indicates that the cytoplasm of the cell is targeted first with these techniques. With the supercritical carbon dioxide treatments, subsequent washes increase the specific activity. This may indicate that the recovery of periplasmic proteins is favoured in the first washes.

However, the large standard deviations show that the trends may not be exact since the values for the reaction rates do overlap with each other during the independent trials. This variability may be reduced by perform another series of experiments to verify the trends.

4.5 Glucose Fructose Oxidoreductase Activity

Glucose fructose oxidoreductase is an enzyme that is located in the periplasmic space of the cell [38]. Permeabilization of the cells allows substrates to readily access the enzymes and permeabilization inactivates or removes other enzymes that can compete for the substrate resulting in side reactions and other products. GFOR activity was normalized to cell dry weight and is reported in Table 4.5 under various treatment conditions. With the GFOR analysis, each mole of glucose and fructose consumed by the reaction should yield a corresponding mole of gluconic acid and sorbitol. Differences between the rates of sorbitol production and glucose consumption would indicate that other side reactions are occurring. The highest rate of sorbitol production occurred when cells were permeabilized under supercritical carbon dioxide conditions. Rates of sorbitol production and glucose consumption were comparable, indicating that side reactions were minor. However, the standard deviation was very high, this variability will be discussed in section 4.5.2. Sorbitol production rates were also high for the freeze/thaw treatment, but the rate of glucose consumption was approximately 43% higher than that of sorbitol production. This indicates that significant side reactions were occurring. Similarly for control cells, sorbitol production and glucose consumption rates were not comparable, with glucose consumption being 117% greater than sorbitol production. HPLC analysis confirmed side reactions were occuring as ethanol was observed as a product. The lowest GFOR activity was observed with the toluene treated cells and was about 23% of the level observed for supercritical carbon dioxide treated cells.

Table 4.5: Summary of GFOR assay (Rates in mM/min/g dry cell)

Treatment	Sorbitol Production	Glucose Consumption	Maximum % yield
Control	1.84 ± 1.04	3.98 ± 1.64	17.33 ± 1.15 %
Supercritical CO_2	2.96 ± 2.55	2.80 ± 1.90	53.33 ± 14.22 %
Toluene	0.69 ± 0.14	0.72 ± 0.34	76.33 ± 4.93 %
Freeze Thaw	2.17 ± 0.54	3.10 ± 1.27	59.67 ± 10.79 %

4.5.1 Control Treatment

The rate of glucose disappearance is generally greater than the rate of sorbitol production for the control cells. Since these cells were not treated in any fashion, they would remain viable cells

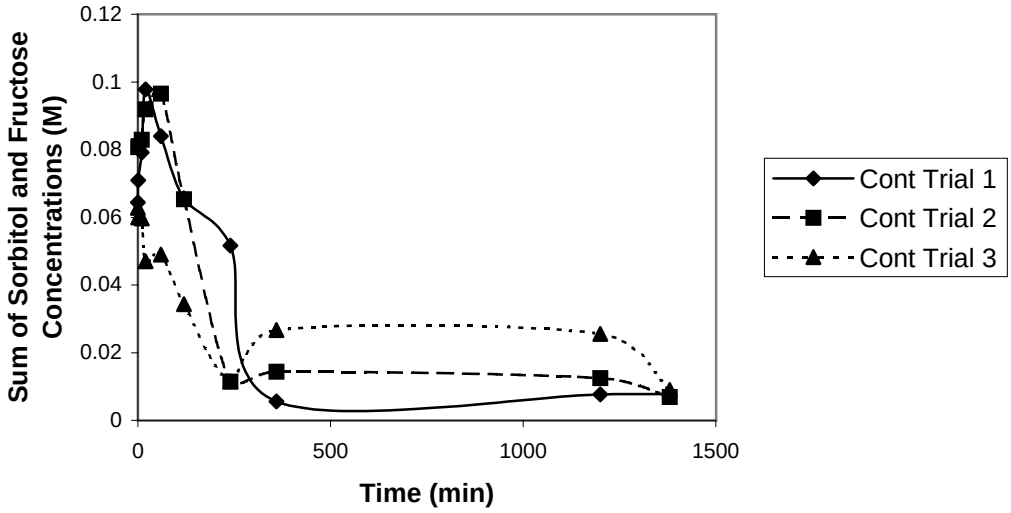

Figure 4.8: The mass balance of sorbitol and fructose for the control treatment (3 experimental runs).

and undergo regular cell metabolism. The amount of sorbitol present reaches a maximum within 1 hour, while glucose is completely consumed within 2 hours (Figures C.10, C.11, C.12). Since glucose is not used primarily for the GFOR reaction in the control cells, it is being consumed for other cell functions, such as cell growth and the production of biomass. Within 10 minutes, the presence of ethanol was observed, indicating that the cells are continuing their regular function to produce ethanol as a method for energy generation. The mass balance (Figure 4.8) shows that the combined presence of fructose and sorbitol decreases within 6 hours. The control cells show the lowest yield of sorbitol ranging from 16% to 18%. This is to be expected since the production of sorbitol is not to be expected when the cells are still active.

4.5.2 Supercritical Carbon Dioxide Treatment

Overall, the rate of glucose consumption is comparable to the rate of sorbitol production. However, analysis of individual trials show that only on the third trial are they similar. Based on the charts of trials 1 and 2, this may be due to the fluctuations that occurred during the first 4 hours (Figures C.13, C.14, C.15). The mass balances for these trials (Figure 4.9)

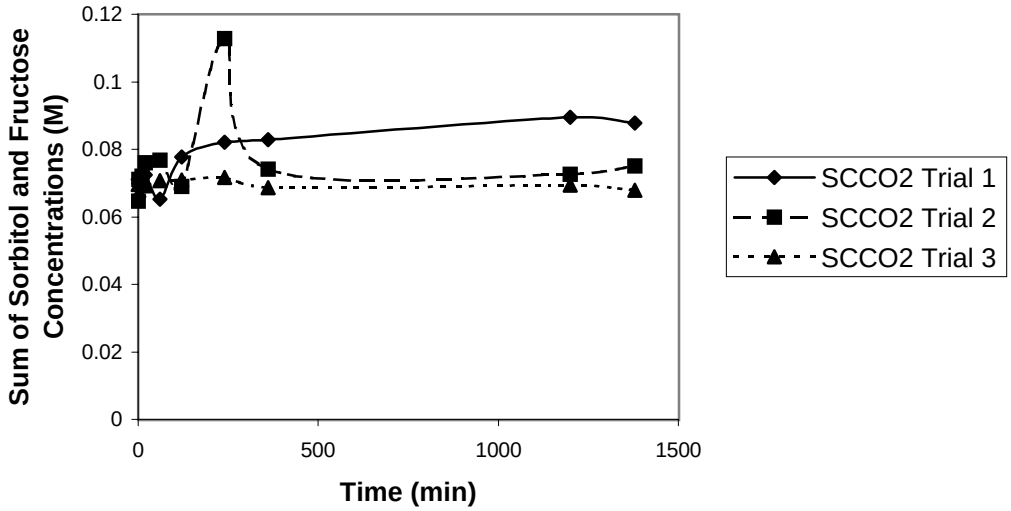

Figure 4.9: The mass balance of sorbitol and fructose for the supercritical carbon dioxide treatment (3 experimental runs).

remain relatively steady with the sum of fructose and sorbitol concentrations staying constant throughout the trial. At the end of the reaction, there is still glucose left in the reactor, indicating that the reaction may not be complete. Over the period from 6 to 20 hours, there does not seem to be a significant increase or decrease in sugar levels; however, activity seems to continue after the 20 hour time point based on the sample at 23 hours. Throughout the three trials, there is no production of ethanol, indicating that the ethanogenic pathway was removed from the system. The yields of sorbitol range from 37% to 63%. These yields seem lower than for freeze/thaw or toluene treated cells; however, since fructose is still present in the solution, it is possible that the yield may increase if the reaction was allowed to go to completion.

4.5.3 Toluene Treatment

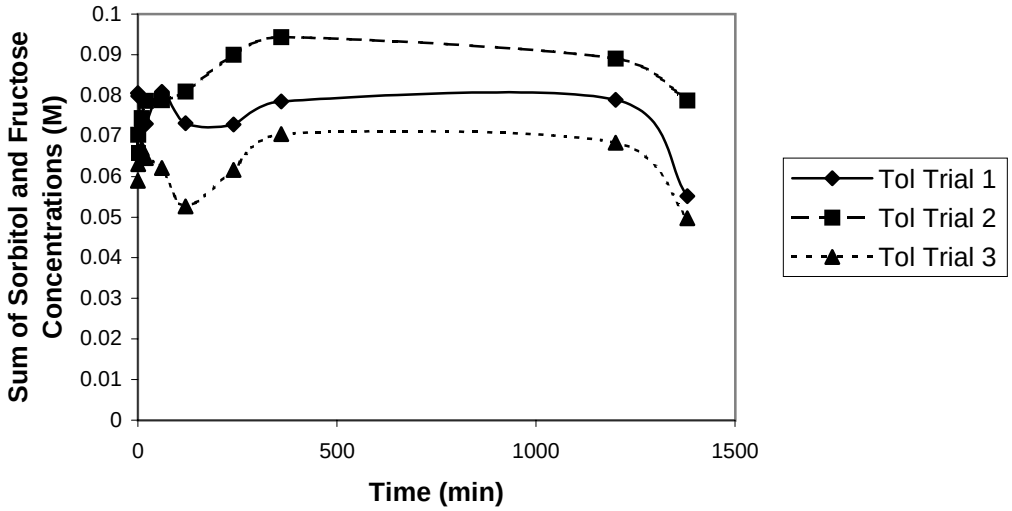

Figure 4.10: The mass balance of sorbitol and fructose for the toluene treatment (3 experimental runs).

The reaction rates for sorbitol production and glucose consumption are fairly similar. As with the data from the supercritical carbon dioxide treatment, the individual trials do not yield similar rates, but the average reaction rates are similar. The glucose is readily consumed within the first 6 hours of the experimental run, thereby limiting further production of sorbitol. After the 6 hours, the remaining sugars are further metabolized and the total amount of the sugars gradually decrease up to the 23 hour endpoint of the experimental run (Figures 4.10, C.16, C.17, C.18). However, in all cases, there was no indication of ethanol production, so the further metabolism of the sugars cannot be attributed to the Entner-Doudoroff pathway [38]. Of the four treatments, toluene treated cells show the highest sorbitol yields ranging from 73% to 82%.

4.5.4 Freeze/Thaw Treatment

The initial reaction rates of sorbitol production and glucose consumption are fairly similar. The glucose is consumed quickly within the first 4 hours of the reaction. This corresponds with the maximum in the production of sorbitol. Sorbitol begins to be consumed after 4 hours, indicated

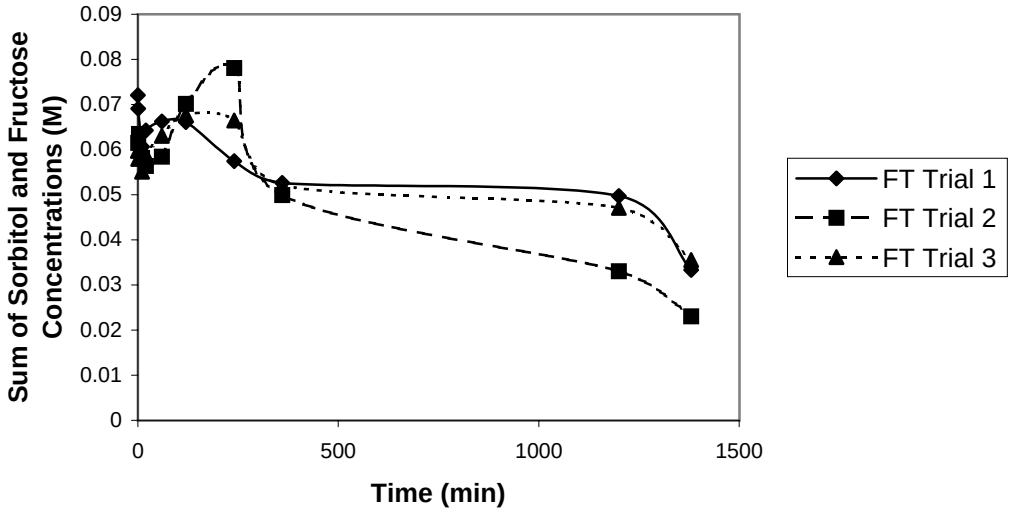

Figure 4.11: The mass balance of sorbitol and fructose for the freeze/thaw treatment (3 experimental runs).

by the gradual drop in sorbitol production (Figure C.19, C.20, C.21). The mass balances show that there is a continual decrease over the time of reaction (Figure 4.11). Along with the presence of ethanol after 20 minutes, this indicates that there is still further metabolic activity beyond that of the GFOR enzymatic system.

4.6 Lipid Analysis

To determine the basis for the different effects of the treatments, lipid analysis was performed. Changes in the lipid composition would indicate removal of certain lipids. All have very similar lipid profiles, with the combination of trans-9-octadecenoate and cis-11-octadecenoate containing about 70% of the lipids in almost all the cases (Figure 4.12) [10]. The exception is with the supercritical treated cells. In these cells, a significant reduction in the concentration of the octadecenoate and an increase in the tetradecanoate composition was observed. Since the lipid composition of the cells is comparable regardless of the cell treatment, one can conclude that the differences observed in GFOR activity are not related directly to solubilization of specific lipids.

Figure 4.13 compares the weight of lipids remaining in the cells. The profiles do not differ significantly with the different treatments. The amount of lipids in the control cells should be the greatest since no lipids should have been removed from the cells. However, the control cells show slightly lower levels of lipids. This may be due to the procedure used to determine the amount of lipids. It is possible that the esterification process is more effective with the treated cells since they are permeabilized and this may allow more lipids to react with the reagents to form esters.

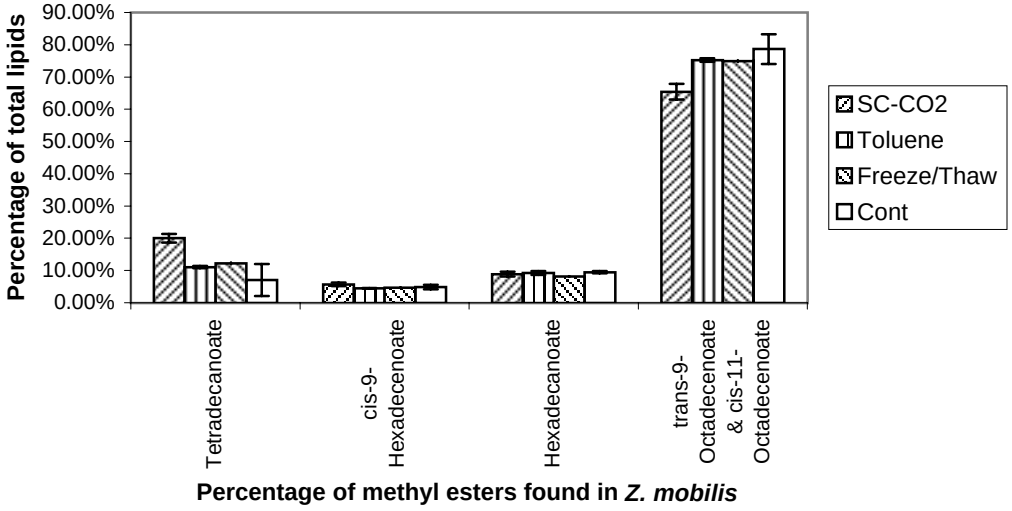

Figure 4.12: Comparison of cell lipid profiles (percentage) between treatments for *Z. mobilis*.

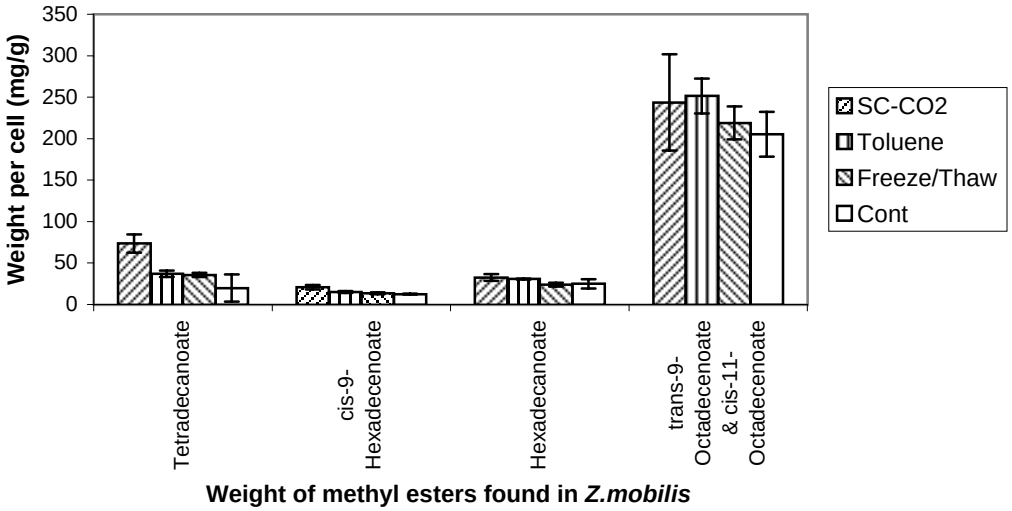

Figure 4.13: Comparison of cell lipid profiles (weight) between treatments for *Z. mobilis*.

4.7 Scanning Electron Microscopy

Analysis of the cells using scanning electron microscopy (SEM) was performed to determine if differences in cell surface morphology were evident as a result of the various treatments.

The control cells (Figure 4.14) are less elongated and relatively wide. The surface of the cells are shown to be smooth with little features of note.

Figure 4.15 shows that the supercritical-treated cells have a slight shrinkage in their shapes. Instead of being oval, the cells show some indentations around the center. Other cells show some texture on the surface of the cells. When compared to the untreated cells in Figure 4.14, this indicates that there is some cell morphology change due to the lack of smoothness and loss of shape.

Figure 4.16 shows examples of toluene-treated cells. These cells are elongated and the cell walls are not as distinct as they are for the control cells. Since toluene acts by solubilizing cellular matter, this may cause the cell membranes to merge together [34].

Figure 4.17 shows that the freeze/thaw treated cells have more pronounced textures on the

surface, The overall shapes of the cells are still oval, with a few cells showing some shrinkage in the center. Since the action of freeze/thaw is caused by formation of ice crystals, it is expected that the cellular membrane would be greatly disrupted [24]. This is evident with the changes of the cellular surface.

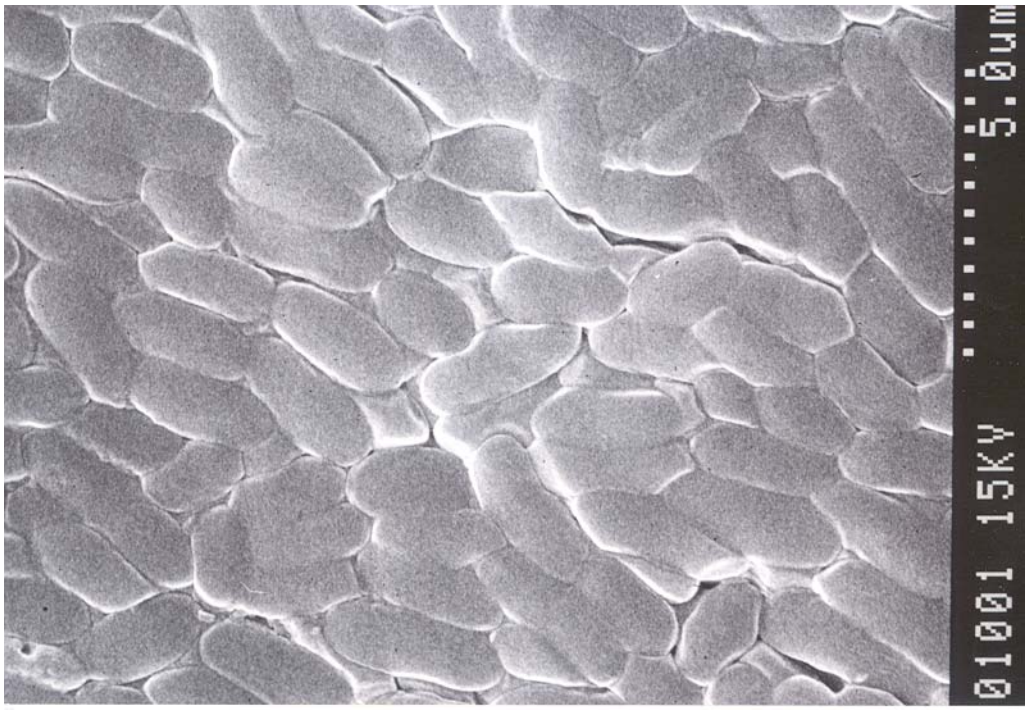

Figure 4.14: SEM of control treated cells.

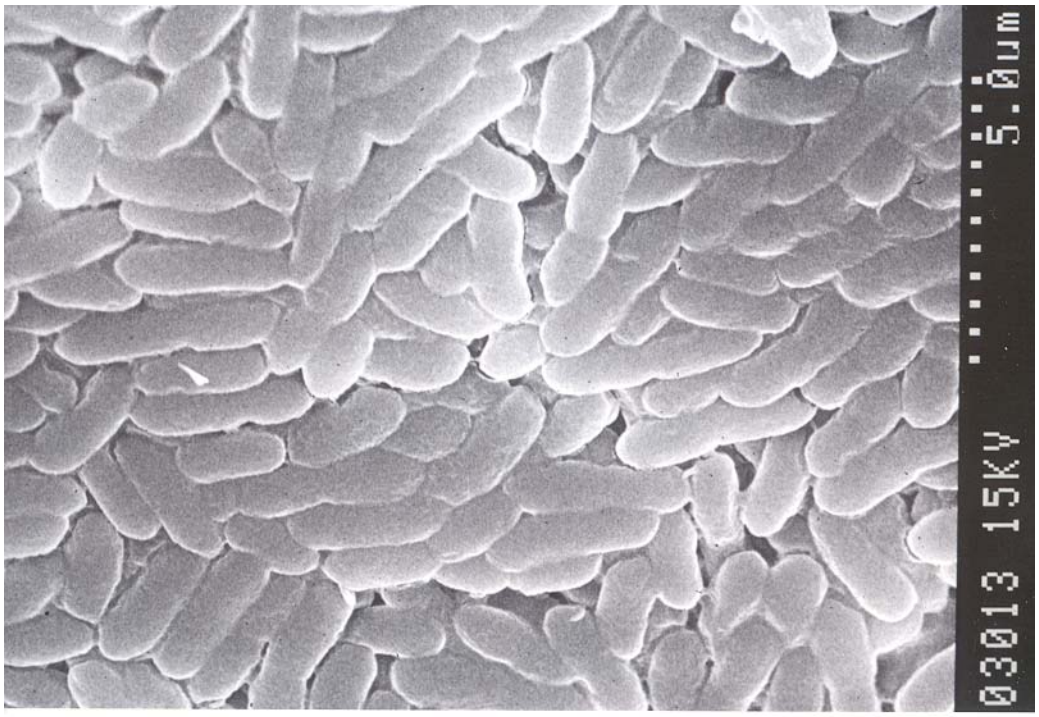

Figure 4.15: SEM of supercritical CO_2 treated cells.

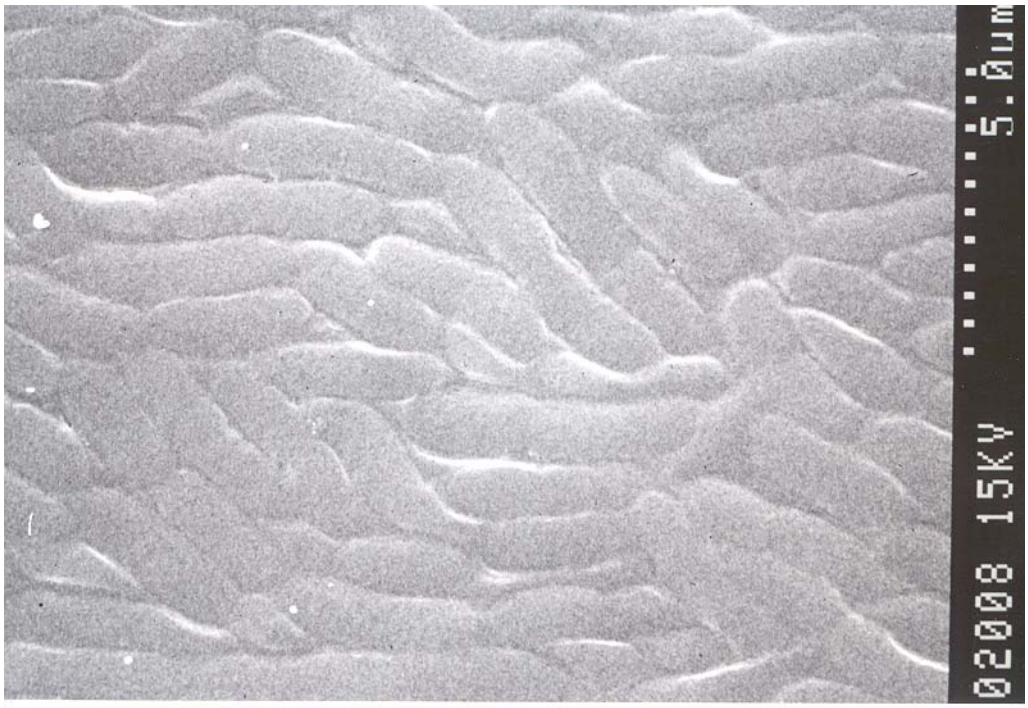

Figure 4.16: SEM of toluene treated cells.

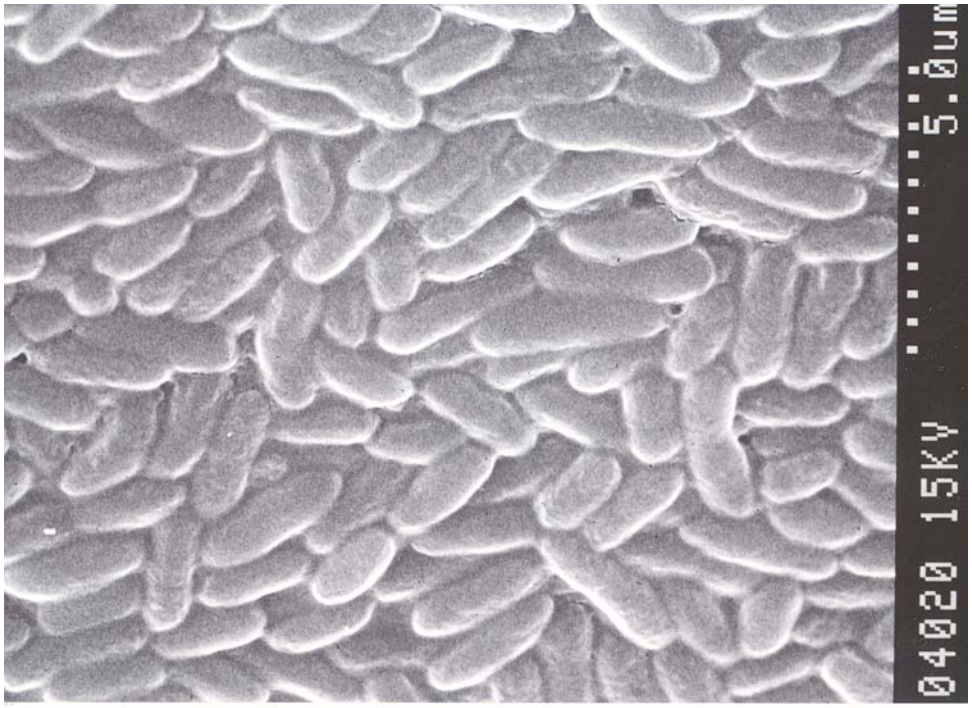

Figure 4.17: SEM of freeze/thaw treated cells.

4.8 Atomic Force Microscopy

Atomic Force Microscopy (AFM) was performed to provide a more detailed examination of the surface morphology of the treated cells. Figure 4.18 shows similar results to the SEM. The control cells can be seen as having smooth cell walls, while the other cells show textures on the cell surface, indicating a change in the cell wall and membrane. At a higher magnification, Figure 4.19 shows a more enhanced view of the cell surfaces. The control cells show pronounced ridges along the cell surface. However, the treated cells show a lack of this structure and they are more disorganized with small groupings randomly around the cell surface. Since the treatments disrupt the cell membrane structure, this would be expected. These differences may be difficult to see due to the resolution of these images. These images are provided as an example of the preliminary use of AFM for determining cell surface characteristics in our lab. Further refinements to the AFM technique and practice may yield more obvious images in the future.

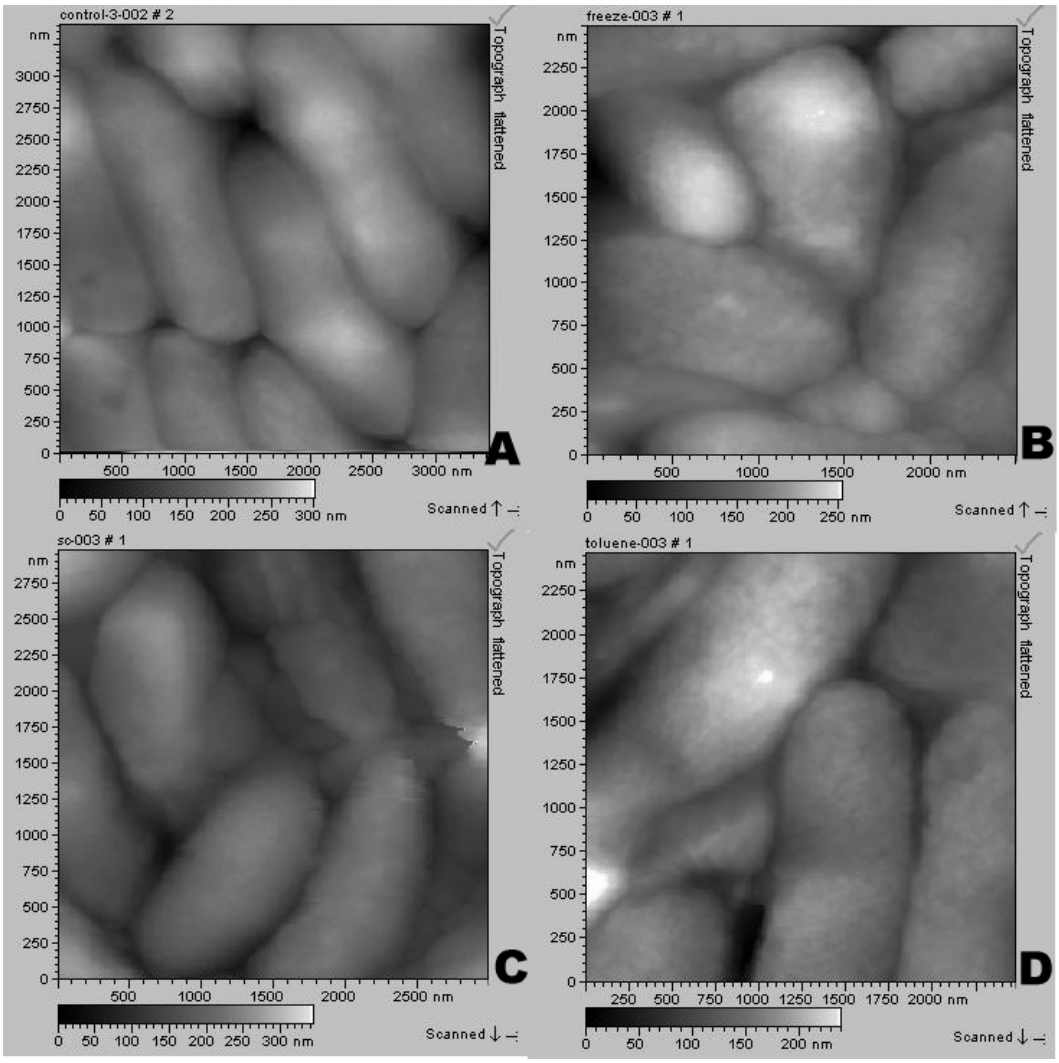

Figure 4.18: AFM of the four cell samples (A - control at 29 000x, B - freeze/thaw at 40 000x, C - supercritical at 34 000x, D - toluene at 40 000x)

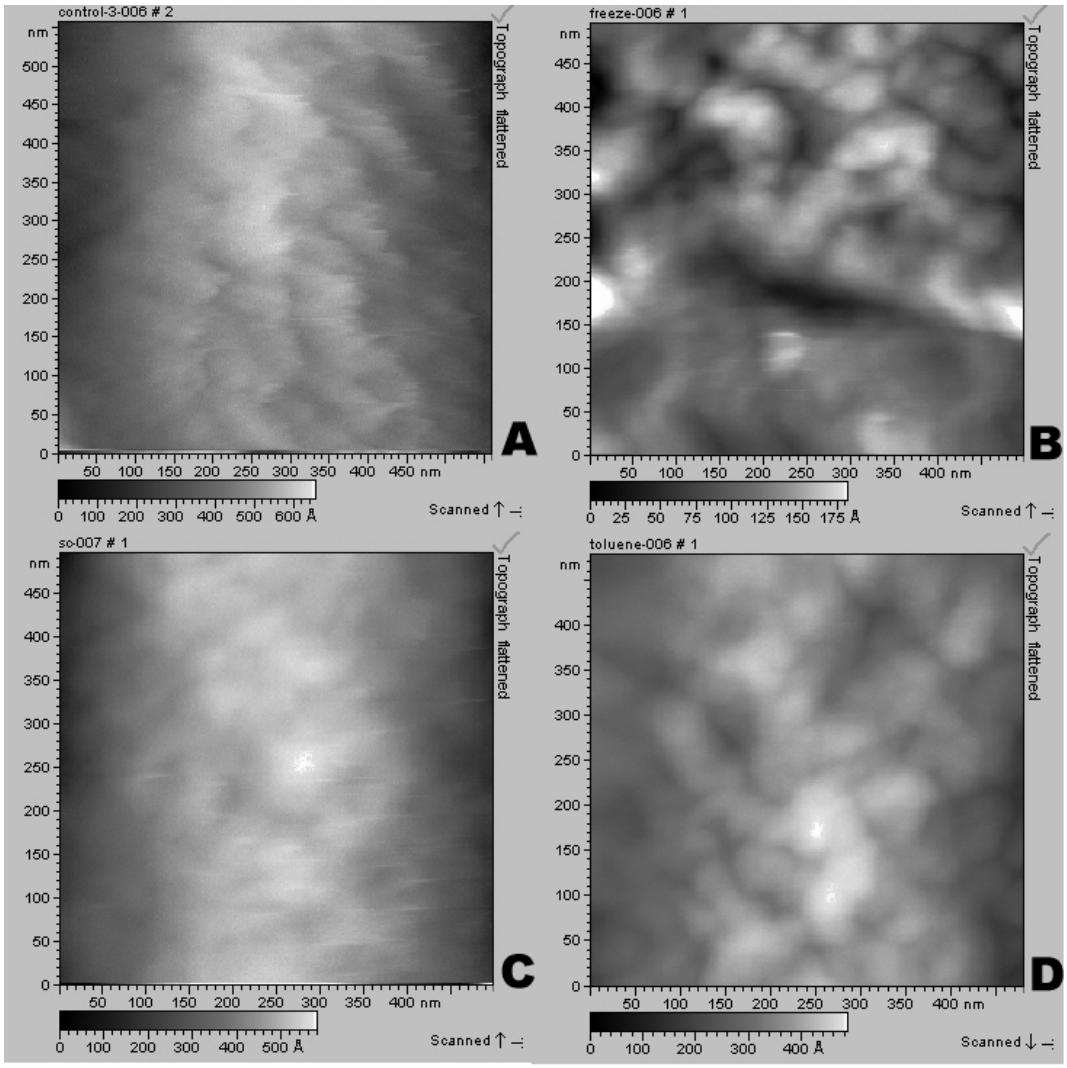

Figure 4.19: AFM of the four cell samples (A - control at 184 000x, B - freeze/thaw at 202 000x, C - supercritical at 202 000x, D - toluene at 213 000x)

4.9 Reaction in the Supercritical Reactor

One of the goals of the research is to determine the feasibility of using supercritical conditions as a reaction medium to produce sorbitol. Ideally, use of supercritical carbon dioxide would permeabilize the cells and provide a medium for the reaction. Since cells were not completely dried before the exposure, in this study, some water was present. Water may be necessary to allow solubilization of the sugars under supercritical conditions [92]. 600 mg each of glucose and fructose were added to the Nytex cloth containing the cells. The reactor was pressurized to 1100 psi in 10 minutes. The cells were exposed to supercritical carbon dioxide for 24 hours and the reactor was depressurized over a period of 10 minutes (Table 4.6). In addition to the sugars on the Nytex, a viscous residue remained at the bottom of the reactor. This residue was analyzed for presence of sugar. Cells were extracted with MES buffer after supercritical carbon dioxide exposure and in trial 2 the residue in the reactor was analyzed. In trials 1 and 3, the percentage of sorbitol conversion based on the total amount of added fructose was less than 1% (0.74% and 0.57% respectively). For trial 2, the percentage of sorbitol conversion was 8.14%. This difference is due to the amount of sugar found in the residue (Table 4.7). However, even when accounting for the sugar in the residue, only half the total weight of sugars was recovered (578 mg). This may be due to sugars that would adhere to the Nytex cloth or to the surface of the reactor, and would be difficult to recover.

Table 4.6: GFOR reaction in Supercritical CO_2 (mg sugar recovered from Nytex cloth)

Sugar	Trial 1	Trial 2	Trial 3
Glucose	83.61	20.65	29.80
Fructose	42.23	24.23	27.51
Sorbitol	4.46	1.63	3.43
Gluconic Acid	2.49	4.84	4.73

Table 4.7: Values for Trial 2 with the GFOR reaction in Supercritical CO_2 (mg sugar)

Sugar	Nytex	Residue	Total
Glucose	20.65	211.70	232.35
Fructose	24.23	201.27	225.5
Sorbitol	1.63	47.19	48.82
Gluconic Acid	4.84	66.20	71.04

Chapter 5

Results and Discussion: *Escherichia coli*

To determine if the results of this study were unique to *Z. mobilis*, results were compared to *E. coli*. *E. coli* was also used as a test organism due to its widespread use in biotechnology and because a simple reporter protein could be used to investigate the effects of the permeabilization methods.

5.1 Green Fluorescent Protein

Green fluorescent protein is used by researchers as a fluorescent marker for recombinant proteins [85]. The fluorescent properties make it easy to detect and quantify when in solution. GFP is also sensitive to changes in protein shape. If the conformation of the protein changes dramatically, the amount of fluorescence will decrease. This makes GFP a good indicator of any possible denaturation of proteins which may occur during isolation.

In this study, *E. coli* which had been activated to produce GFP was permeabilized using the various treatments detailed in Chapter 3. Then the cells were washed, with the washes analyzed for GFP content based on their fluorescence. Figure 5.1 shows the summary of the recovery of GFP. The overall results for GFP mirror the results for protein recovery obtained previously with *Z. mobilis*. The freeze/thaw and toluene treatments yield the greatest presence of GFP. The supercritical carbon dioxide treatment show the next highest amount of GFP, while the control washes show the lowest GFP content.

While the amount of recovered GFP is very small for the control treatment, the majority of the GFP was recovered from the first wash. For the supercritical carbon dioxide treatment, the same trends previously determined with *Z. mobilis* were observed. The greatest amount of the GFP is found in the first wash, while the subsequent washes show a drastic reduction. The toluene treatment showed the greatest GFP in the second wash, with the other washes showing significantly lower amounts of GFP. Again, a sample of the toluene solution was analyzed (wash 0) and very little GFP was found in the permeabilization solution. For the freeze/thaw treatment, the first wash removed the largest portion of the total recovered GFP. Since the recovery pattern is similar to that of total proteins recovered from *Z. mobilis*, GFP seems to be present throughout the cell. If GFP were present in the cytosol, the expected trend would be that exhibited by G-6-P DH activity.

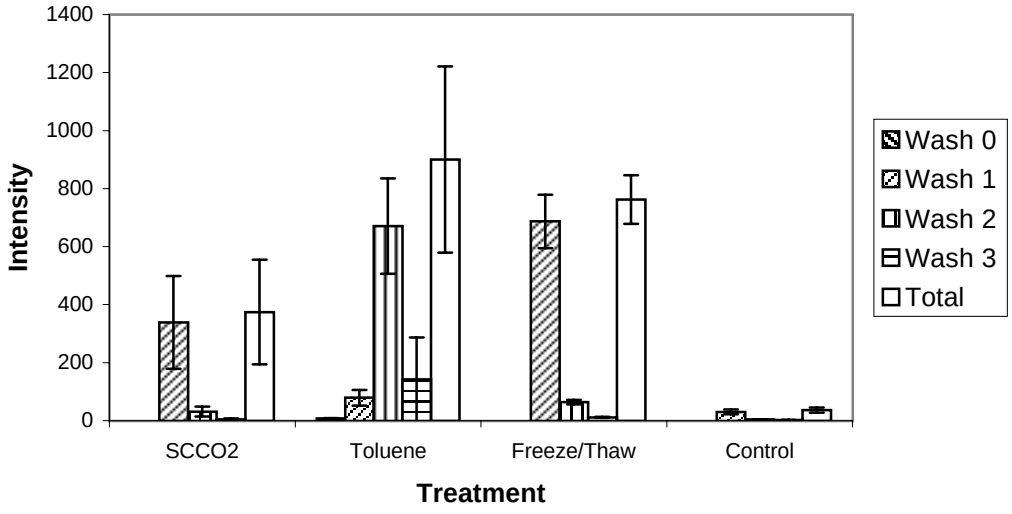

Figure 5.1: Comparison of the four permeabilization treatments on GFP intensity (average of 3 replicates)

5.1.1 Lipid Analysis

The lipid profile for *E. coli* is much more complex than that for *Z. mobilis*. This can be attributed to the different membrane compositions of the organisms. The different compositions

may be affected by the different native environments. *Z. mobilis* is found in environments with high concentrations of ethanol and so the high concentration of octadecenoic acids in the membrane help to protect the organism from ethanol damage [10]. The lipid analysis (Figure 5.2) shows very similar profiles between the different treatments. The only difference in the treatments is the high percentage of cis-9-hexadecenoate for the toluene-treated cells. This corresponds with a slight decrease in hexadecanoate and octadecenoate. When comparing the weight of recovered lipids (Figure 5.3), very little difference in profiles is seen. Again, the control treatment shows the lowest amount of fatty acids which is contrary to what is expected. As with the *Z. mobilis* results, this may be due to the incomplete esterification of the control cells.

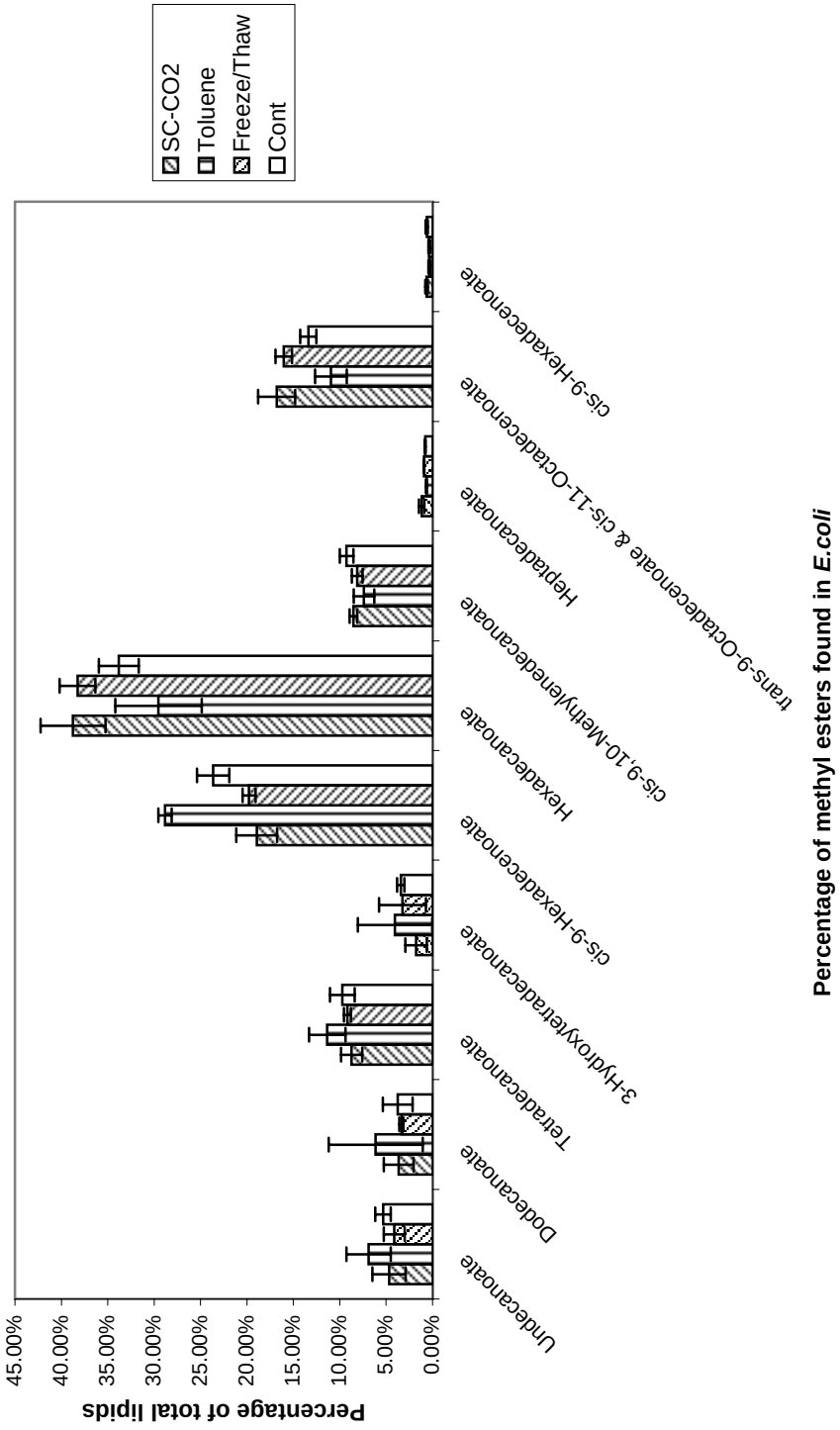

Figure 5.2: Comparison of cell lipid profiles (percentage) between treatments for *E. coli*.

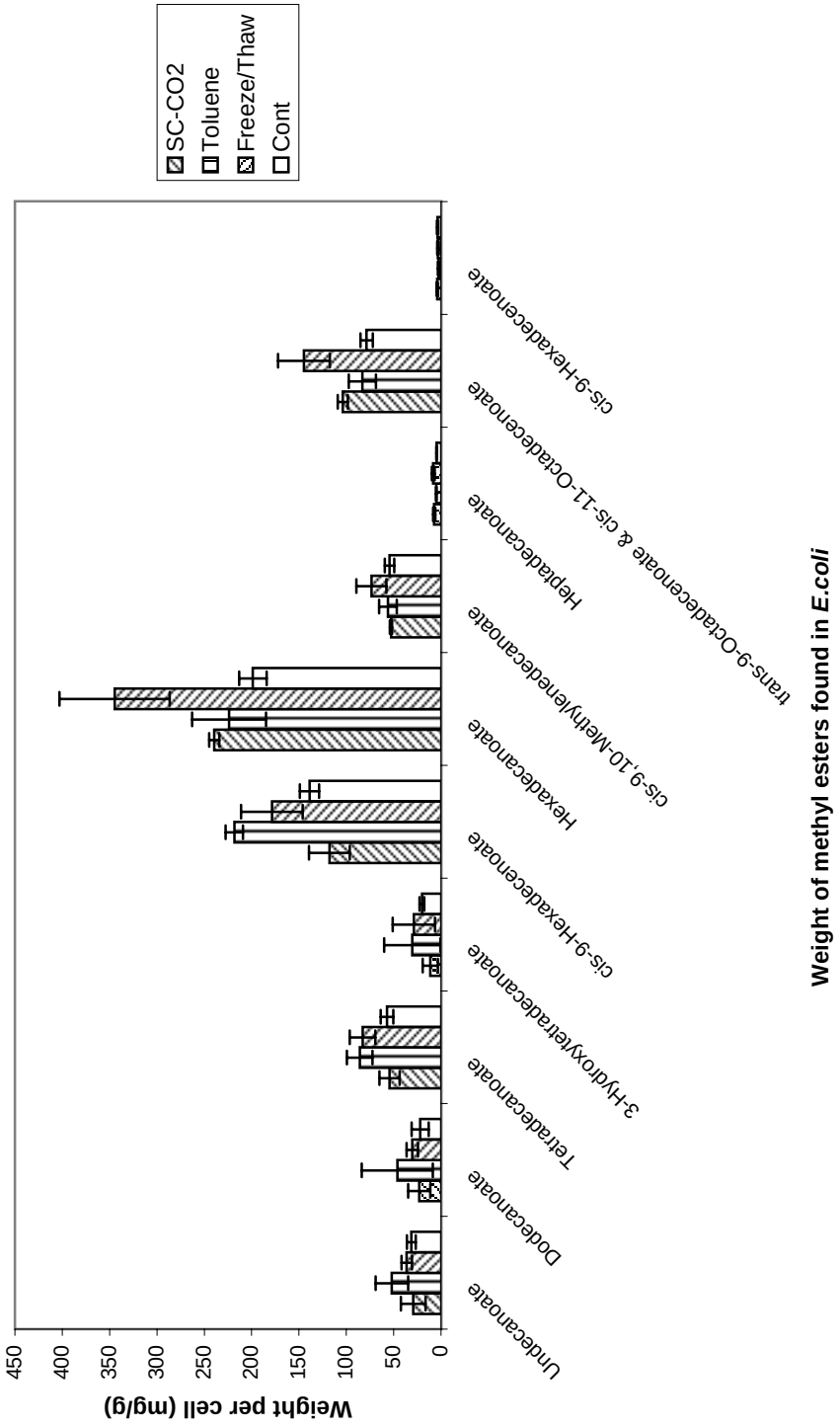

Figure 5.3: Comparison of cell lipid profiles (weight) between treatments for *E. coli*.

Chapter 6

Conclusions and Recommendations

6.1 Conclusions

Within this research, the use of supercritical carbon dioxide has been shown to be a possible tool for cell permeabilization. The total amount of protein that can be released through supercritical treatment is not as large as the amount released by either toluene or freeze/thaw method. In fact, the amount of protein released by the supercritical treatment is not significantly greater than the control. However, the electrophoresis gels show little indication of proteins from the control samples which may indicate some discrepancy between the BCA assay and the gels. The types of proteins released through supercritical treatment are similar to those released through the freeze/thaw method based on molecular weight distribution. Both treatments are effective for higher molecular weight proteins, while the toluene treatment does not seem to release high molecular weight proteins. With all the treatments, there is no evidence of protease activity, indicating that the proteases are not recovered or are inactive.

The G-6-P dehydrogenase shows some activity with all the permeabilization procedures. However, only in the case of the freeze/thaw treatment, do the activities show any significant difference from the other treatments. With the toluene and supercritical treatments, the standard deviation is very high and they have very low specific activities which are marginally higher than the control treatment. This indicates that only the toluene and supercritical treatments do not favour recovery of cytoplasmic proteins as shown by the freeze/thaw treatment.

Supercritical treated cells show some unique characteristics relating to GFOR activity. The reaction does not appear to be complete after 23 hours, unlike the other cell treatments where

glucose is consumed rapidly within the first 6 hours. Even after 23 hours, there are significant amounts of glucose and fructose, as well as sorbitol and gluconic acid. The sorbitol yield is relatively high, comparable to the yield of the freeze/thaw treatments. However, since there is still glucose and fructose in the solution, there is a possibility of a further increase in yield. Unlike the freeze/thaw and control treatments, no ethanol or any side reactions occur with supercritical-treated cells. The lack of side reactions is also characteristic of the toluene-treated cells.

The use of supercritical carbon dioxide for biotransformation was shown to be feasible. The yields were not as high as in the aqueous reactor; however, the results are promising.

The lipid profiles of *Z. mobilis* show similar lipid profiles for all the cells except for a slight reduction in the octadecenoate component in the supercritical cells. This would indicate that octadecenoate was removed from the cellular membrane, causing the membrane to be permeable. The SEM and AFM micrographs only show the result of the treatments. They do show that some changes in cell morphology and on the cell surface do occur with any of the treatments.

Active GFP was extracted from the *E. coli* and the amounts of GFP removed mirror the amount of protein removed from the *Z. mobilis* cells after treatment. The lipid profiles show little to explain the permeabilization, even with the case of *E. coli* where toluene was found to have a different profile. This difference in profile can be attributed to the removal of hexadecanoate from the cells by toluene. This removal is an indication of how permeabilization occurs with toluene treatment.

6.2 Recommendations

For further studies, an increase in the number of cell washes may yield a more accurate amount of proteins recovered and yield more data regarding the types of proteins recovered in each wash. Protein profiles on the type of proteins recovered in each wash would be easily constructed by running more electrophortic gels.

Another method for handling cells when placed in the supercritical reactor should be found. There is a problem with cell recovery due to the loss of cells after the treatment and subsequent removal from the Nytex cloth.

The HPLC method that was used for sugar determination was problematic due to difficulties in resolution between the fructose and glucose. This may be the reason for some of

the fluctuations during the first 4 hours of the GFOR assay. There are occasions where the fructose and glucose will increase and then drop down. Due to the lack of peak resolution at high concentrations of sugars, i.e. glucose and fructose at the start, the total amount of sugars may have been incorrect when determined from the HPLC plots.

Further experiments with the supercritical carbon dioxide as a reaction medium should be conducted as preliminary results indicate that it may be a suitable medium.

References

[1] O. Aaltonen and M. Rantakyla. Biocatalysis in supercritical CO_2. *Chemical Technology*, 21:240–248, 1991.

[2] J.E. Bailey and D.F. Ollis. *Biochemical engineering fundamentals*. McGraw-Hill Inc., Toronto, second edition, 1986.

[3] C. Baldwin and C.W. Robinson. Disruption of *Saccharomyces cerevisiae* using enzymatic lysis combined with high-pressure homogenization. *Biotechnology Techniques*, 4(5):329, 334 1990.

[4] K.D. Barrow, J.G. Collins, D.A. Leigh, P.C. Rogers, and R.G. Warr. Sorbitol production by *Zymomonas mobilis*. *Applied Microbiology and Biotechnology*, 20:225–232, 1984.

[5] T. Becker, J.R. Ogez, and S.E. Builder. Downstream Processing of Proteins. *Biotechnology Advances: Research Reviews and Patent Abstracts*, 1:247–261, 1983.

[6] M. Berger, K. Laumen, and M.P. Schneider. Enzymatic esterification of glycerol I. Lipase-catalyzed synthesis of regioisomerically pure 1,2-sn-diacylglycerols. *Journal. American Oil Chemists' Society*, 69(10):955–960, 1992.

[7] M. Berger, K. Laumen, and M.P. Schneider. Lipase-catalyzed esterification of hydrophilic diols in organic solvents. *Biotechnology Letters*, 14(7):553–558, 1992.

[8] S. Bringer, T. Hartner, K. Poralla, and S. Hermann. Influence of ethanol on the hopanoid content and the fatty acid pattern in batch and continuous cultures of *Zymomonas mobilis*. *Archives of Microbiology*, 140:312–316, 1985.

[9] J.S.G. Brookman. Mechanism of Cell Disintegration in a High Pressure Homogenizer. *Biotechnology and Bioengineering*, 16:371–383, 1974.

[10] V.C. Carey and L.O. Ingram. Lipid composition of *Zymomonas mobilis*: Effects of ethanol and glucose. *Journal of Bacteriology*, 154(3):1291–1300, 1983.

[11] E. Cernia and C. Palocci. Lipases in supercritical fluids. In *Lipases Part B: Enzyme Characterization and Utilization*, volume 287 of *Methods in enzymology*, pages 465–473. New York : Academic Press, 1997.

[12] T. Chatterjee, B.K. De, and D.K. Bhattacharyya. Bioconversions of citral and (±)-citronellal by *Saccharomyces cerevisae*-2415. *Indian Journal of Chemistry*, 38B:1025–1029, 1999.

[13] Y. Chisti and M. Moo-Young. Disruption of microbial cells for intracellular products. *Enzyme and Microbial Technology*, 8:194–204, 1986.

[14] L. Chordia and L. Dolata. Growth for supercritical extraction - The supercritical process may soon gain supercritical mass. *Chemical Processing*, 62(3):43–45, 1999.

[15] U.H. Chun and P.L. Rogers. The simultaneous production of sorbitol from fructose and gluconic acid from glucose using an oxidoreductase of *Zymomonas mobilis*. *Applied Biochemistry and Biotechnology*, 29:19–24, 1988.

[16] R.H. Cumming, J. Tuffnell, and G. Street. The Dependence of Protein Release from *Bacillus amyloliquefaciens* on the Growth Phase in Batch Culture. *Biotechnology and Bioengineering*, 27:887–889, 1985.

[17] R.L. Dabora and C.L. Cooney. Intracellular lytic enzyme systems and their use for disruption of *Escherichia coli*. In *Advances in Biochemical Engineering/Biotechnology*, volume 43 of *Applied Molecular Genetics*, pages 11–29. Springer-Verlag, 1990.

[18] J. Darbyshire. *Large scale enzyme extraction and recovery*, volume 5 of *Topics in Enzyme and Fermentation Biotechnology*, chapter 3, pages 147–186. John Wiley and Sons, Toronto, 1977.

[19] J Deutsch. *Enzymes 1: Oxidoreductases, Transferases*, volume 3 of *Methods of Enzymatic Analysis*, chapter 2.7, pages 190–197. Verlag chemie, Third edition, 1983.

[20] M.S. Doulah. Mechanism of Disintegration of Biological Cells in Ultrasonic Cavitation. *Biotechnology and Bioengineering*, 19:649–660, 1977.

[21] Z. Duvnjak, G. Turcotte, and Z.D. Duan. Production of sorbitol and ethanol from Jerusalem artichokes by *Saccharomyces cerevisiae* ATCC 36859. *Applied Microbiology and Biotechnology*, 35:711–715, 1991.

[22] L. Edebo. *Disintegration of Cells*, pages 249–271. Fermentation Advances. Academic Press, 1969.

[23] V.H. Edwards. *Separation Techniques for the Recovery of Materials from Aqueous Solutions*, pages 273–298. Fermentation Advances. Academic Press, 1969.

[24] C.R. Engler. *Comprehensive biotechnology*, chapter 20, pages 305–324. Ellis Horwood, 1985.

[25] H. Felix. Permeabilized cells. *Analytical Biochemistry*, 120:211–234, 1982.

[26] H. Felix. Bioconversions in Permeabilized Cells. In *Extractive Bioconversions*, pages 259–278. Marcel Dekker, Inc., 1991.

[27] H.C. Ferraz, C.P. Borges, and T.L.M. Alves. Sorbitol and Gluconic Acid Production Using Permeabilizaed *Zymomonas mobilis* Cells Confined by Hollow-Fiber Membranes. *Applied Biochemistry and Biotechnology*, 89:43–53, 2000.

[28] A. Fersht. *Structure and Mechanism in Protein Science*. W.H. Freeman and Company, 1999.

[29] D. Gollhofer, B. Nidetzky, M. Fuerlinger, and K. Kulbe. Efficient protection of glucose-fructose oxidoreductase from *Zymomonas mobilis* against irreversible inactivation during its catalytic action. *Enzyme and Microbial Technology*, 17:235–241, 1995.

[30] I. Goodarznia and M.H. Eikani. Supercritical carbon dioxide extraction of essential oils: Modeling and simulation. *Chemical Engineering Science*, 53(7):1387–1395, 1998.

[31] P. Gunasekaran and K.C. Raj. Ethanol fermentation technology - *Zymomonas mobilis*. *Current Science*, 77(1):56–68, 1999.

[32] P.J. Halling. Thermodynamic predictions for biocatalysis in nonconventional media: Theory, tests, and recommendations for experimental design and analysis. *Enzyme and Microbial Technology*, 16:178–206, 1994.

[33] D.C. Harris. *Quantitative Chemical Analysis*. W.H. Freeman and Company, third edition, 1991.

[34] S.T.L. Harrison. Bacterial Cell Disruption: A key unit operation in the recovery of intracellular products. *Biotechnology Advances*, 9:217–240, 1991.

[35] S.T.L. Harrison, J.S. Dennis, and H.A. Chase. Combined chemical and mechanical processes for the disruption of bacteria. *Bioseparation*, 2:95–105, 1991.

[36] P.J. Hetherington, M. Follow, P. Dunnill, and M.D. Lilly. Release of protein from Baker's Yeast (*Saccharomyces cerevisia*) by disruption in an industrial homogeniser. *Transactions of the Institution of Chemical Engineers*, 49:142–148, 1971.

[37] D. Hettwer and H. Wang. Protein Release from *Escherichia coli* Cells Permeabilized with Guanidine-HCl and Triton X100. *Biotechnology and Bioengineering*, 33:886–895, 1989.

[38] K-H Jang, S. Jung, H-S Chang, and U-H Chun. Improvement of the process for sorbitol production with *Zymomonas mobilis* immobilised in κ-carrageenan. *Process Biochemistry*, 31(5):485–492, 1996.

[39] S. Kamat, E.J. Beckman, and A.J. Russell. Enzyme activity in supercritical fluids. *Critical Reviews in Biotechnology*, 15:41–71, 1995.

[40] S.S. Kesava and T. Panda. Ethanol production by immobilized whole cells of *Zymomonas mobilis* in a continuous flow expanded bed bioreactor and a continuous flow stirred tank bioreactor. *Journal of Industrial Microbiology*, 17:11–14, 1996.

[41] S.S. Kesava, T. Panda, and S.K. Rakshit. Production of ethanol by immobilised whole cells of *Zymomonas mobilis* in an expanded bed bioreactor. *Process Biochemistry*, 31:449–456, 1996.

[42] D-M Kim and H-S Kim. Continuous production of gluconic acid and sorbitol from Jerusalem artichoke and glucose using an oxidoreductase of *Zymomonas mobilis* and Inulinase. *Biotechnology and Bioengineering*, 39:336–342, 1992.

[43] R.L. Kingston, R.K. Scopes, and E.N. Baker. The structure of glucose-fructose oxidoreductase from *Zymomonas mobilis*: an osmoprotective periplasmic enzyme containing nondissociable NADP. *Structure*, 4(12):1413–1428, 1996.

[44] A. Kondo, Y. Liu, M. Furuta, Y. Fujita, T. Matsumoto, and H. Fukuda. Preparation of high activity whole cell biocatalyst by permeabilization of recombinant flocculent yeast with alcohol. *Enzyme and Microbial Technology*, 27:806–811, 2000.

[45] M-R Kula and H. Schutte. Purification of proteins and the disruption of microbial cells. *Biotechnology Progress*, 3(1):31–42, 1987.

[46] D.-H. Kweon, N.S. Han, K.-M. Park, and J-H. Seo. Overproduction of *Phytolacca insularis* protein in batch and fed-batch culture of recombinant *Escherichia coli*. *Process Biochemistry*, 36:537–542, 2001.

[47] R. Leon, P. Fernandes, H.M. Pinheiro, and J.M.S. Cabral. Whole-cell biocatalysis in organic media. *Enzyme and Microbial Technology*, 23:483–500, 1998.

[48] M.D. Lilly and P. Dunnill. *Isolation of Intracellular Enzymes from Micro-organisms - The Development of a Continuous Process*, pages 225–247. Fermentation Advances. Academic Press, 1969.

[49] J. Limon-Lason, M. Hoare, C.B. Orsborn, D.J. Doyle, and P. Dunnill. Reactor Properties of a High-Speed Bead Mill for Microbial Cell Rupture. *Biotechnology and Bioengineering*, 21:745–774, 1979.

[50] Y. Liu, Y. Fujita, A. Kondo, and F. Hideki. Preparation of High-Activity Whole Cell Biocatalysts by Permeabilization of Recombinant Yeasts with Alcohol. *Journal of Bioscience and Bioengineering*, 89(6):554–558, 2000.

[51] H.-F. Lo, L.-L. Lin, H.-L. Chen, W.-H. Hsu, and C.-T. Chang. Enzymic properties of a SDS-resistant *Bacillus* sp. TS-23 α-amylase produced by recombinant *Escherichia coli*. *Process Biochemistry*, 36:743–750, 2001.

[52] H. Lodish, D. Baltimore, A. Berk, S.L. Zipursky, P. Matsudaira, and J. Darnell. *Molecular Cell Biology*. Scientific American Books, third edition, 1995.

[53] H. Loos, R. Krämer, H. Sahm, and G.A. Sprenger. Sorbitol promotes growth of *Zymomonas mobilis* in environments with high concentrations of sugar: Evidence for a physiological function of glucose-fructose oxidoreductase in osmoprotection. *Journal of Bacteriology*, 176(24):7688–7693, 1994.

[54] H. Loos, M. Völler, B. Rehr, Y.D. Stierhof, H. Sahm, and G.A. Sprenger. Glucose-fructose oxidoreductase, a periplasmic enzyme of *Zymomonas mobilis*. *FEMS Microbiology Letters*, 84:211–216, 1991.

[55] A.J. Mesiano, E.J. Beckman, and A.J. Russell. Supercritical biocatalysis. *Chemical Reviews*, 99:623–633, 1999.

[56] M.J.F. Michielsen, C. Frielink, R.H. Wijffels, J. Tramper, and H.H. Beeftink. D-malate production by permeabilized *Pseudomonas pseudoal cligenes*; optimization of conversion and biocatalyst productivity. *Journal of Biotechnology*, 79:13–26, 2000.

[57] H. Mogren, M. Lindblom, and G. Hedenskog. Mechanical Disintegration of Microorganisms in an Industrial Homogenizer. *Biotechnology and Bioengineering*, 16:261–274, 1974.

[58] E.K. Moore, M. Hoare, and P. Dunnill. Disruption of baker's yeast in a high-pressure homogenizer: New evidence on mechanism. *Enzyme and Microbial Technology*, 12:764–770, 1990.

[59] N. Moseyko. Expression of pH-sensitive green fluorescent protein in *Arabidopsis thaliana*. *Plant, Cell and Environment*, 24:557–563, 2001.

[60] M.J. North. *Proteolytic enzymes - a practical approach*, chapter 6, pages 105–124. Practical Approach Series. IRL Press, 1989.

[61] M. Nozaki and O. Hayaishi. *Separation and Purification of Proteins*, volume 5B of *Methods in Microbiology*, chapter 6, pages 425–454. Academic Press, New York, 1971.

[62] P. O'Mullan, M. Szakacs-Dobozi, and D.E. Eveleigh. Identification of saccharolytic enzymes of *Zymomonas mobilis* CP4. *Biotechnology Letters*, 13(2):137–142, 1991.

[63] C. Parker, N. Peekhaus, X. Zhang, and T. Conway. Kinetics of sugar transport and phosphorylation influence glucose and fructose cometabolism by *Zymomonas mobilis*. *Applied and Environmental Microbiology*, 63(9):3519–3525, 1997.

[64] A. Pawluk, R.K. Scopes, and K. Griffiths-Smith. Isolation and properties of the glycolytic enzymes from *Zymomonas mobilis*. *Biochemistry Journal*, 238:275–281, 1986.

[65] R.H. Perry, editor. *Perry's Chemical Engineers' Handbook*. McGraw-Hill Inc., Sixth edition, 1984.

[66] J.T. Polak, M. Balaban, A. Peplow, and A.J. Phlips. *Supercritical Fuild Science and Technology*, chapter 28, pages 449–467. Number 406 in ACS Symposium Series. American Chemical Society, Washington,DC, 1989.

[67] S.L. Putnam and A.L. Koch. Complications in the Simplest Cellular Enzyme Assay: Lysis of *Escherichia coli* for the Assay of β-Galactosidase. *Analytical Biochemistry*, 63(2):350–360, 1975.

[68] B. Rehr and H. Sahm. Process for Obtaining Sorbitol and Gluconic Acid or Gluconate. US Patent 5,102,795, 1992.

[69] B. Rehr, C. Wilhelm, and H. Sahm. Production of sorbitol and gluconic acid by permeabilized cells of *Zymomonas mobilis*. *Applied Biochemistry and Biotechnology*, 35:144–148, 1991.

[70] S. Roy, R.C. Anantheswaran, and R.B. Beelman. Sorbitol Increases Shelf Life of Fresh Mushrooms Stored in Conventional Packages. *Journal of Food Science*, 60(6):1254–1259, 1995.

[71] M. Sasser. *Methods in Phytobacteriology*, chapter I.11, pages 199–204. Akademiai Kiado, Budapest, Hungary, 1990.

[72] T. Sauer, C.W. Robinson, and B.R. Glick. Disruption of Native and Recombinant *Escherichia coli* in a High-Pressure Homogenizer. *Biotechnology and Bioengineering*, 33:1330–1342, 1989.

[73] P. Schlieper and E. De Robertis. Triton X-100 as a channel-forming substance in artificial lipid bilayer membranes. *Archives of Biochemistry and Biophysics*, 184:204–208, 1977.

[74] H. Schütte, K.H. Kroner, H. Hustedt, and M.-R. Kula. Experiences with a 20 litre industrial bead mill for the disruption of microorganisms. *Enzyme and Microbial Technology*, 5:143–148, 1983.

[75] R.K. Scopes, V. Testolin, A. Stoter, K. Griffiths-Smith, and E.M. Algar. Simultaneous purification and characterization of glucokinase, fructokinase and glucose-6-phosphate dehydrogenase from *Zymomonas mobilis*. *Biochemistry Journal*, 228:627–634, 1985.

[76] N. Shaw. *Lipid Composition as a Guide to the Classification of Bacteria*, volume 17 of *Advances in Applied Microbiology*, pages 63–108. Academic Press, New York, 1974.

[77] H. Shi and W.W. Su. Display of green fluorescent protein on *Escherichia coli* cell surface. *Enzyme and Microbial Technology*, 28:25–34, 2001.

[78] T. Shibasaki, H. Mori, and A. Ozaki. Cloning of an isozyme of proline 3-hydroxylase and its purification from recombinant *Escherichia coli*. *Biotechnology Letters*, 22:1967–1973, 2000.

[79] B. Sikyta. *Methods in Industrial Microbiology*. Ellis Horwood Ltd, Toronto, 1983.

[80] M. Silva-Martinez, D. Haltrich, S. Novalic, and B. Kulbe, K.D.; Nidetzky. Simultaneous enzymatic synthesis of gluconic acid and sorbitol - Continuous process development using glucose-fructose oxidoreductase from *Zymomonous mobilis*. *Applied Biochemistry and Biotechnology*, 70-72:863–868, 1998.

[81] S.J. Singer and G.L. Nicolson. Fluid mosaic model of the structure of cell membranes. *Science*, 175:720–731, 1972.

[82] H. Souzu. Studies on the damage to *Escherichia coli* cell membrane caused by different rates of freeze-thawing. *Biochimica et Biophysica Acta*, 603:13–26, 1980.

[83] J. Swartz. Advances in *Escherichia coli* production of therapeutic proteins. *Current Opinion in Biotechnology*, 12:195–201, 2001.

[84] H. Tang, E. Gulari, and E.W. Rothe. Large mirage effect in supercritical CO_2. *Journal of Supercritical Fluids*, 18:193–200, 2000.

[85] R.Y. Tsien. The Green Fluorescent Protein. *Annual Reviews in Biochemistry*, 67:509–544, 1998.

[86] A.M.M. van Eijis, J.M.P. Wokke, and B. ten Brink. Supercritical extraction of fermentation products. In *Preconcentration and Drying of Food Materials*, volume 5 of *Process Technology Proceedings*, pages 135–143, 1988.

[87] A.M.M. van Eijis, J.M.P. Wokke, B. ten Brink, and K.A. Dekker. Downstream processing of fermentation broths with supercritical carbon dioxide. In *Proceedings of the International Symposium on Supercritical Fluids*, pages 799–805, 1988.

[88] P.K. Vohra, R. Sharma, D.R. Kashyap, and R. Tewari. Enhanced production of penicillin G acylase from a recombinant *Escherichia coli*. *Biotechnology Letters*, 23:531–535, 2001.

[89] D.I.C. Wang, C.L. Cooney, A.L. Demain, P Dunnill, A.E. Humphrey, and M.D. Lilly. *Fermentation and Enzyme Technology*. John Wiley & Sons, Toronto, 1979.

[90] T. Wiegert, H. Sahm, and G.A. Spenger. Export of the periplasmic NADP-containing glucose-fructose oxidoreductase of *Zymomonas mobilis*. *Archives of Microbiology*, 166:32–41, 1996.

[91] S.L. Wolfe. *Molecular and Cellular Biology*. Wadsworth Publishing Company, 1993.

[92] J-S Yau and F-N Tsai. Solubilities of D(-)fructose and D(+)glucose in subcritical and supercritical carbon dioxide. *Journal of Supercritical Fluids*, 7:129–133, 1994.

[93] B-D Yin, Y-C Chen, S-C Lin, and W-H Hsu. Production of D-amino acid precursors with permeabilized recombinant *Escherichia coli* with D-hydantoinase activity. *Process Biochemistry*, 35:915–921, 2000.

[94] M. Zachariou and R.K. Scopes. Glucose-fructose oxidoreductase, a new enzyme isolated from *Zymomonas mobilis* that is responsible for sorbitol production. *Journal of Bacteriology*, 167(3):863–869, 1986.

[95] Y. Zheng and G.T. Tsao. Avicel Hydrolysis by Cellulase Enzyme in Supercritical CO2. *Biotechnology Letters*, 18(4):451–454, 1996.

Appendix A

Calibration Curves

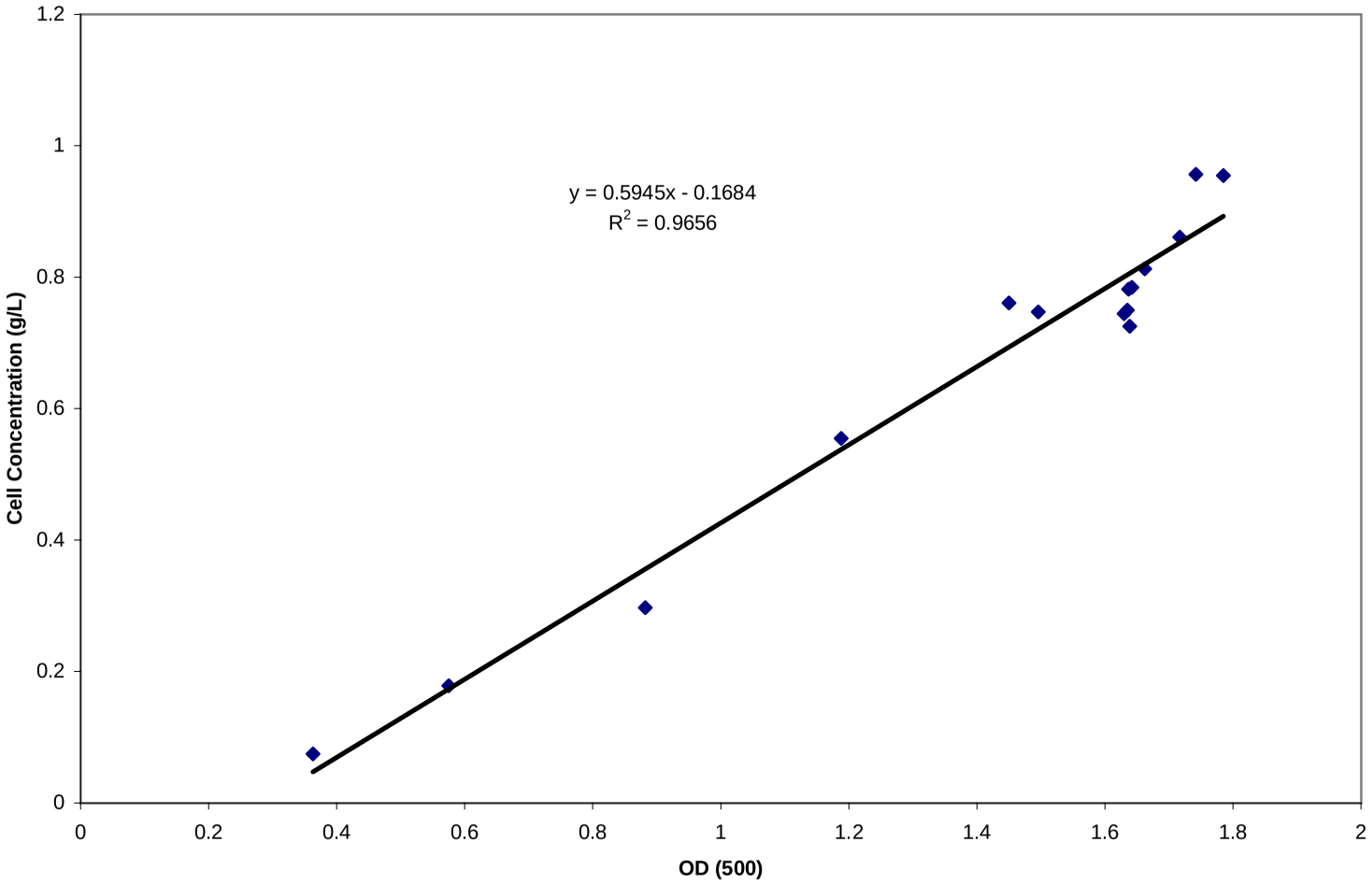

Figure A.1: Calibration curve for *Z. mobilis* at 500 nm.

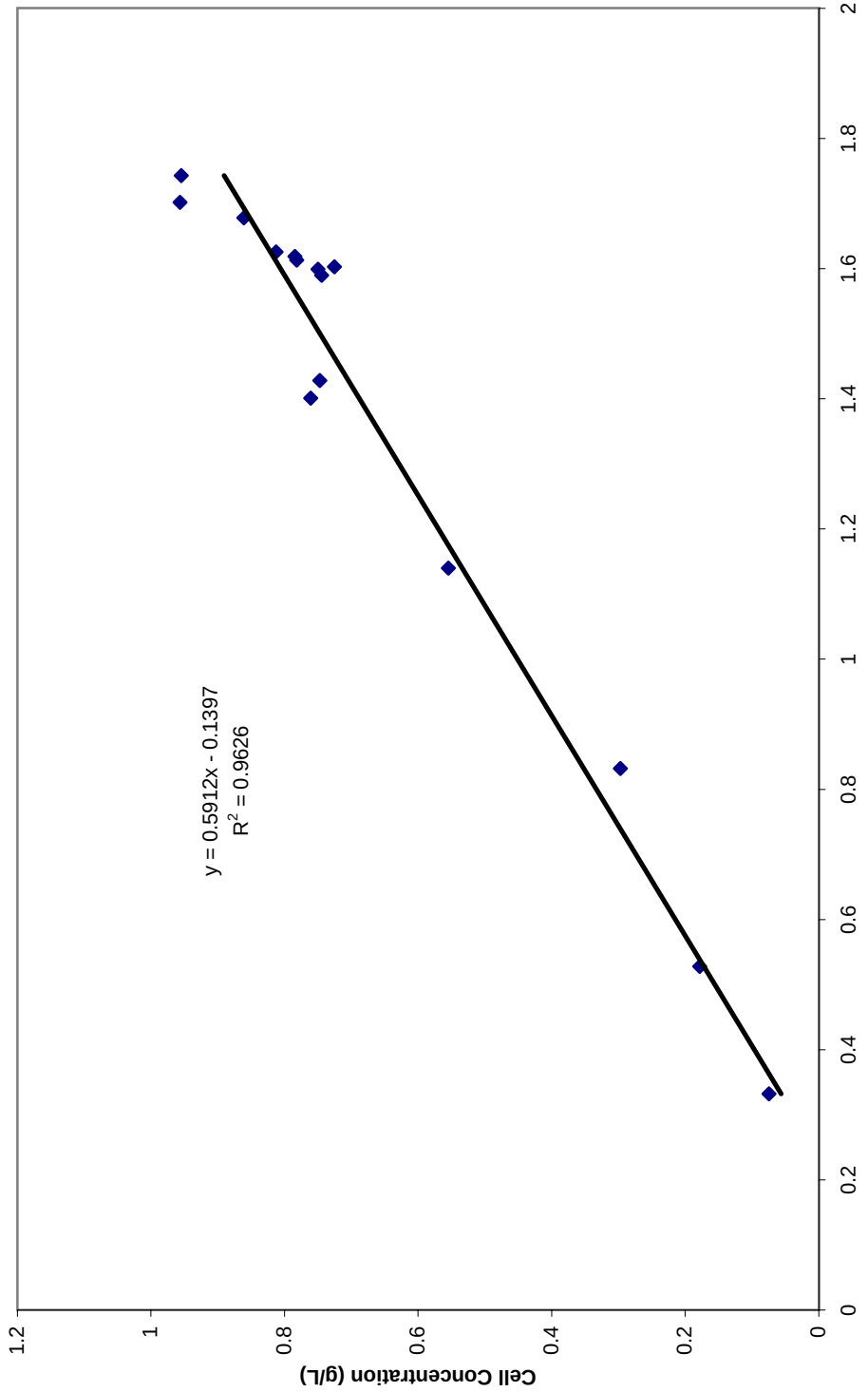

Figure A.2: Calibration curve for *Z. mobilis* at 550 nm.

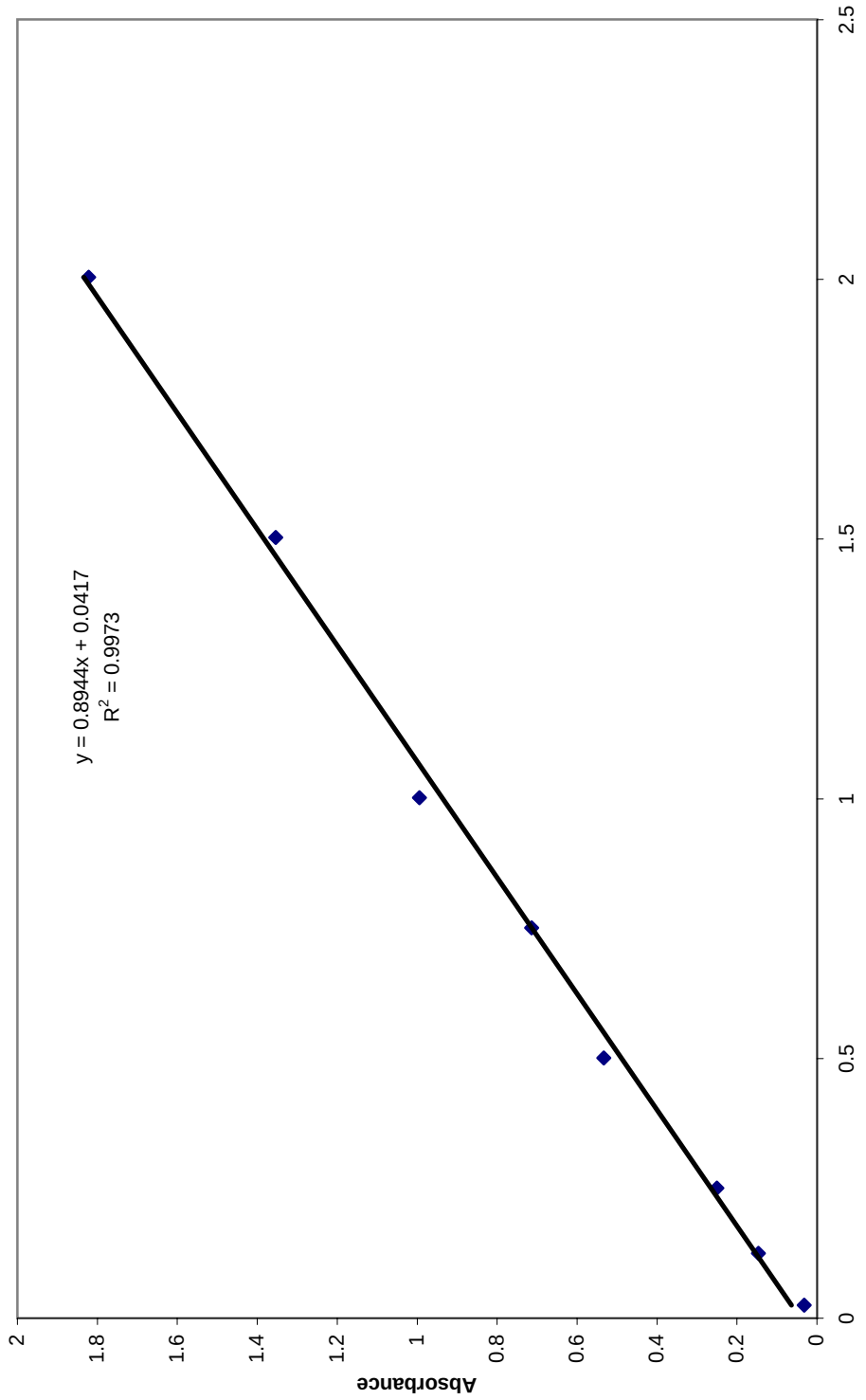

Figure A.3: Calibration curve for BCA at 562 nm.

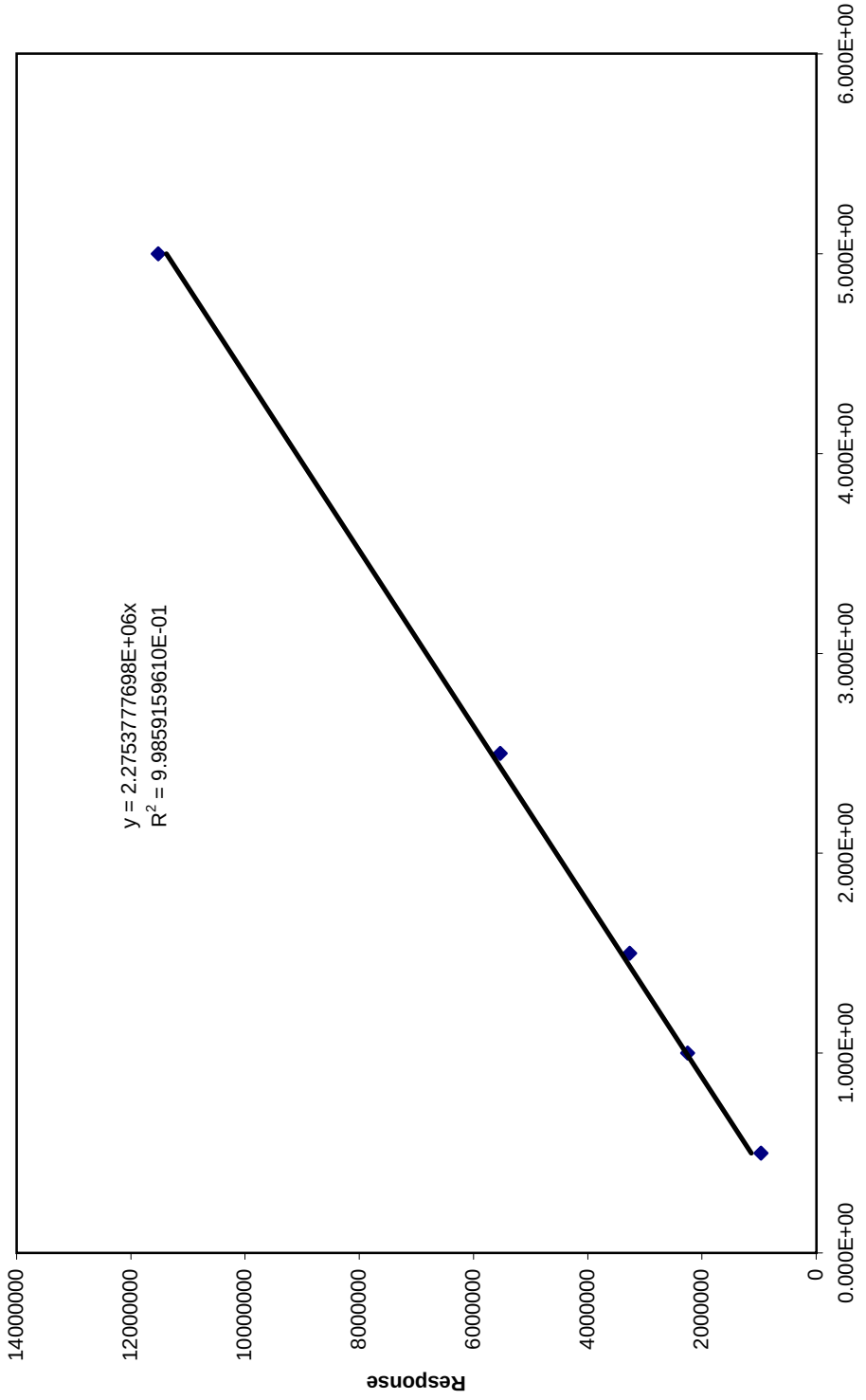

Figure A.4: Calibration curve for Glucose (HPLC).

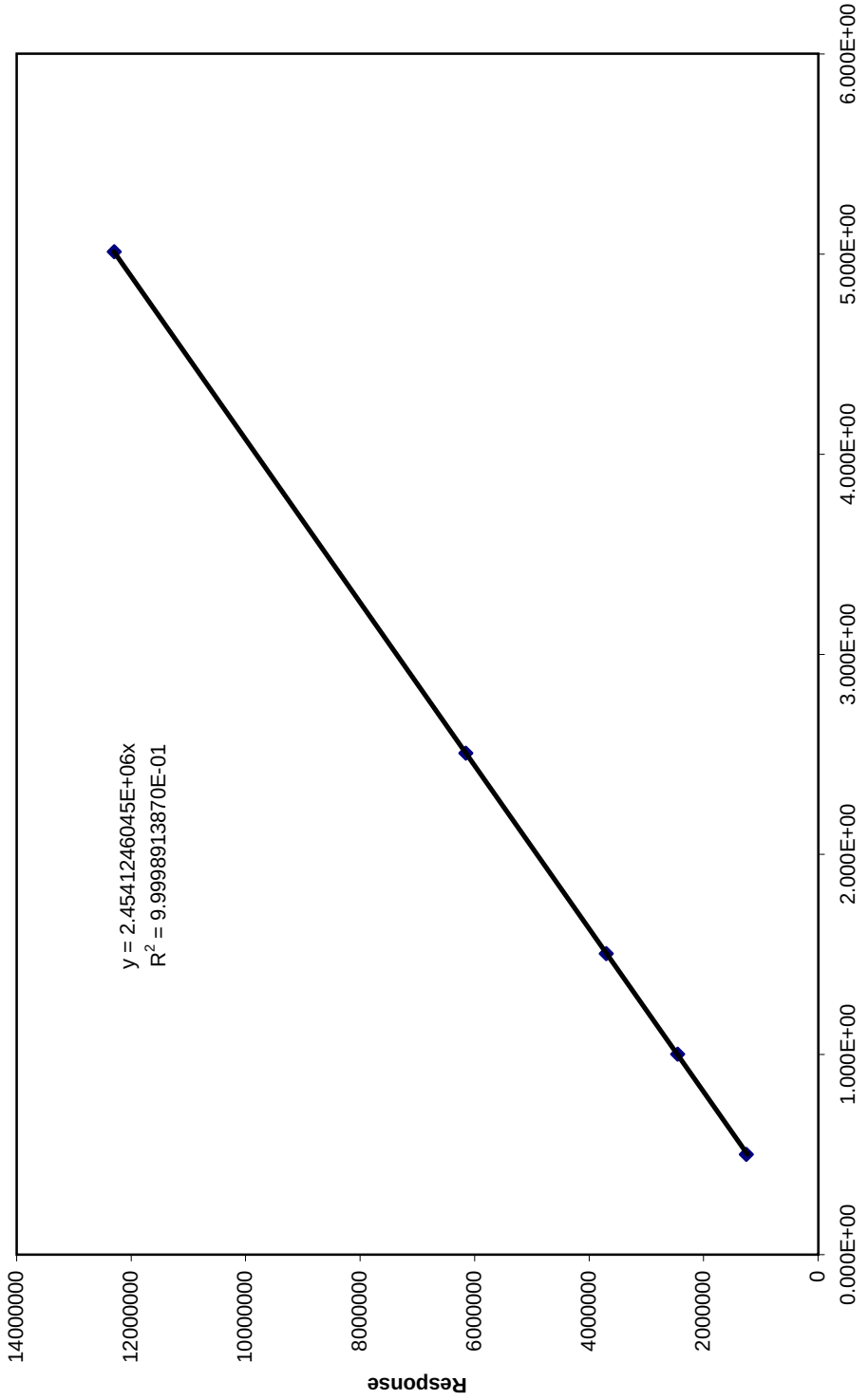

Figure A.5: Calibration curve for Fructose (HPLC).

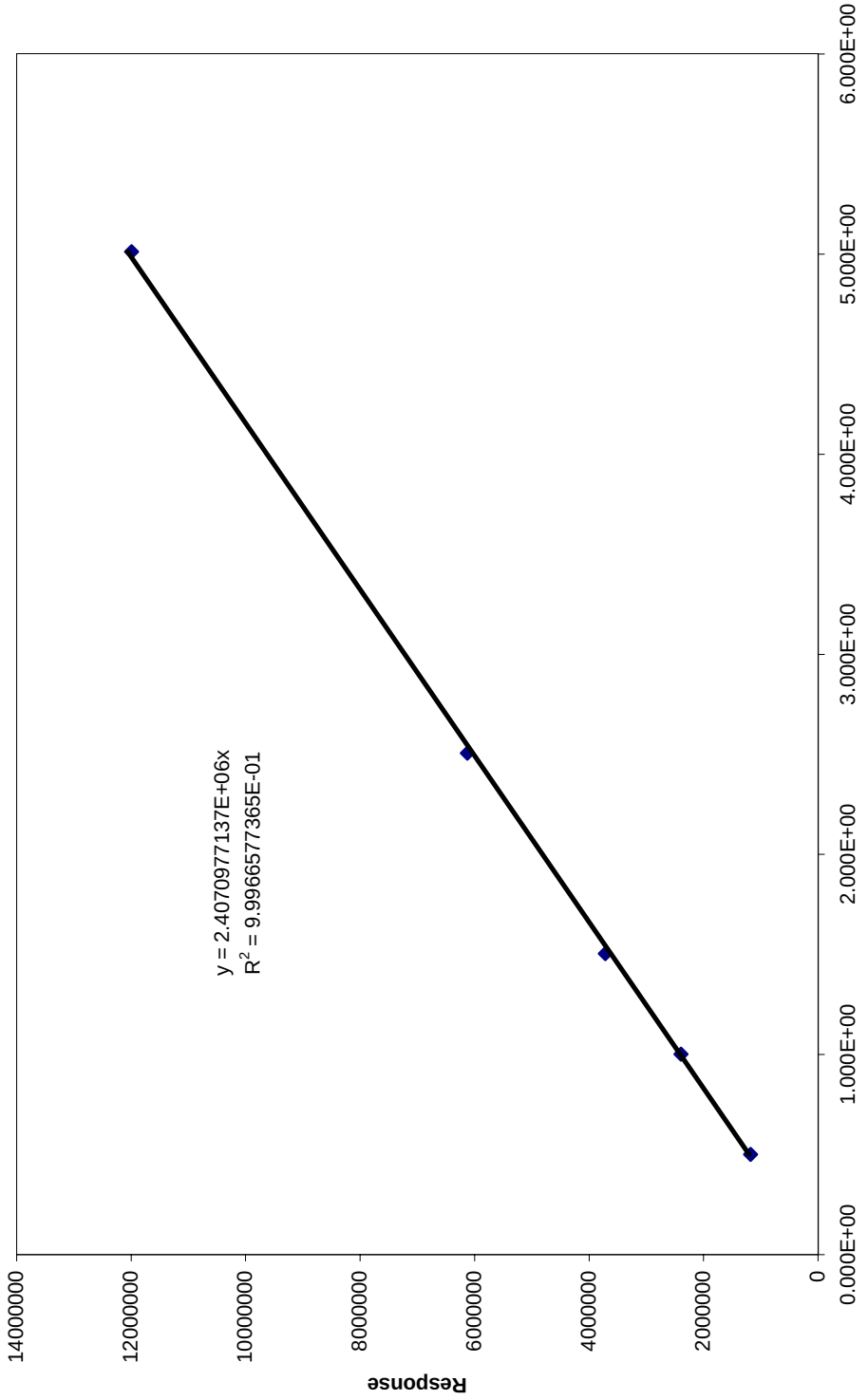

Figure A.6: Calibration curve for Sorbitol (HPLC).

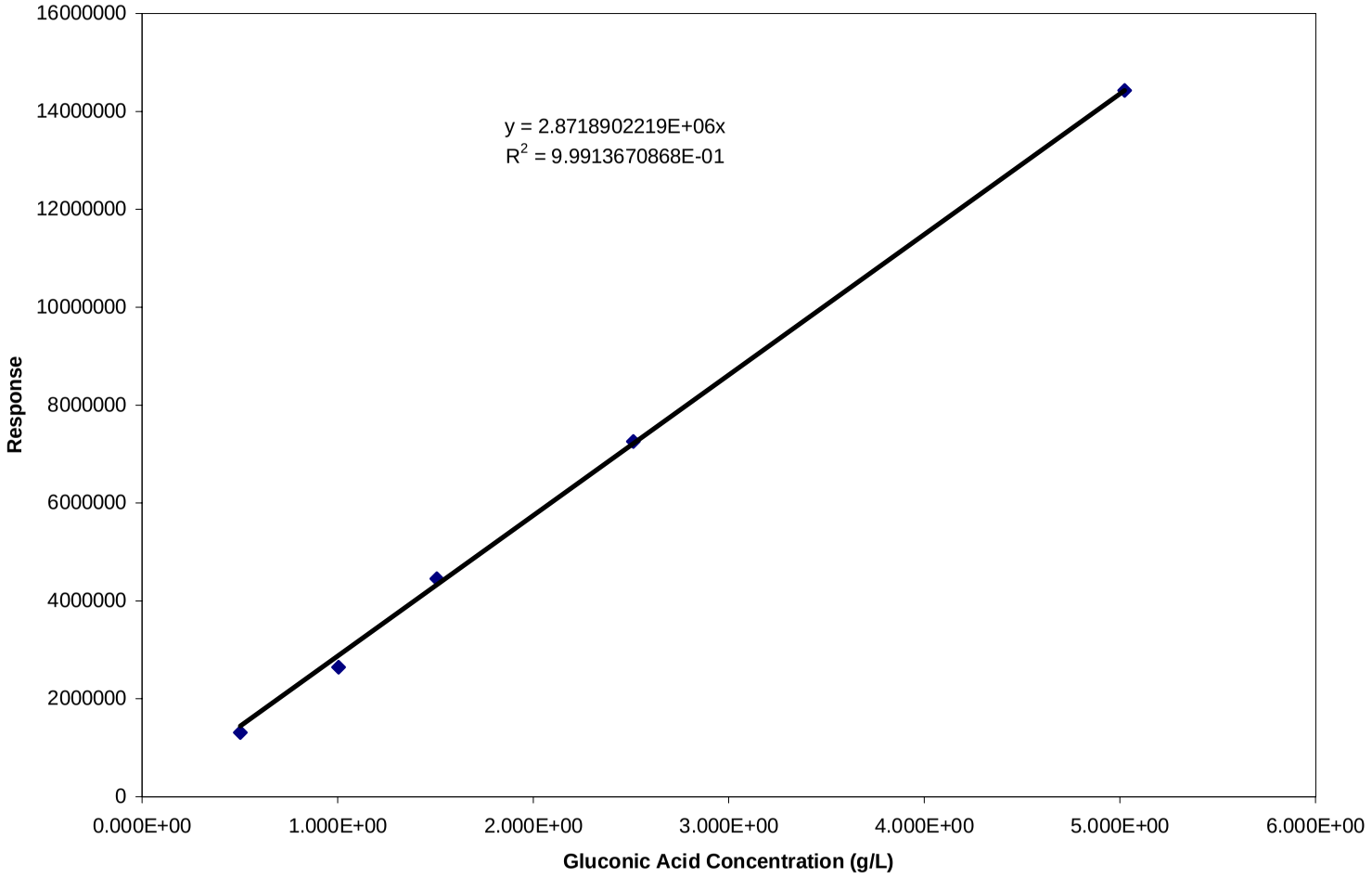

Figure A.7: Calibration curve for Gluconic Acid(HPLC).

Appendix B

Sample chromatograms

Sample Information

SampleName	20hr	Sample Type	Unknown
Vial	11	Date Acquired	7/16/01 1:02:25 AM
Injection	1	Acq Method Set	Sugars
Injection Volume	50.00 ul	Processing Method	HPLC Sugars
Channel	SATIN	Date Processed	7/16/01 2:40:52 AM
Run Time	28.0 Minutes		

Auto-Scaled Chromatogram

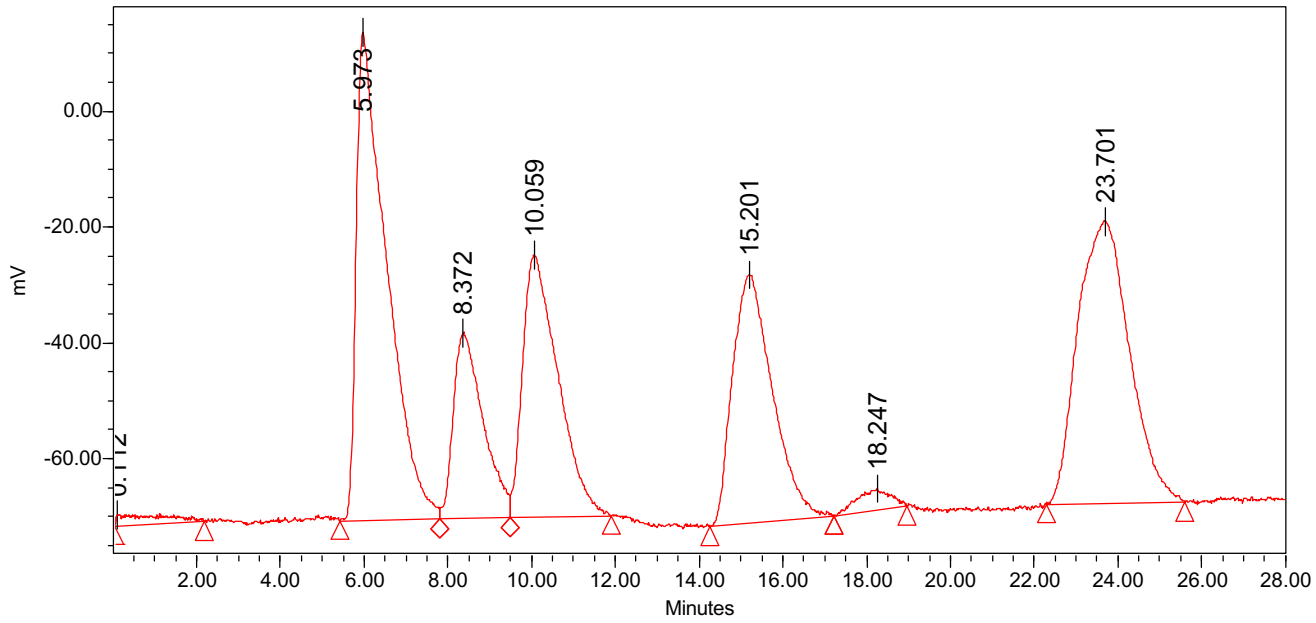

Peak Results

	Name	RT	Area	Height	Amount	Units
1		0.112	144745	1902		
2		5.973	4259223	84335		
3		8.372	1593348	32054		
4		10.059	2665077	45314		
5		15.201	2844339	42876		
6		18.247	211716	3830		
7		23.701	4194792	48874		

Data File C:\HPCHEM\1\DATA\MATT\aug20025.D Sample Name: zmftC

Z mob ft - C 01/08/21

Injection Date	: 8/21/01 5:50:26 AM	Seq. Line	: 6
Sample Name	: zmftC	Vial	: 206
Acq. Operator	: Matt	Inj	: 1
		Inj Volume	: 1 µl
Sequence File	: C:\HPCHEM\1\SEQUENCE\FAME2.S		
Method	: C:\HPCHEM\1\METHODS\FAME2.M		
Last changed	: 8/20/01 2:50:44 PM by Matt		

Gas chromatographic method for the determination of fatty acid methyl esters. Splitless injection mode is used.

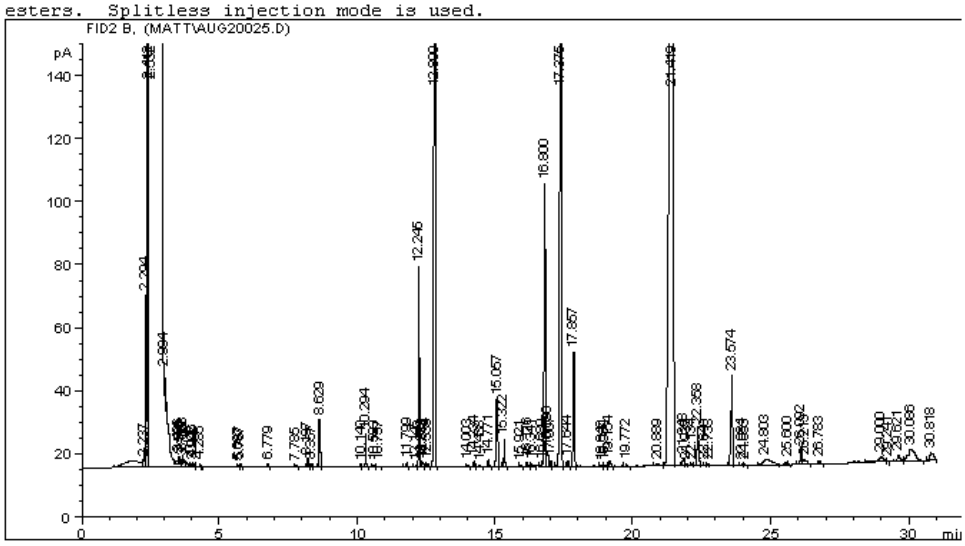

Area Percent Report

Sorted By	:	Signal
Multiplier	:	1.0000
Dilution	:	1.0000

Signal 1: FID2 B,

Peak #	RetTime [min]	Type	Width [min]	Area [pA*s]	Height [pA]	Area %
1	2.237	BV	0.5841	88.56893	1.79214	0.00101
2	2.294	VV	0.0292	110.43729	54.47725	0.00126
3	2.412	VV S	0.0233	3.72449e5	2.30945e5	4.24400
4	2.532	VB S	0.2658	8.39602e6	5.26506e5	95.67114
5	2.994	BB X	0.0604	24.07290	5.41459	0.00027
6	3.496	BV T	0.0546	7.67341	1.92104	8.744e-5
7	3.560	VV T	0.0397	5.06404	1.72911	5.770e-5
8	3.653	VV T	0.0309	5.58081	2.61556	6.359e-5
9	3.709	VB T	0.0516	4.92172	1.30133	5.608e-5
10	3.992	VV X	0.0337	1.63272	7.42580e-1	1.860e-5

Instrument 1 8/21/01 6:21:31 AM Matt Page 1 of 3

Figure B.1: Sample GC chromatogram (*Z. mobilis*).

Data File C:\HPCHEM\1\DATA\MATT\aug20003.D Sample Name: ecscA

E Coli SCCO2 - A 01/08/19

Injection Date	: 8/20/01 4:02:02 PM	Seq. Line	: 3
Sample Name	: ecscA	Vial	: 203
Acq. Operator	: Matt	Inj	: 1
		Inj Volume	: 1 µl
Sequence File	: C:\HPCHEM\1\SEQUENCE\FAME2.S		
Method	: C:\HPCHEM\1\METHODS\FAME2.M		
Last changed	: 8/20/01 2:50:44 PM by Matt		

Gas chromatographic method for the determination of fatty acid methyl esters. Splitless injection mode is used.

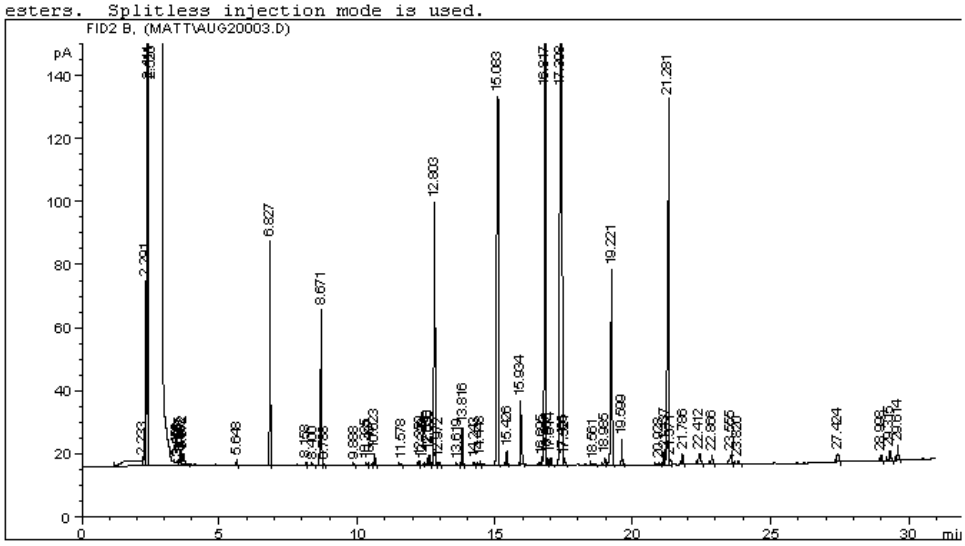

Area Percent Report

Sorted By	:	Signal
Multiplier	:	1.0000
Dilution	:	1.0000

Signal 1: FID2 B,

Peak #	RetTime [min]	Type	Width [min]	Area [pA*s]	Height [pA]	Area %
1	2.233	BV	0.4681	83.31533	2.10564	0.00094
2	2.291	VV	0.0283	114.27560	58.45620	0.00129
3	2.411	VV S	0.0227	3.65630e5	2.34307e5	4.13549
4	2.520	VB S	0.2429	8.47213e6	5.81306e5	95.82473
5	3.453	BV X	0.0460	1.49092	4.39805e-1	1.686e-5
6	3.505	VV X	0.0321	1.31588	5.99273e-1	1.488e-5
7	3.577	VV X	0.0286	4.47842	2.31378	5.065e-5
8	3.602	VV X	0.0296	3.80706	2.14045	4.306e-5
9	3.672	VB X	0.0441	9.98366	3.09996	0.00011
10	5.648	BB	0.0314	4.12799	2.05809	4.669e-5

Instrument 1 8/20/01 4:33:07 PM Matt Page 1 of 2

Figure B.2: Sample GC chromatogram (*E. coli*).

Appendix C

Raw Data

SC CO2										
Wash 1	8.971463974	3.269488304	4.440537064	2.721894833	0.8948695	2.045122	7.092973	4.332492	12.903627	3.7007288
Wash 2	4.697323118	1.038543344	4.802358603	1.26773184	1.2677318	1.291656	11.81092	3.643232	5.4041922	4.0452794
Wash 3	3.279662538	1.307795322	2.236714966	1.006728226	0.484721	0.896983	0.802372	1.312876	2.6446047	0.3955951
Total	16.94844963	5.61582697	11.47961063	4.996354898	2.6473224	4.233761	19.70627	9.2886	20.952424	8.1416033
Freeze Thaw										
Wash 1	28.25189667	22.29314812	29.21149171	45.16989694	14.053455	32.13253				
Wash 2	6.330836601	6.313419548	4.66616826	47.95517209	17.375181	12.608				
Wash 3	5.792500155	1.819120887	2.173283847	26.73258646	14.56449	13.27158				
Total	40.37523342	30.42568856	36.05094382	119.8576555	45.993125	58.01211				
Toluene										
Wash 1	0.864761396	3.799097248	7.5713813	7.85010033	4.0531441	0				
Wash 2	4.249074513	0.794582431	23.97604078	11.91266477	5.0081403	3.292372				
Wash 3	11.57285621	7.647855899	8.833278184	35.76942613	15.049973	6.214672				
Wash 4	7.72947223	3.542513338	14.93244645	32.18619715	8.4320729	10.0813				
Total	24.41616435	15.78404892	55.31314672	87.71838838	32.54333	19.58834				
Control										
Wash 1	1.338609125	1.670696902	3.067830084	8.28707305	2.1080182	1.148502				
Wash 2	0.701176208	0.321287866	1.551961101	1.65741461	1.0348453	0.727385				
Wash 3	1.784812166	4.144613468	5.702554745	4.301385535	0.9837418	0.038283				
Total	3.824597499	6.136598235	10.32234593	14.2458732	4.1266054	1.91417				

Figure C.1: Protein Data (mg).

Time	Sample 1						Avg	StdDev
0								
1	0.013	0.000	0.002	0.000	0.003	0.000	0.003	0.005
2	0.025	0.000	0.002	0.000	0.003	0.000	0.005	0.010
3	0.041	0.000	0.002	0.005	0.004	0.000	0.009	0.016
4	0.056	0.000	0.002	0.010	0.005	0.000	0.012	0.022
5	0.076	0.003	0.004	0.014	0.005	0.000	0.017	0.029
6	0.089	0.003	0.004	0.016	0.005	0.000	0.019	0.035
7	0.097	0.006	0.004	0.021	0.004	0.002	0.022	0.037
8	0.104	0.006	0.004	0.024	0.005	0.002	0.024	0.040
9	0.094	0.009	0.004	0.026	0.005	0.002	0.023	0.036
10	0.084	0.012	0.004	0.027	0.005	0.002	0.022	0.032
11	0.082	0.015	0.004	0.027	0.006	0.002	0.023	0.030
Time	Sample 2							
1	0.005	0.032	0.000	0.000	0.012	0.003	0.009	0.012
2	0.015	0.048	0.000	0.000	0.014	0.003	0.013	0.018
3	0.024	0.064	0.000	0.004	0.014	0.006	0.019	0.024
4	0.029	0.080	0.004	0.004	0.014	0.006	0.023	0.030
5	0.034	0.096	0.004	0.004	0.016	0.006	0.027	0.036
6	0.039	0.112	0.004	0.008	0.016	0.008	0.031	0.042
7	0.044	0.128	0.004	0.011	0.016	0.008	0.035	0.048
8	0.049	0.144	0.004	0.015	0.016	0.008	0.039	0.054
9	0.049	0.161	0.004	0.015	0.018	0.008	0.042	0.060
10	0.054	0.177	0.007	0.019	0.018	0.008	0.047	0.066
11	0.054	0.161	0.007	0.023	0.018	0.008	0.045	0.059
Time	Sample 3							
1	0.006	0.004	0.000	0.001	0.008	0.000	0.003	0.003
2	0.015	0.002	0.000	0.001	0.010	0.054	0.014	0.020
3	0.023	0.002	0.000	0.003	0.010	0.054	0.015	0.020
4	0.031	0.002	0.000	0.004	0.010	0.054	0.017	0.021
5	0.036	0.004	0.001	0.004	0.013	0.107	0.027	0.041
6	0.040	0.004	0.001	0.006	0.013	0.107	0.028	0.041
7	0.042	0.005	0.001	0.007	0.013	0.107	0.029	0.041
8	0.046	0.006	0.001	0.009	0.015	0.161	0.040	0.061
9	0.040	0.007	0.001	0.010	0.015	0.161	0.039	0.061
10	0.042	0.010	0.002	0.009	0.017	0.161	0.040	0.061
11	0.059	0.012	0.002	0.010	0.017	0.214	0.052	0.082

Figure C.2: Control Data (G-6-P DH) (absorbance).

Time	Sample 1									Avg	StDev
1.000	0.008	0.006	0.000	0.015	0.000	0.001	0.001	0.006	0.003	0.004	0.005
2.000	0.024	0.009	0.001	0.035	0.000	0.006	0.004	0.010	0.007	0.011	0.012
3.000	0.037	0.009	0.006	0.044	0.000	0.012	0.009	0.013	0.009	0.015	0.015
4.000	0.052	0.011	0.010	0.057	0.000	0.017	0.013	0.017	0.012	0.021	0.020
5.000	0.066	0.019	0.011	0.070	0.000	0.023	0.015	0.020	0.014	0.026	0.025
6.000	0.080	0.019	0.012	0.081	0.000	0.026	0.017	0.022	0.015	0.030	0.030
7.000	0.093	0.023	0.013	0.095	0.000	0.030	0.027	0.025	0.018	0.036	0.034
8.000	0.104	0.030	0.015	0.108	0.000	0.034	0.034	0.027	0.020	0.041	0.038
9.000	0.113	0.040	0.015	0.121	0.000	0.038	0.040	0.029	0.022	0.047	0.042
10.000	0.122	0.047	0.017	0.130	0.000	0.043	0.044	0.031	0.024	0.051	0.045
11.000	0.132	0.051	0.019	0.147	0.000	0.047	0.050	0.033	0.027	0.056	0.050
Time	Sample 2										
1.000	0.014	0.030	0.001	0.000	0.004	0.003	0.000	0.010	0.003	0.007	0.010
2.000	0.038	0.036	0.005	0.000	0.004	0.004	0.001	0.015	0.005	0.012	0.015
3.000	0.058	0.042	0.008	0.005	0.004	0.006	0.004	0.020	0.008	0.017	0.020
4.000	0.070	0.048	0.011	0.005	0.004	0.008	0.009	0.024	0.010	0.021	0.023
5.000	0.085	0.054	0.013	0.009	0.004	0.010	0.012	0.029	0.012	0.025	0.027
6.000	0.099	0.054	0.015	0.014	0.004	0.012	0.014	0.033	0.014	0.029	0.030
7.000	0.113	0.065	0.018	0.014	0.004	0.014	0.017	0.038	0.016	0.033	0.035
8.000	0.124	0.071	0.021	0.014	0.004	0.017	0.022	0.042	0.018	0.037	0.038
9.000	0.135	0.077	0.024	0.019	0.009	0.019	0.025	0.046	0.020	0.042	0.041
10.000	0.146	0.077	0.026	0.024	0.009	0.021	0.029	0.050	0.022	0.045	0.043
11.000	0.153	0.089	0.026	0.024	0.009	0.023	0.032	0.055	0.024	0.048	0.046
Time	Sample 3										
1.000	0.005	0.000	0.000	0.000	0.0064	0.019	0.000	0.0062	0.0362	0.008	0.012
2.000	0.010	0.000	0.002	0.000	0.0128	0.026	0.000	0.0078	0.0621	0.013	0.020
3.000	0.014	0.005	0.002	0.000	0.0128	0.026	0.000	0.0093	0.0828	0.017	0.026
4.000	0.020	0.005	0.002	0.006	0.0193	0.026	0.000	0.0109	0.1087	0.022	0.034
5.000	0.024	0.009	0.005	0.006	0.0193	0.026	0.004	0.0124	0.1294	0.026	0.040
6.000	0.029	0.014	0.005	0.012	0.0257	0.045	0.000	0.0132	0.1553	0.033	0.048
7.000	0.034	0.014	0.005	0.018	0.0257	0.058	0.004	0.0147	0.1812	0.039	0.056
8.000	0.039	0.014	0.005	0.024	0.0257	0.064	0.004	0.0155	0.2071	0.044	0.064
9.000	0.045	0.019	0.007	0.030	0.0321	0.058	0.008	0.0171	0.2278	0.049	0.069
10.000	0.050	0.019	0.007	0.036	0.0321	0.051	0.012	0.0178	0.2537	0.053	0.077
11.000	0.054	0.024	0.007	0.042	0.0385	0.058	0.012	0.0186	0.2796	0.059	0.085

Figure C.3: Supercritical carbon dioxide Data (G-6-P DH) (absorbance).

Time	Sample 1						
0.000						Avg	StdDev
1.000	0.000	0.000	0.000	0.000	0.024	0.005	0.011
2.000	0.027	0.009	0.000	0.000	0.027	0.013	0.014
3.000	0.027	0.009	0.000	0.000	0.027	0.013	0.014
4.000	0.027	0.009	0.000	0.000	0.027	0.013	0.014
5.000	0.027	0.019	0.000	0.004	0.027	0.015	0.013
6.000	0.027	0.019	0.000	0.004	0.031	0.016	0.014
7.000	0.054	0.019	0.000	0.004	0.031	0.021	0.022
8.000	0.054	0.019	0.000	0.009	0.031	0.022	0.021
9.000	0.054	0.019	0.000	0.009	0.031	0.022	0.021
10.000	0.054	0.028	0.000	0.009	0.031	0.024	0.021
11.000	0.080	0.038	0.000	0.009	0.031	0.031	0.031
Time	Sample 2						
1.000	0.006	0.013	0.001	0.001	0.014	0.007	0.006
2.000	0.019	0.027	0.001	0.003	0.019	0.014	0.011
3.000	0.027	0.040	0.002	0.005	0.024	0.019	0.016
4.000	0.031	0.047	0.002	0.006	0.028	0.023	0.019
5.000	0.036	0.054	0.003	0.007	0.033	0.027	0.021
6.000	0.044	0.054	0.003	0.008	0.038	0.029	0.022
7.000	0.050	0.067	0.003	0.009	0.042	0.034	0.027
8.000	0.056	0.080	0.004	0.010	0.047	0.039	0.032
9.000	0.061	0.087	0.004	0.011	0.051	0.043	0.035
10.000	0.065	0.100	0.005	0.014	0.055	0.048	0.039
11.000	0.072	0.107	0.005	0.016	0.060	0.052	0.042
Time	Sample 3						
1.000	0.0030	0.0021	0.0000	0.0003	0.003	0.002	0.001
2.000	0.0083	0.0049	0.0006	0.0007	0.004	0.004	0.003
3.000	0.0127	0.0076	0.0006	0.0011	0.005	0.005	0.005
4.000	0.0154	0.0097	0.0006	0.0013	0.006	0.007	0.006
5.000	0.0184	0.0111	0.0006	0.0014	0.007	0.008	0.007
6.000	0.0207	0.0111	0.0006	0.0017	0.008	0.008	0.008
7.000	0.0237	0.0118	0.0013	0.0018	0.009	0.009	0.009
8.000	0.0267	0.0139	0.0013	0.0020	0.010	0.011	0.010
9.000	0.0296	0.0139	0.0019	0.0024	0.011	0.012	0.011
10.000	0.0311	0.0146	0.0019	0.0027	0.012	0.012	0.012
11.000	0.0326	0.0174	0.0019	0.0030	0.013	0.013	0.013

Figure C.4: Toluene Data - Page 1 (G-6-P DH) (absorbance)

Time	Sample 4						
1.000	0.0040	0.0000	0.0000	0.0000	0.002	0.001	0.002
2.000	0.0058	0.0030	0.0004	0.0000	0.003	0.002	0.002
3.000	0.0080	0.0060	0.0004	0.0002	0.003	0.003	0.003
4.000	0.0106	0.0090	0.0004	0.0003	0.003	0.005	0.005
5.000	0.0142	0.0120	0.0004	0.0003	0.003	0.006	0.007
6.000	0.0155	0.0120	0.0004	0.0006	0.004	0.006	0.007
7.000	0.0164	0.0135	0.0004	0.0009	0.004	0.007	0.007
8.000	0.0168	0.0150	0.0004	0.0011	0.004	0.007	0.008
9.000	0.0173	0.0165	0.0008	0.0013	0.004	0.008	0.008
10.000	0.0164	0.0165	0.0008	0.0013	0.004	0.008	0.008
11.000	0.0177	0.0135	0.0008	0.0014	0.004	0.008	0.008

Figure C.5: Toluene Data - Page 2 (G-6-P DH) (absorbance).

Time	Sample 1						Avg	StdDev
0								
1	0.036	0.004	0.007	0.014	0.072	0.037	0.028	0.026
2	0.098	0.018	0.020	0.061	0.110	0.066	0.062	0.038
3	0.178	0.037	0.027	0.108	0.134	0.087	0.095	0.057
4	0.231	0.060	0.036	0.135	0.152	0.105	0.120	0.070
5	0.267	0.084	0.045	0.152	0.165	0.120	0.139	0.077
6	0.305	0.106	0.051	0.160	0.175	0.132	0.155	0.086
7	0.344	0.127	0.058	0.164	0.183	0.141	0.169	0.095
8	0.375	0.145	0.066	0.165	0.189	0.149	0.181	0.103
9	0.398	0.161	0.076	0.166	0.194	0.155	0.192	0.108
10	0.414	0.177	0.083	0.166	0.197	0.160	0.200	0.112
11	0.427	0.192	0.084	0.167	0.200	0.165	0.206	0.116
Time	Sample 2							
1	0.005	0.004	0.005	0.001	0.053	0.023	0.015	0.020
2	0.019	0.007	0.012	0.017	0.091	0.040	0.031	0.032
3	0.021	0.012	0.023	0.038	0.123	0.056	0.046	0.041
4	0.027	0.016	0.035	0.048	0.151	0.071	0.058	0.049
5	0.052	0.020	0.049	0.053	0.174	0.085	0.072	0.054
6	0.081	0.022	0.062	0.057	0.195	0.097	0.086	0.059
7	0.103	0.024	0.069	0.058	0.213	0.109	0.096	0.065
8	0.125	0.024	0.078	0.057	0.229	0.120	0.105	0.071
9	0.143	0.027	0.086	0.058	0.243	0.129	0.114	0.076
10	0.156	0.032	0.088	0.060	0.255	0.138	0.121	0.080
11	0.153	0.036	0.095	0.061	0.265	0.147	0.126	0.082
Time	Sample 3							
1	0.011	0.003	0.000	0.007	0.010	0.006	0.006	0.004
2	0.025	0.006	0.000	0.034	0.015	0.016	0.016	0.012
3	0.039	0.009	0.002	0.055	0.019	0.022	0.024	0.020
4	0.054	0.016	0.007	0.069	0.022	0.028	0.033	0.024
5	0.066	0.019	0.009	0.082	0.025	0.034	0.039	0.029
6	0.077	0.025	0.012	0.096	0.027	0.039	0.046	0.033
7	0.090	0.028	0.014	0.111	0.029	0.045	0.053	0.039
8	0.104	0.035	0.019	0.125	0.031	0.050	0.061	0.044
9	0.116	0.038	0.021	0.139	0.032	0.055	0.067	0.049
10	0.127	0.041	0.028	0.151	0.033	0.060	0.073	0.053
11	0.137	0.044	0.033	0.163	0.034	0.064	0.079	0.057

Figure C.6: Freeze/Thaw Data (G-6-P DH) (absorbance).

sc010628

Time	Glucose	Fructose	Sorbitol	Gluconic Acid
0	0.0808205	0.0711559	0	0
1	0.0763693	0.066061	0	0
10	0.0787488	0.0703732	0	0
20	0.0781291	0.0723388	0	0
60	0.0737541	0.0652986	0	0
120	0.0606775	0.0753231	0.0024297	0.0047563
240	0.0587781	0.0725932	0.0095594	0.011655
360	0.051083	0.067132	0.0157586	0.0262935
1200	0.0474049	0.0622868	0.0272559	0.0347622
1380	0.03899	0.0430111	0.044773	0.0578521

sc010713

Time	Glucose	Fructose	Sorbitol	Gluconic Acid
0	0.064522	0.0646201	0	0
1	0.0686378	0.071111	0	0.0012374
10	0.0670776	0.0698083	0.0022806	0.0032532
20	0.0676734	0.0715783	0.0044018	0.0059788
60	0.0662792	0.070629	0.0061578	0.0085888
120	0.0563695	0.0598411	0.0090708	0.0108618
240	0.0802043	0.0865946	0.0262101	0.0331985
360	0.0445196	0.0493746	0.0248292	0.0299614
1200	0.0387773	0.0443266	0.0281904	0.0370932
1380	0.023316	0.0361584	0.0389169	0.0486532

sc010716

Time	Glucose	Fructose	Sorbitol	Gluconic Acid
0	0.0717192	0.069658	0	0
1	0.072817	0.0717697	0	0
10	0.0685387	0.0684789	0.0022203	0.0032394
20	0.0645022	0.0647608	0.0045122	0.0065263
60	0.0636946	0.0651475	0.0055763	0.00698
120	0.0630852	0.0617668	0.0090853	0.0105566
240	0.0553778	0.0559439	0.0157008	0.0203689
360	0.0451489	0.0455881	0.0231174	0.0301532
1200	0.0401283	0.0446749	0.0246225	0.0310986
1380	0.0257696	0.041716	0.0260865	0.0365486

ft010702

Time	Glucose	Fructose	Sorbitol	Gluconic Acid
0	0.0764024	0.0720422	0	0
1	0.0695418	0.0664465	0.0026278	0.0027837
10	0.0562238	0.0526094	0.0080536	0.010028
20	0.0512857	0.0507806	0.013455	0.0168732
60	0.0470335	0.0501249	0.0161333	0.0205571
120	0.0294388	0.0420235	0.0241081	0.030162
240	0.0119813	0.0269786	0.0304378	0.0368795
360	0.0017816	0.0157812	0.0368254	0.0450309
1200	0.0023427	0.012099	0.037643	0.0411839
1380	0	0	0.0333652	0.0384629

ft010711

Time	Glucose	Fructose	Sorbitol	Gluconic Acid
0	0.0634781	0.0634502	0	0
1	0.0499019	0.0544255	0.0070706	0.0088402
10	0.0309713	0.0388498	0.0193302	0.0246168

Figure C.7: GFOR Data - Page 1 (moles/L).

20	0.022267	0.034649	0.0217213	0.0263229
60	0.0192834	0.0332264	0.0252422	0.0315557
120	0.0113875	0.0365122	0.0336339	0.0378642
240	0	0.0432888	0.0347903	0.0261182
360	0	0.0237959	0.0261146	0.0169296
1200	0	0.0091167	0.0239014	0.0096361
1380	0	0	0.0230179	0

ft010715

Time	Glucose	Fructose	Sorbitol	Gluconic Acid
0	0.0610839	0.0596842	0	0
1	0.0433878	0.0471325	0.0107975	0.0135417
10	0.0188619	0.0253591	0.0297125	0.0373008
20	0.0127029	0.0226553	0.036174	0.0429197
60	0.0103414	0.020603	0.042419	0.0520421
120	0.0056455	0.0221429	0.0455215	0.0551517
240	0	0.0259049	0.0405658	0.0486181
360	0	0.0172753	0.0348859	0.03752
1200	0	0.0135503	0.0335231	0.0352711
1380	0	0	0.0355064	0.028443

tol010630

Time	Glucose	Fructose	Sorbitol	Gluconic Acid
0	0.0803169	0.0805403	0	0
1	0.0742498	0.079866	0	0
10	0.0648205	0.0676797	0.0044988	0.0080346
20	0.0611529	0.0636982	0.0092684	0.0106814
60	0.0577078	0.0640892	0.0167723	0.0211434
120	0.0405481	0.0467988	0.026295	0.0365999
240	0.0172519	0.0269312	0.0458571	0.0606776
360	0	0.0200884	0.0583992	0.0796901
1200	0	0.0205015	0.0584057	0.0816306
1380	0	0	0.055159	0.0766822

tol010707

Time	Glucose	Fructose	Sorbitol	Gluconic Acid
0	0.0576765	0.0658275	0	0
1	0.0558154	0.0692388	0.0010869	0.0036754
10	0.0502378	0.0661783	0.0082148	0.0144119
20	0.047642	0.0648368	0.0137728	0.0190685
60	0.0425788	0.0597177	0.0190694	0.0264009
120	0.0387184	0.051238	0.0296754	0.0441316
240	0.0329054	0.0472927	0.0427223	0.0633754
360	0	0.045589	0.0487061	0.0770539
1200	0	0.0437331	0.0452967	0.0747065
1380	0	0.0393266	0.0394055	0.0736421

tol010714

Time	Glucose	Fructose	Sorbitol	Gluconic Acid
0	0.0569833	0.0589769	0	0
1	0.0583709	0.0630645	0	0.0018225
10	0.0475478	0.0534166	0.0134964	0.0187969
20	0.0385508	0.0465642	0.0179815	0.0234701
60	0.0330224	0.0401933	0.0218975	0.0301098
120	0.02126	0.0285821	0.0240247	0.0325345
240	0.0147841	0.0231345	0.038481	0.0508834
360	0	0.0171641	0.053318	0.0746865

Figure C.8: GFOR Data - Page 2 (moles/L).

1200	0	0.0181318	0.0501952	0.0735562
1380	0	0.0015997	0.0481019	0.0725268

cont010701

Time	Glucose	Fructose	Sorbitol	Gluconic Acid
0	0.0581177	0.0644278	0	0
1	0.0561859	0.070928	0	0
10	0.0392847	0.0736745	0.0054316	0.0066094
20	0.0261387	0.0881677	0.0096433	0.0031795
60	0	0.0744702	0.0094986	0
120	0	0.0562385	0.0093851	0
240	0	0.045008	0.0066563	0
360	0	0	0.0055992	0
1200	0	0	0.0076133	0
1380	0	0	0.0077309	0

cont010706

Time	Glucose	Fructose	Sorbitol	Gluconic Acid
0	0.0773391	0.0810475	0	0
1	0.0642685	0.0807202	0	0
10	0.0488732	0.0790009	0.0039326	0
20	0.0416201	0.0826771	0.0091918	0
60	0.0321691	0.0847308	0.0118552	0.0013307
120	0	0.0532738	0.0120268	0
240	0	0	0.0114106	0
360	0	0	0.0143478	0
1200	0	0	0.0125082	0
1380	0	0	0.0068815	0

cont010712

Time	Glucose	Fructose	Sorbitol	Gluconic Acid
0	0.0615631	0.062806	0	0
1	0.0552645	0.0599166	0	0
10	0.0427384	0.0560001	0.0036284	0
20	0.0174871	0.0403222	0.0066463	0.001878
60	0.0068071	0.0412775	0.0077433	0.0022275
120	0	0.0239594	0.010374	0
240	0	0	0.011547	0
360	0	0.0171641	0.0095483	0
1200	0	0.0181318	0.0074299	0
1380	0	0.0015997	0.0073411	0

Figure C.9: GFOR Data - Page 3 (moles/L).

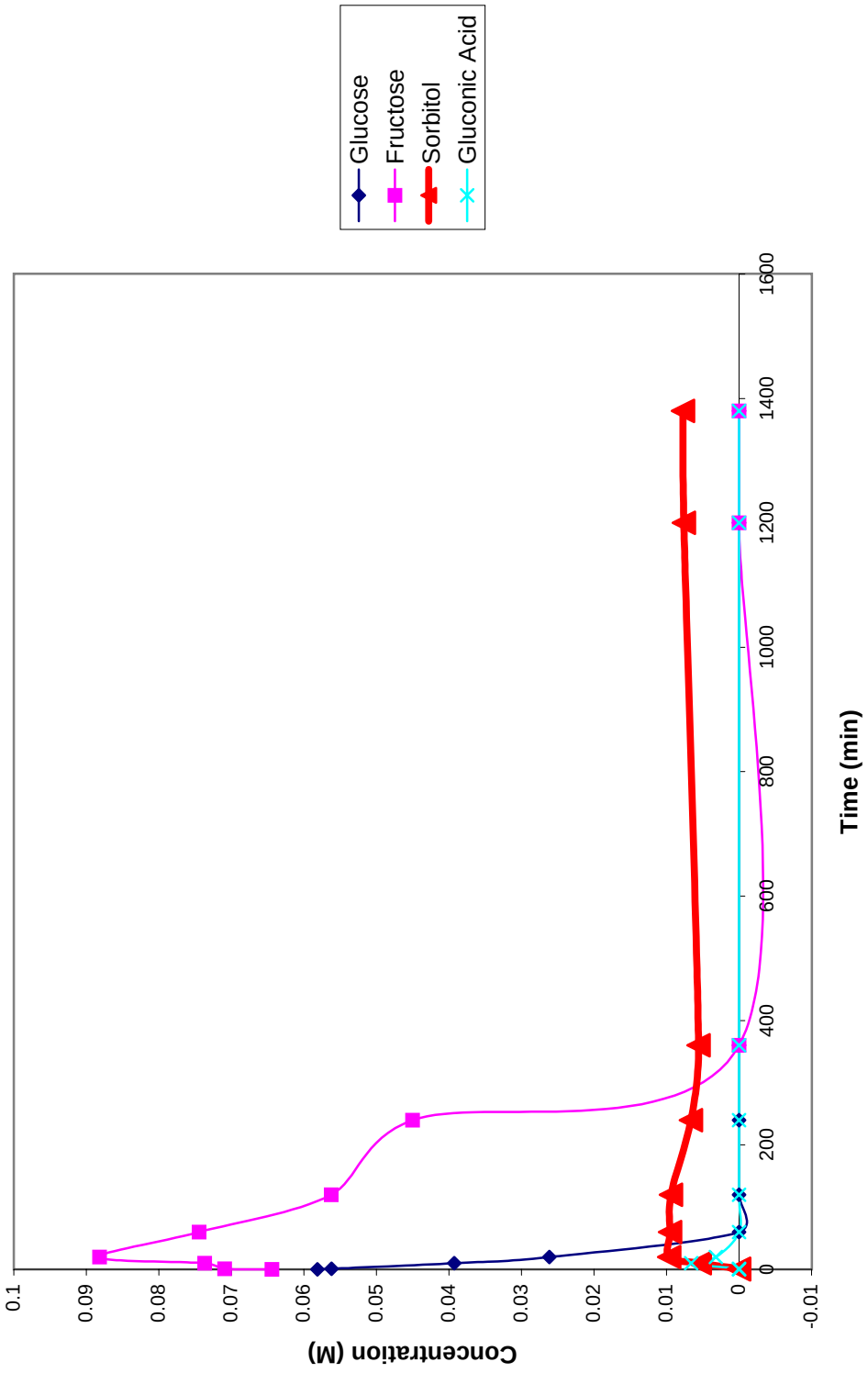

Figure C.10: Time course for control run 1.

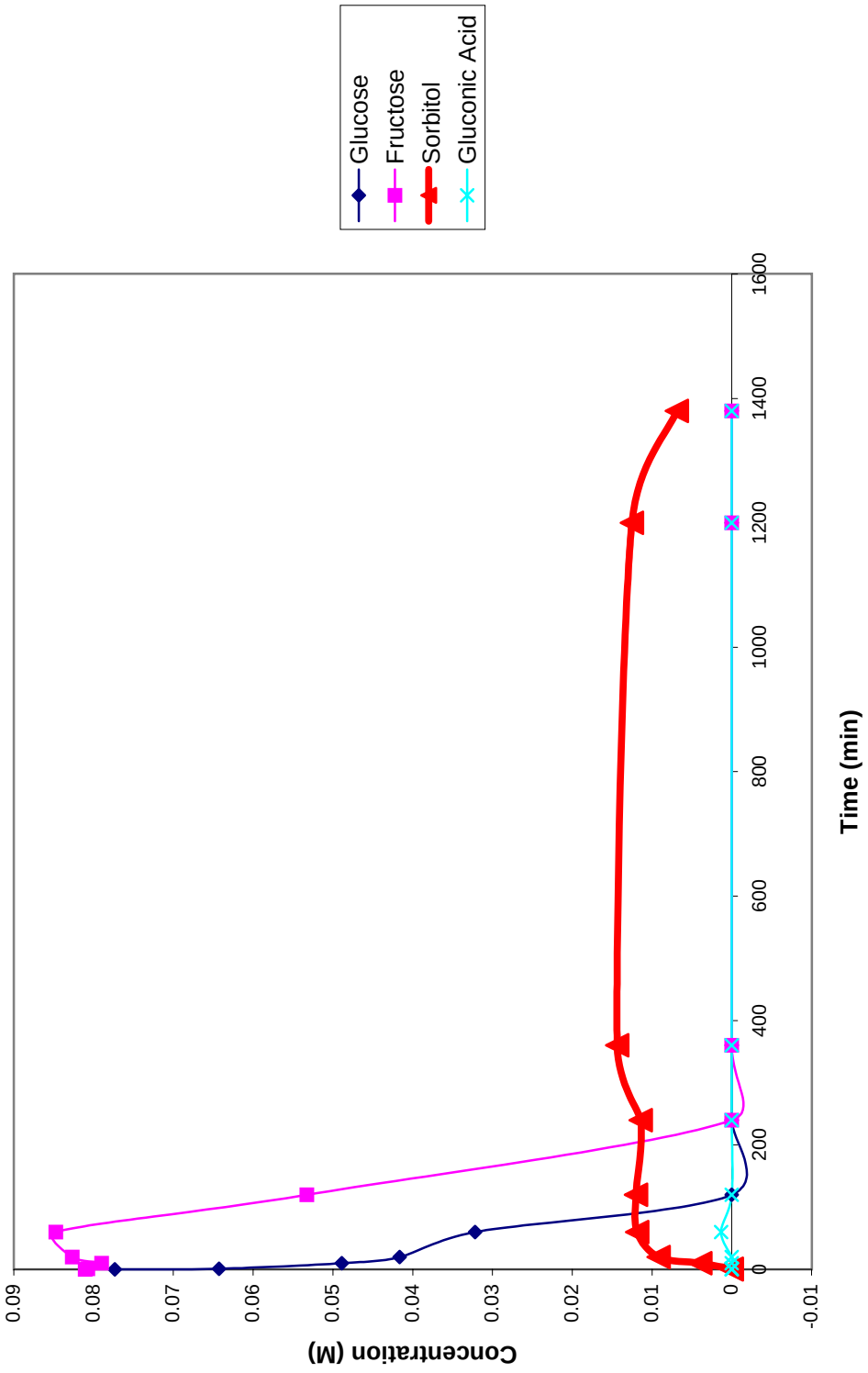

Figure C.11: Time course for control run 2.

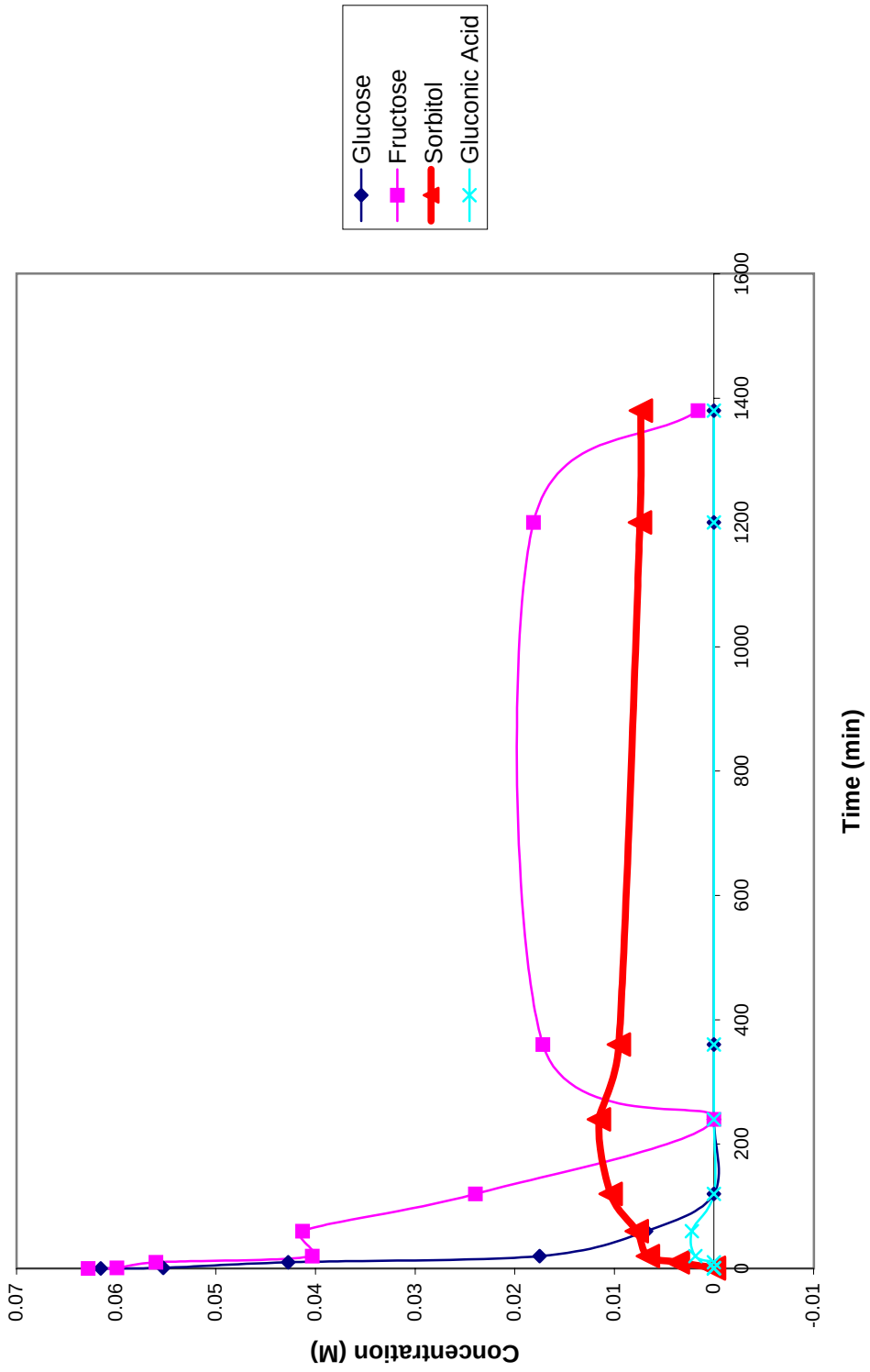

Figure C.12: Time course for control run 3.

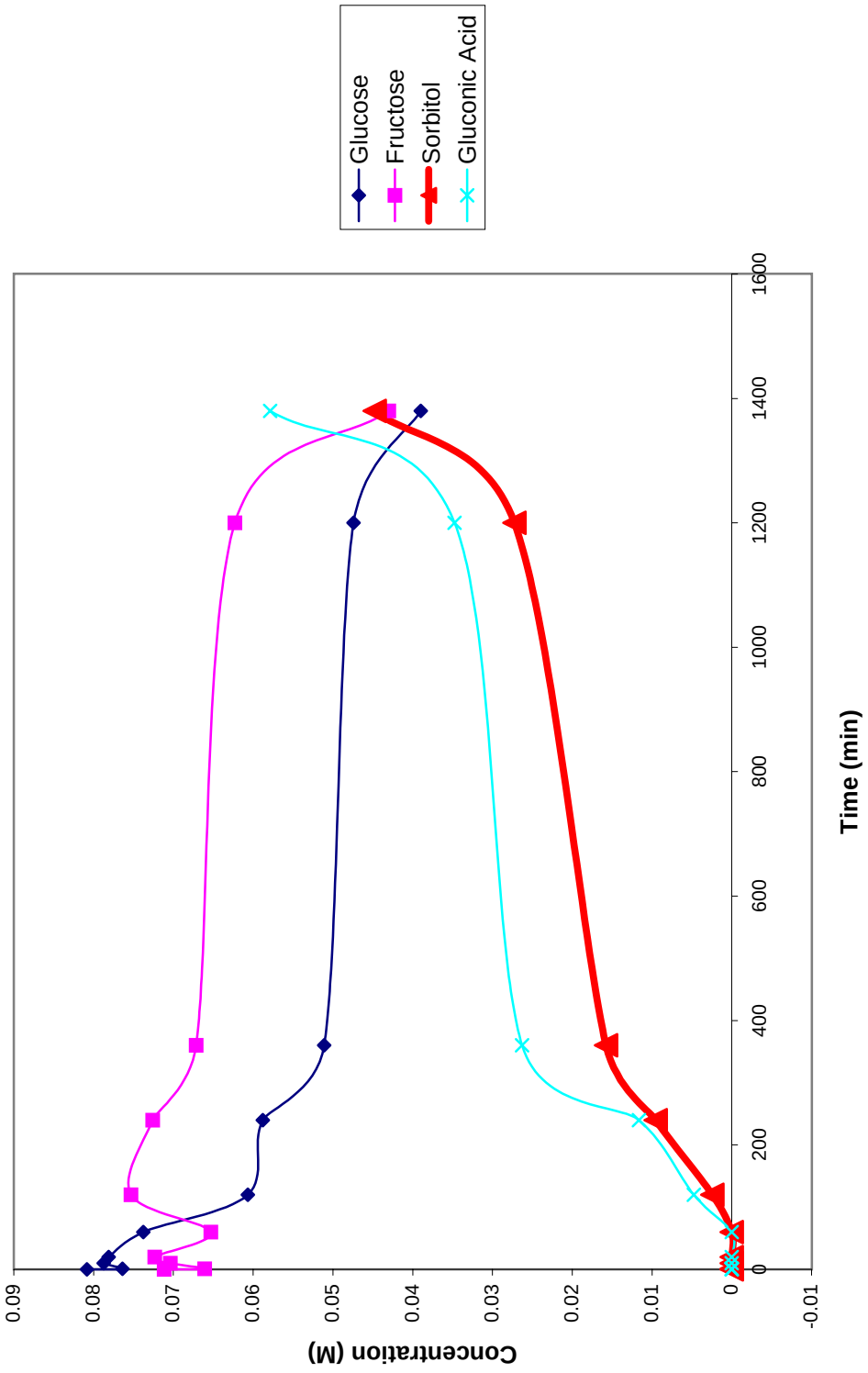

Figure C.13: Time course for sc-co2 run 1.

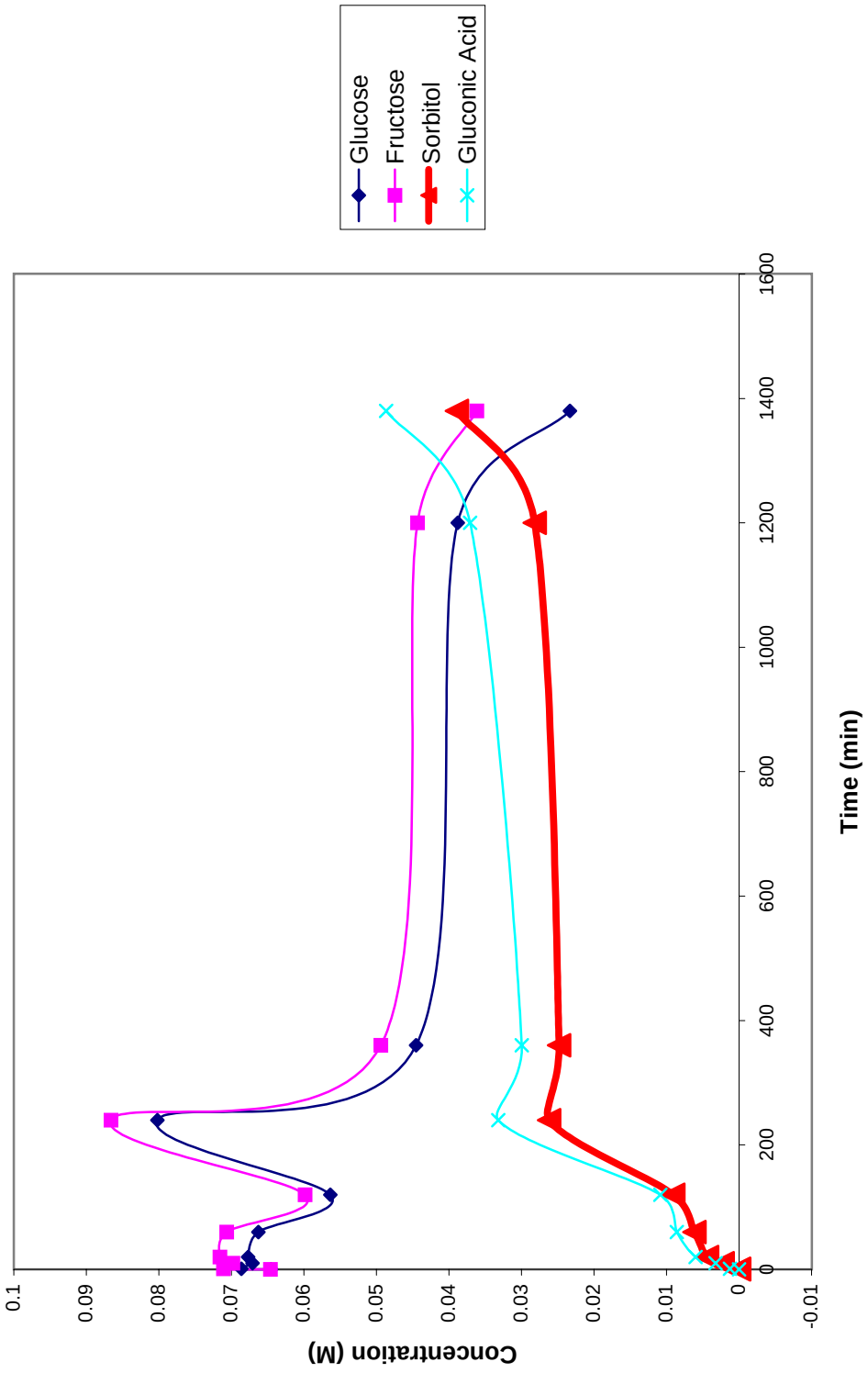

Figure C.14: Time course for sc-co2 run 2.

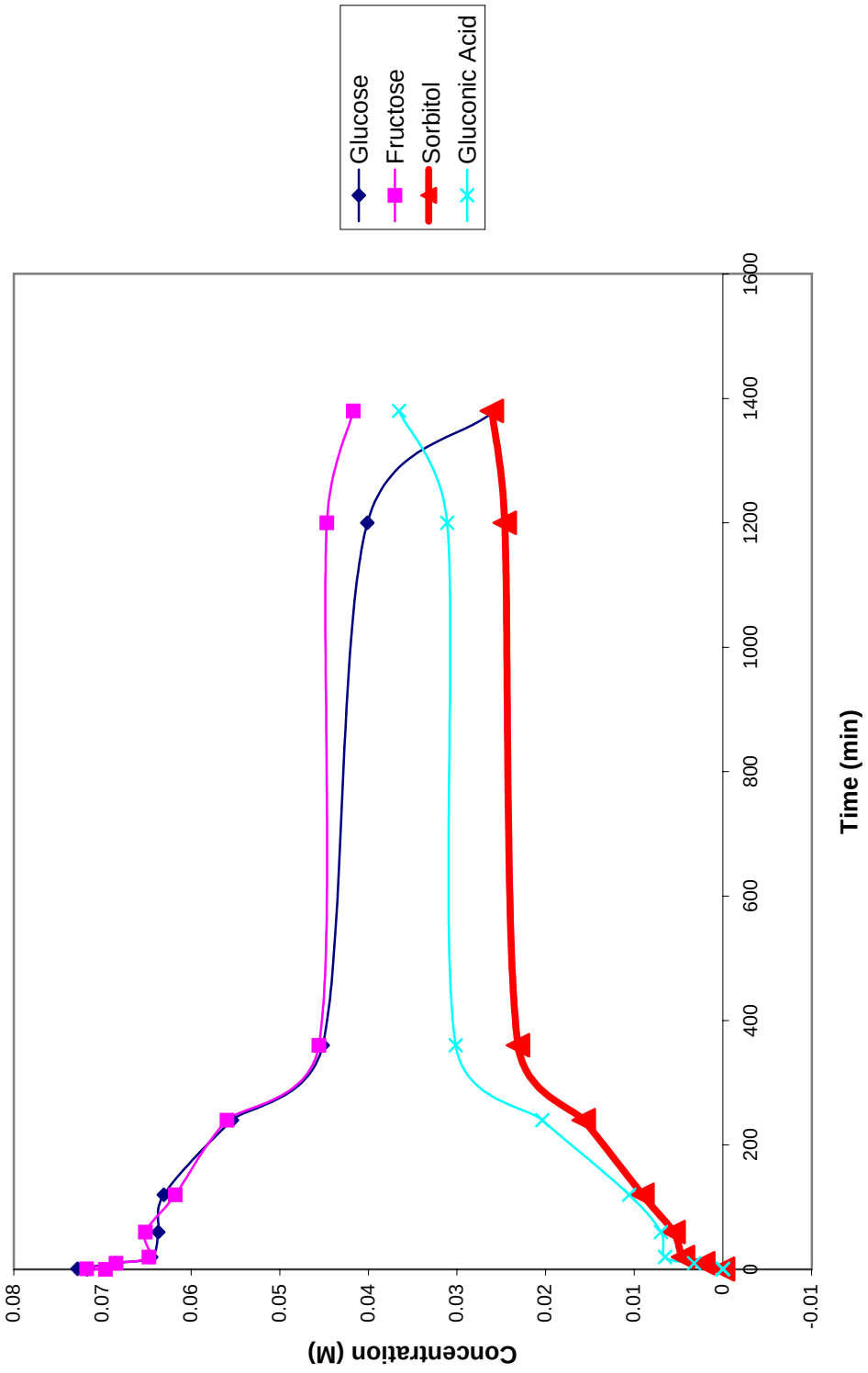

Figure C.15: Time course for sc-co2 run 3.

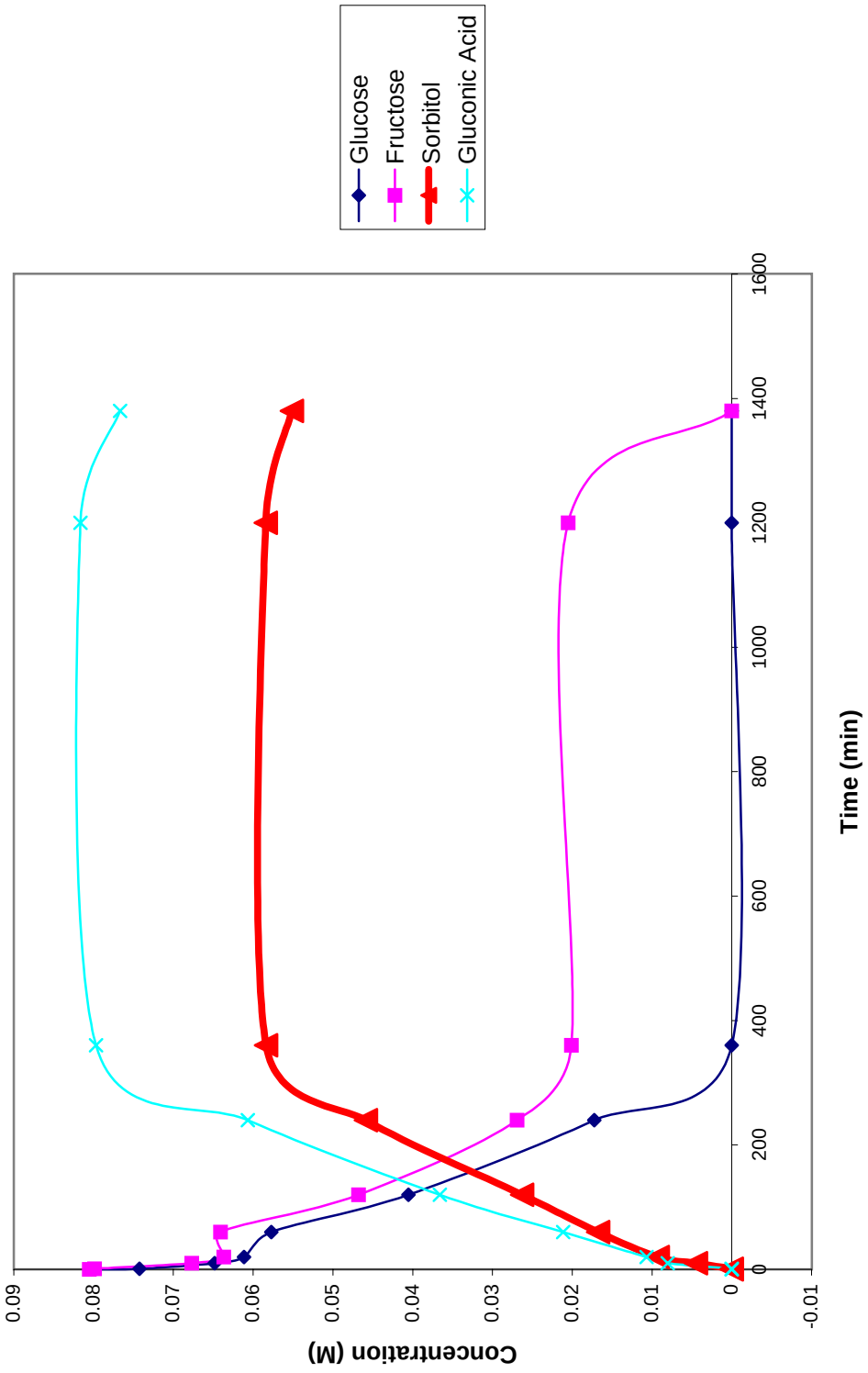

Figure C.16: Time course for toluene run 1.

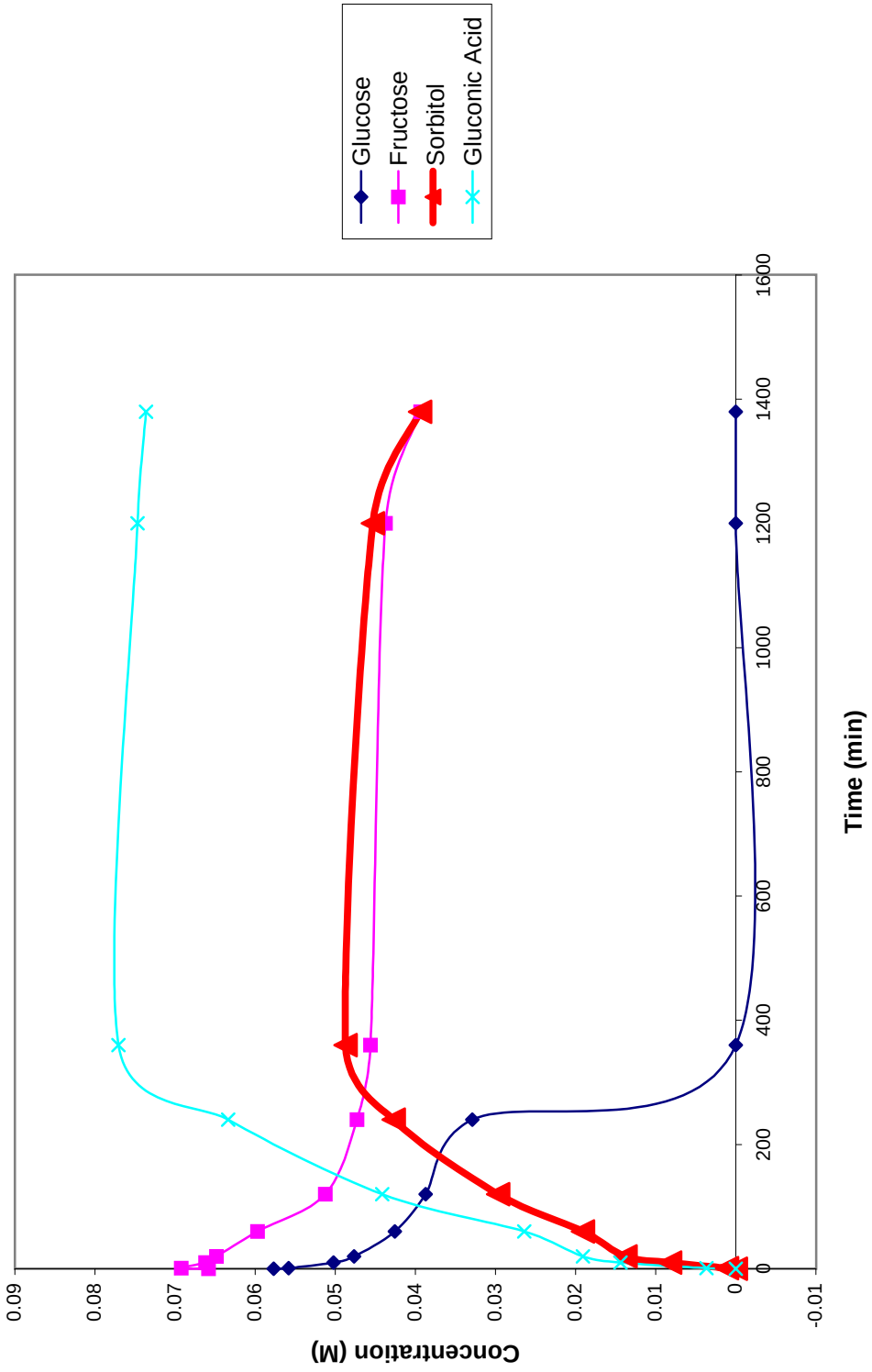

Figure C.17: Time course for toluene run 2.

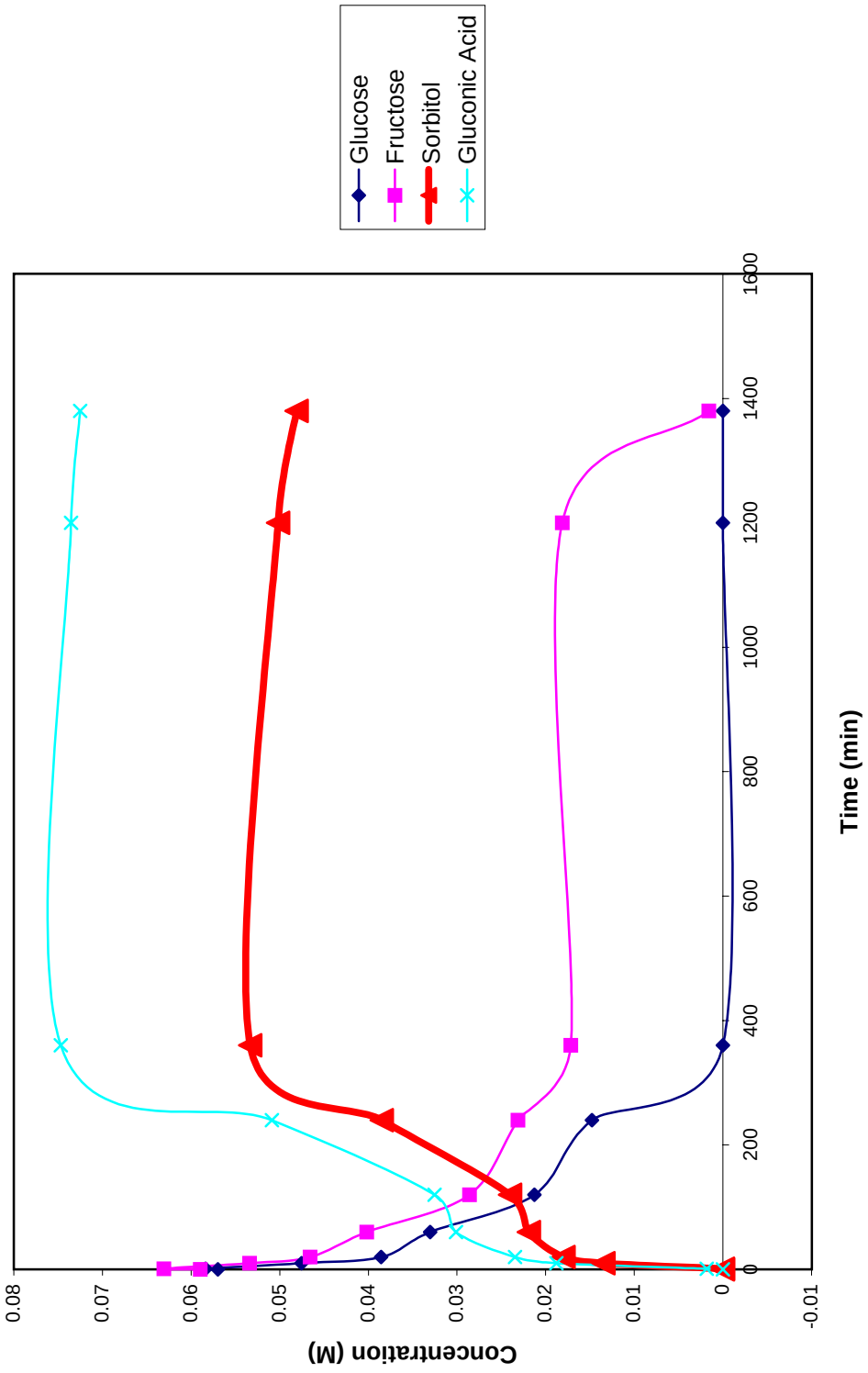

Figure C.18: Time course for toluene run 3.

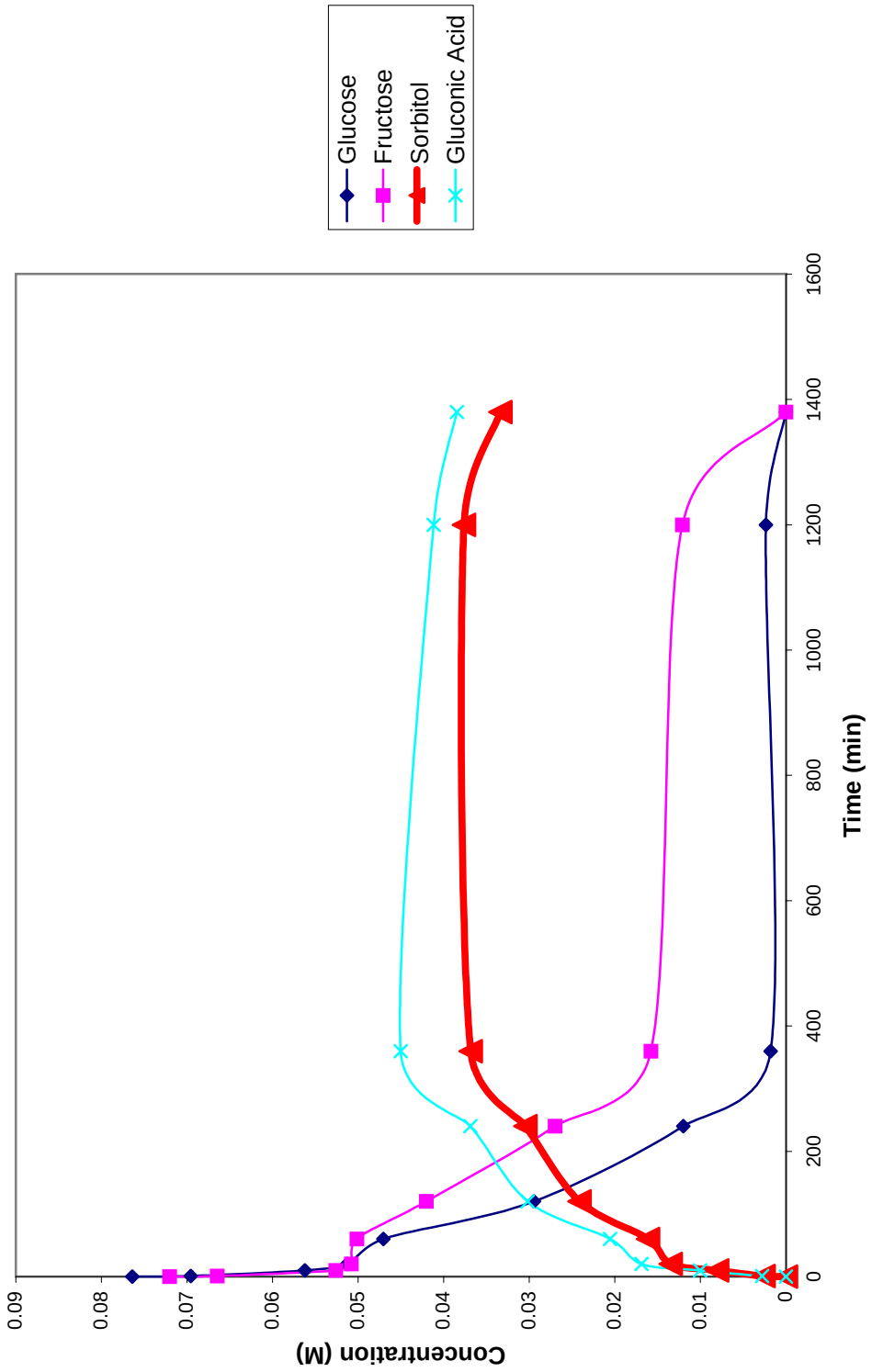

Figure C.19: Time course for freeze/thaw run 1.

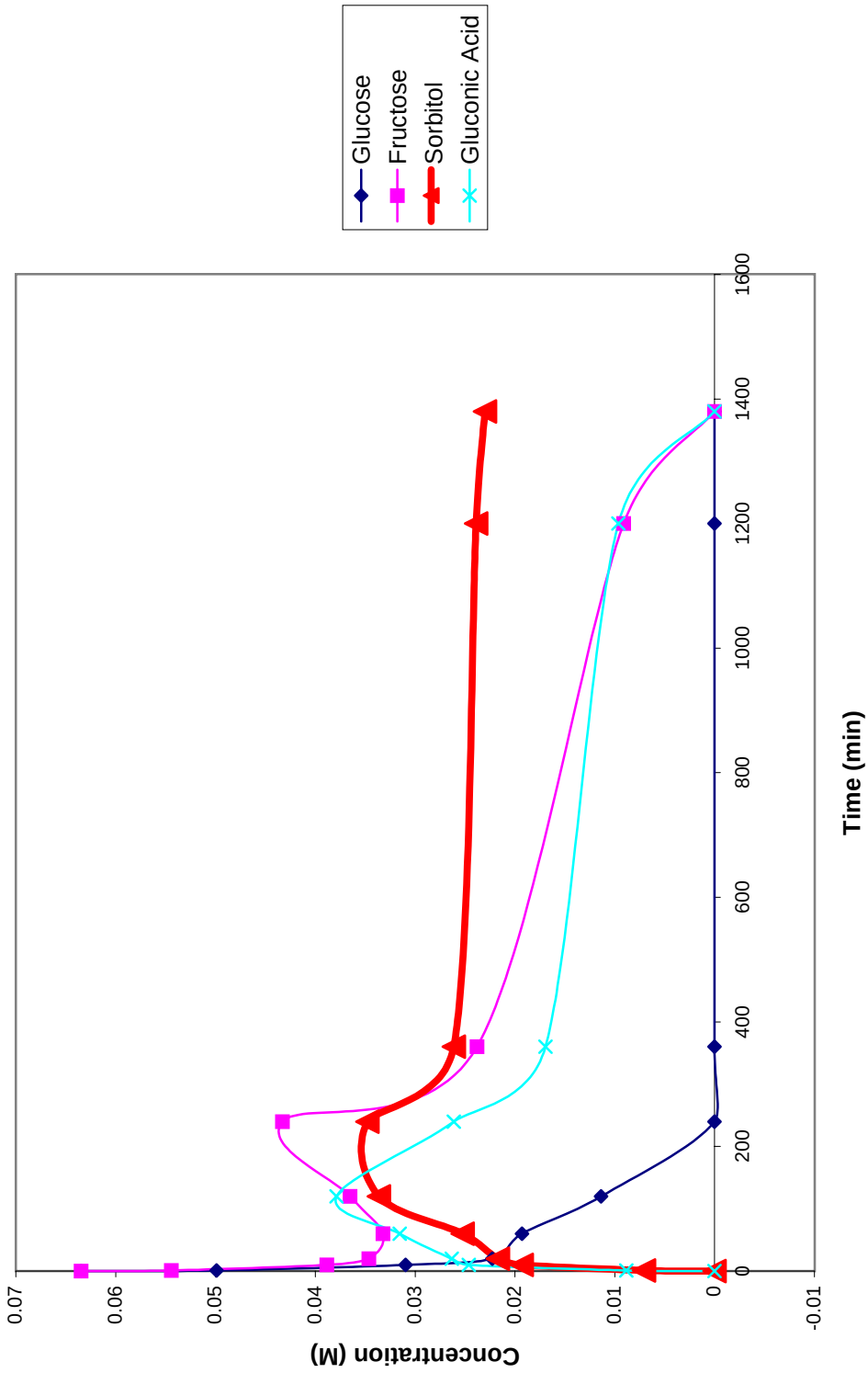

Figure C.20: Time course for freeze/thaw run 2.

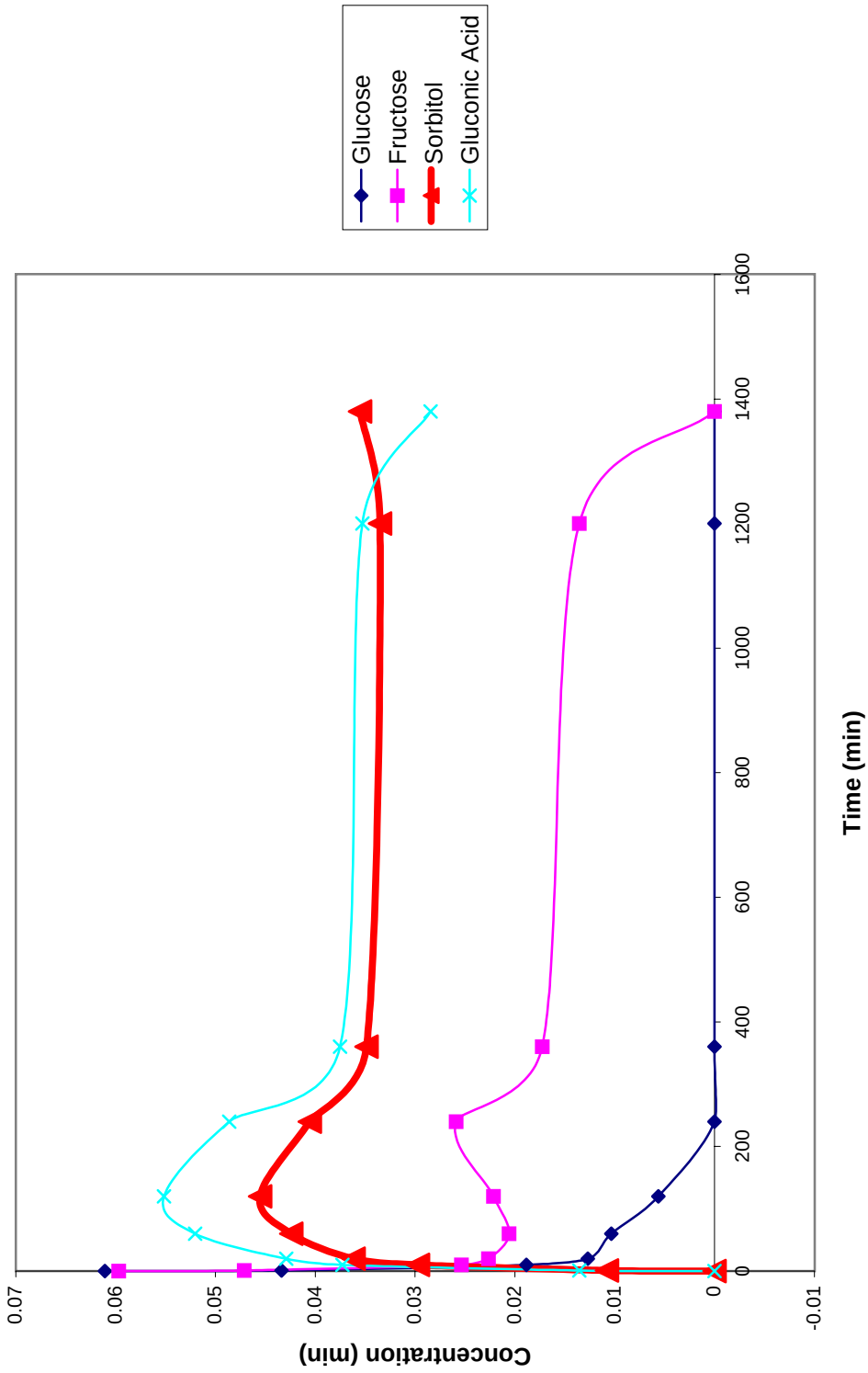

Figure C.21: Time course for freeze/thaw run 3.